The role of peroxisomes in sterol biosynthesis by the cellular slime mould *Dictyostelium discoideum*

Mayyadah Abdullah Mohammed Alkuwayti, BSc

This thesis is submitted to the University of Sheffield for the degree of Doctor of Philosophy

Department of Molecular Biology and Biotechnology

University of Sheffield

September 2014

ABSTRACT

In eukaryotic cells, the mevalonate pathway of isoprenoid biosynthesis provides the cell with essential precursors for several cellular processes. For example, one product, FDP (farnesyl diphosphate) is a fundamental precursor for sterol biosynthesis and it is also used for protein prenylation. In the slime mould *Dictyostelium discoideum* some of the mevalonate pathway enzymes possess a peroxisomal targeting signal. This suggested that part of the mevalonate pathway may take place in the peroxisomes.

In this study, the intracellular locations of the mevalonate pathway enzymes were investigated by transforming *D. discoideum* amoebae to express each enzyme as a fusion protein with either GFP (green fluorescent protein) or mRFP (monomeric red fluorescent protein). It was found that three of the mevalonate pathway enzymes are peroxisomal: 3-hydroxy-3-methylglutaryl-coenzyme A synthase isozyme B, phosphomevalonate kinase and farnesyl diphosphate synthase. HMG-CoA reductase is associated with the endoplasmic reticulum and the other four enzymes of the mevalonate pathway were most likely to be in the cytosol: HMG-CoA synthase isozyme A, mevalonate kinase, diphosphomevalonate decarboxylase and IDP-isomerase.

The intracellular location of the first five enzymes involved in sterol biosynthesis from farnesyl diphosphate was also identified by using the GFP or mRFP tagged enzyme approach. Some of these enzymes possess a strong peroxisomal targeting signal type 1 (PTS1). It was shown that the first four enzymes of the pathway: squalene synthase, squalene epoxidase, oxidosqualene cyclase and cycloartenol - C-24-methyltransferase are peroxisomal whereas the two isozymes of the fifth enzyme, methylsterol monooxygenase, are associated with the endoplasmic reticulum.

It was also demonstrated that the first four enzymes on the sterol biosynthesis pathway are strongly associated with the peroxisomal membrane. However, the

putative PTS1 present at the C-terminus of squalene synthase, oxidosqualene cyclase and cycloartenol-C-24-methyltransferase would imply that each of these enzymes should be a peroxisomal matrix protein. We therefore investigated whether the putative PTS1s are involved in directing these three enzymes into the peroxisomes. It was found that squalene synthase was largely peroxisomal even when its PTS1 was absent but the PTS1 in oxidosqualene synthase and cycloartenol-C-24-methyltransferase was essential for entry of these enzymes into peroxisomes.

It appears that the sterol biosynthesis in *D. discoideum* is unusual since the enzymes squalene synthase, squalene epoxidase, oxidosqualene cyclase and cycloartenol -C-24-methyltransferase are accumulated in the peroxisomes whereas in all other organisms studied they are in the endoplasmic reticulum.

ACKNOWLEDGEMENTS

Praise to Allah the Almighty, Creator and Sustainers of the Universe.

Firstly, I would like to express my sincere gratitude and appreciation to my supervisors Dr Donald Wattas and Dr Ewald Hettema for their excellent supervision, constructive guidance, invaluable feedback, and encouragement during my PhD journey.

Secondly, special thanks for my sponsor King Faisal University and Ministry for Higher Education in Saudi Arabia, for their financial and academic support, represented by the cultural attaché in London during my PhD study.

I am grateful for Dr Patrick Baker for the three dimensional structure pictures.

I offer my regards and blessings to the rest of the members of the Hettema lab, Alison, Jimmy, Gemma, Joanne, Nadal, Peter, Mohammed, John and Murtakab.

My greatest indebtedness to my husband Mohammed Alsaif for his encouragement, inspiration, patience and support. The thanks extended to my little boy Othman for his patience during my busy days.

I owe a special thanks to my Mum and Dad for their emotional, continues prayers and love.

I am grateful also to my father in law for his daily phone support and encouragement.

Big thanks to my sisters especially Abeer for the video calls and encouragement, brothers and friends for their moral support and endless encouragement.

TABLE OF CONTENTS

ABBREVIATIONS

A15	Actin 15 promoter
aa	Amino acids
ADP	Adenosine diphosphate
APS	Ammonium persulphate
ATP	Adenosine triphosphate
A.thaliana	*Arabidopsis thaliana*
BF	Bright field
CHO	Chinese hamster ovary
C. roseus	*Catharanthus roseus*
C-terminal	Carboxyl-terminal
DNA	Deoxyribonucleic acid
dATP	Deoxyadenosine triphosphate
dCTP	Deoxycytidine triphosphate
dGTP	Deoxyguanosine triphosphate
dH_2O	Deionised water
DMPD	Diphosphomevalonate Decarboxyase
dNTPs	Equimolar mixture of dATP, dTTP, dCTP, dGTP
DTT	Dithiothreitol
dTTP	Deoxythymidine triphosphate
Dd	*Dictyostelium discoidium*
D. fasciculatum	*Dictyosteleum fasciculatum*
E.coli	*Escherichia coli*
ECL	Enhanced chemiluminescence

EDTA	ethylenediaminetetraacetic acid
ER	Endoplasmic reticulum
FDPS	Farnesyl diphosphate synthase
GFP	Green fluorescent protein
HMGS	3-Hydroxy-3-methylglutaryl-Coenzyme A Synthase
HMGR	Hydroxy-3-methylglutaryl-Coenzyme A Reductase
hr	Hour(s)
HRP	Horseradish peroxidase
Hs	*Homo sapiens*
IDP-isomerase isomerase	Isopentenyl Diphosphate: Dimethylallyl Diphosphate (IDP)
IgG	Immunoglobulin G
IRD	Infantile Refsum disease
Mm	*Mus musculus*
mPTS	Peroxisomal membrane protein targeting signal
mRFP	monomeric Red fluorescent protein
MSM	Methylsterol monooxygenase
MVK	Mevalonate kinase
NALD	Neonatal adrenoleukodystrophy
N-terminal	Amino-terminal
nt	Nucleotides
OD	Optical density
ORF	Open reading frame
OSC	Oxidosqualene Cyclase
PEG	Polyethylene glycol
PBD	Peroxisome biogenesis disorder
PCR	Polymerase chain reaction

PED	Single peroxisomal enzyme deficiency
PMK	Phosphomevalonate kinase
PMP	Peroxisomal membrane protein
P.pallidum	*Polysphondylium pallidum*
PTS	Peroxisome targeting signal
RCDP	Rhizomelic chondrodysplasia punctata
Rn	*Rattus norvegicus*
S.cerevisiae	*Saccharomyces cerevisiae*
SDS	Sodium dodecyl sulphate
SDS-PAGE	Sodium dodecyl sulphate-polyacrylamide gel electrophoresis
S.epoxidase	Squalene epoxidase
SMT	Cycloartenol -C-24-methyltransferase
SQS	Squalene synthase
SSRs	Simple sequence repeats
TEMED	N, N, N-Tetramethylethylenediamine
WB	Woronin body
WT	Wild type
ZS	Zellweger syndrome

AMINO ACIDS

Ala	A	Alanine
Cys	C	Cysteine
Asp	D	Aspartic acid
Glu	E	Glutamic acid
Phe	F	Phenylalanine
Gly	G	Glycine
His	H	Histidine
Ile	I	Isoleucine
Lys	K	Lysine
Leu	L	Leucine
Met	M	Methionine
Asn	N	Asparagine
Pro	P	Proline
Gln	Q	Glutamine
Arg	R	Arginine
Ser	S	Serine
Thr	T	Threonine
Val	V	Valine
Trp	W	Tryptophan
Tyr	Y	Tyrosine
X		Unknown

UNIPROT GENES NUMBERS

Gene name	Uniprot number
HMGSA	P54872
HMGSB	Q86HL5
HMGR1	P34135
HMGR2	P34136
MVK	Q86AG7
PMK	Q54CW0
DMPD	Q54YQ9
IDP-isomerase	Q9NH02
SQS	Q54DR1
S.epoxidase	Q54BK7
SMT	Q553T0
OSC	Q55D85
MSMA	Q55D52
MSMB	Q55D54

LIST OF TABLES

LIST OF FIGURES

Chapter1

Introduction

Peroxisomes were discovered over 50 years ago by a Swedish PhD student Rhodin (1954). They were characterized as enclosed organelles surrounded by a single membrane. Later on, further biochemical studies were carried out by the group of De Duve (1966) in order to investigate the peroxisomal enzymes that may be involved in cellular metabolisme. Recently around 50 peroxisomal enzymes have been identified which are involved mainly in producing hydrogen peroxide and the degradation of fatty acids by β-oxidation.

Peroxisomes have attracted the interest of scientists because it was realised there is a connection between peroxisomal function deficiency and several human diseases. For example, the entire absence of peroxisomes leads to a severe disease such as Zellweger-syndrome (ZS) in which the child dies in his first year. A defect in multiple peroxisomal functions can also lead to less severe diseases such as neonatal adrenoleukodystrophy (NALD) and Infantile Refsum's disease (IRD) in which the patients may survive into adulthood (Steinberg et al., 2006, Wanders and Waterham, 2006). Attempts to understand these genetic diseases were started in humans but these genes are conserved also in the yeast *Saccharomyces cerevisiae* and other yeast species. Therefore, it has been convenient to use yeast as a model system due to the ability of yeast to grow in different conditions, and even in the absence of peroxisomes. Furthermore, genetic studies in yeast are easier to perform than in human cells.

Despite many investigations, some suggested roles for the peroxisome remain controversial. In particular, it has been unclear whether the enzymes of the mevalonate pathway of isoprenoid metabolisme are peroxisomal. However, it has been established recently in the slime mould *Dictyostelium discoideum* that the final enzyme, farnesyl diphosphate synthase, of the mevalonate pathway is

peroxisomal (Nuttall et al., 2012). This led to the idea of using *Dictyostelium discoideum* to investigate whether any of the other enzymes on the pathway are peroxisomal.

It was also noticed that the enzyme squalene synthase that converts two molecules of farnesyl diphosphate, the first committed enzyme of sterol biosynthesis, appeared to have a peroxisomal targeting signal. Investigations were therefore also carried out to determine whether peroxisomes are involved in sterol biosynthesis in *D. discoideum*.

This thesis describes the results of these investigations of the mevalonate pathway and sterol biosynthesis.

1.1 Peroxisomes

Peroxisomes (microbodies, glyoxysomes, glycosomes and Woronin-bodies), are single membrane organelles present in almost all eukaryotic cells. They appear as spherical structures ranging from 0.1 to 1μm in diameter. Based on the organism and cell type peroxisomes can carry out a wide variety of biochemical reactions (Lazarow and Fujiki, 1985).

Rhodin (1954) was one of the first researchers who described peroxisomes, initially termed microbodies. Based on electron micrographs of mouse kidney cells, peroxisomes were described as organelles enclosed in a single membrane. In the mid sixties de Duve and Baudhuin began to study peroxisome biochemistry. They managed to separate the peroxisomes from other cells organelles by density gradient centrifugation and found that the newly identified organelle contains several enzyme such as D-amino acid oxidase, urate oxidase and catalase. The peroxisome is so-called because of the role of catalase in the breakdown of hydrogen peroxide (Baudhuin et al., 1965, De Duve and Baudhuin, 1966).

About 50 enzymes have since been found within peroxisomes which play an important role in a variety of biochemical pathways. Mainly they are involved in reactions producing hydrogen peroxide of which degradation of long-chain fatty acids is particularly important. In mammalian cells, two β-oxidation pathways occur in the peroxiomes in addition to the fatty acids α-oxidation which responsible of the degradation of a special group of lipids comprising very long straight chain fatty acids (VLCFA), long chain dicarboxylic acids, branched-chain fatty acids. These lipids cannot be oxidized by the mitochondrial β-oxidation pathway (Brown and Baker, 2003). By contrast, in fungi and plants, the fatty acid β-oxidation pathway is restricted to the peroxisomes (Poirier et al., 2006). Furthermore, in mammals peroxisomal enzymes can be involved in various activities such as the synthesis of ether lipids (plasmalogens), cholesterol and bile acids and in breakdown of reactive oxygen species (Brown and Baker, 2008, Rucktaschel et al., 2011).

In plants, different types of peroxisomes have been identified. One such type termed glyoxysomes exists in germinating seeds. Glyoxysomes are involved in the glyoxylate cycle by which fatty acids stored in the seeds are converted into sugars. Other types of peroxisomes were found in plant leaves supporting the mitochondrial photorespiration (Brown and Baker, 2003). In addition, plant peroxisomes are involved in many biochemical processes such as producing hormones such as jasmonates (phytohormones), indole-3 acetic acid, reactive oxygen species and the catabolism of some branched chain amino acids, purines and polyamines (Platta and Erdmann, 2007a, Brown and Baker, 2008).

Specific types of peroxisomes, considered initially to be different organelles, have been investigated. In this context, Woronin-bodies of filamentous fungi were identified as a special form of peroxisome (Baker and Sparkes, 2005). They have role in repairing the septal pores of damaged hyphae in order to avoid cytosolic bleeding (Platta and Erdmann, 2007b). Furthermore, glycosomes present in parasitic protozoa *Trypanosoma*, contain the key enzymes of glycolysis and are considered to be a type of peroxisome.

1.2 Peroxisomal diseases

Peroxisomes have attracted considerable attention owing to the association of peroxisomal deficiency or malfunction with several genetic disorders. Peroxisomal disorders can be classified into two categories (I) Peroxisomal biogenesis disorders (PBDs) and (II) Single peroxisomal enzyme deficiencies (PEDs). PBDs give the most severe clinical symptoms and are caused by a deficiency in more than one peroxisomal function (Fujiki, 2000). The other group of PEDs is linked to a defect in a single peroxisomal function (Steinberg et al., 2006, Wanders and Waterham, 2006).

The PBDs consist of cerebro-hepato-renal sydrome, usually known as Zellweger-syndrome (ZS), neonatal adrenoleukodystrophy (NALD), infantile Refsum's disease (IRD) and rhizomelic chondrodysplasia punctata (RCDP). The first three syndromes (ZS, NALD and IRD) are sub-grouped as Zellweger spectrum syndrome (ZSDs) because mutation within the same gene can lead to these disorders. Zellweger-syndrome is characterized by deficiency in the import of peroxisomal matrix proteins and by the decreased number of peroxisomes. ZS is considered to be the most severe form of PBD and is associated with a wide range of abnormalities such as craniofacial and eye abnormalities, severe hypotonia and neuronal migration defects causing brain dysfunction (Steinberg et al., 2006). NALD and IRD are classified as less severe PBD syndromes. Therefore, patients affected by moderate NALD and IRD may survive to adulthood. These disorders are characterized by craniofacial abnormalities similar to the ZS facial features though less severe, liver diseases, seizures, physical weakness and learning disabilities (Wanders and Waterham, 2006).

The second group PEDs is caused by a deficiency of one peroxisomal function such as β-oxidation or α-oxidation of fatty acid, ether phospholipid biosynthesis and glyoxylate detoxification (Wanders and Waterham, 2006).

1.3 Peroxisome Biogenesis (Peroxins/*PEX* genes)

The essential genes for peroxisome biogenesis were identified in the late 1980s based on observation in *Saccharomyces cerevisiae*. These indicated that growth on oleic acid can increase the number of peroxisomes in yeast cells (Veenhuis et al., 1987). Furthermore, it has been shown by Erdmann and his colleagues that functional peroxiomes are essential for *S.cerevisiae* to grow on oleic acid as a sole carbon source (Erdmann et al., 1989). Later on, this approach was adopted as a fundamental basis for genetic screening in order to detect mutants deficient in peroxisome biogenesis i.e. strains deficient in peroxisome biogenesis grow in media containing glucose but not in media in which oleate is the sole carbon source.

In mammals, further genetic screens have been carried out utilizing Chinese Hamster Ovary (CHO) cells, in which peroxisomes are essential for plasmalogen synthesis. This study provided a crucial tool for the identification of a further mutation that affected peroxisomal assembly (Tsukamoto et al., 1990). A number of important genes for peroxisome biogenesis have also been identified by a complementation assay in *S. cerevisiae* and CHO peroxisome-deficient mutants (Erdmann et al., 1989, Tsukamoto et al., 1990). Investigations using a similar genetic approach were also performed in various yeast species such as *Hansenula polymorpha*, *Pichia pastoris* and *Yarrowia lipolytica* (Gould et al., 1992, Liu et al., 1992).

Proteins essential for peroxisome function are called peroxins and are encoded by the PEX genes. Distel et al (1996) have given a summary of the PEX genes that have been identified in various organisms. This term referred to their function in peroxisome biogenesis and the import of peroxisomal matrix and membrane protein (Distel et al., 1996).

Recently, a novel approach in biological sciences has been developed supporting the identification of a new peroxins. This approach consists of proteomic assays and DNA microarray screens for oleic-acid-induced yeast genes. Nowadays, up to 32 PEX genes have been demonstrated (Table 1.1) (Smith et al., 2002, Tam et al., 2003, Vizeacoumar et al., 2003, Vizeacoumar et al., 2004).

Table 1.1: Peroxins

Peroxin	General and Molecular Function
Pex1∗	Matrix protein import (AAA-ATPase required for the recycling of Pex5)
Pex2∗	Matrix protein import (Ring-finger protein)
Pex3∗	*de novo* synthesis+ Membrane docking factor for Pex19p
Pex4∗	Matrix protein import (E2-enzyme required for mono-ubiquitination and recycling of Pex5)
Pex5∗	Matrix protein import (PTS1-Receptors)
Pex6∗	Matrix protein import (AAA-ATPase required for the recycling of Pex5)
Pex7∗	Matrix protein import (PTS receptor)
Pex8∗	Matrix protein import (Connect between the docking and the RING)
Pex10∗	Matrix protein import (RING-finger protein, links Pex4 to the importomer)
Pex11∗	Involved in proliferation
Pex12∗	Matrix protein import (Required for Pex5 recycling)
Pex13∗	Matrix protein import (Involved in receptor docking)
Pex14∗	Matrix protein import (Involved in receptor docking)
Pex15∗	Membrane anchor for Pex6
Pex16	Peroxisome biogenesis
Pex17∗	Matrix protein import + Peroxisome biogenesis
Pex18∗	Matrix protein import (Import of PTS2)
Pex19∗	*de novo* synthesis + Import of PMPs
Pex20	Matrix protein import (PTS2 co-receptor in fungi)
Pex21∗	Matrix protein import (PTS2 co-receptor in yeast)
Pex22∗	Matrix protein import (Membrane anchor for Pex4)
Pex23	Matrix protein import in *Yarrowia lipolytica*
Pex24	Required for peroxisome assembly in *Yarrowia lipolytica*
Pex25∗	Regulate size and maintenance
Pex26	Matrix protein import (Membrane anchor for Pex6 in human cells)
Pex27∗	Regulate size and number
Pex28∗	Regulate size and number
Pex29∗	Regulate size and number
Pex30∗	Regulate size and number
Pex31∗	Regulate size and number
Pex32∗	Regulate size and number
Pex36∗	Regulate size and number

∗ Proteins present in *S.cerevisiae*

1.4 Peroxisomal matrix protein import pathway

It is well known that the peroxisome does not contain any DNA and therefore peroxisomal matrix proteins are encoded by the nuclear genome and, after synthesis in the cytosol by free polyribosomes, are imported post-translationally into peroxisomes (Rucktaschel et al., 2011, Fujiki, 2000).

The pathway for importing the matrix proteins into the peroxisome consists of four distinct steps (Figure 1.1): targeting signal and cargo interaction; receipt of the cargo by the docking complex in the peroxisomal membrane; translocation into the peroxisome and release of the cargo. Finally, recycling of the receptor occurs (Brown and Baker, 2008).

The sorting of the peroxisomal matrix proteins from the cytosol into the peroxisomal matrix requires a peroxisomal targeting signal (PTS). There are two types of PTS: Peroxisomal targeting signal type 1 (PTS1) is the major signal that is used by the peroxisomal matrix proteins. This signal is located at the extreme carboxy- terminus and comprises a (S/A/C) (K/R/H) (L/M) tripeptide consensus sequence (Gould et al., 1989). The -SKL tripeptide sequence has been described as the strongest PTS1 in various organisms (Petriv et al., 2002).

By contrast, a few matrix proteins are targeted by the peroxisomal targeting signal type 2 (PTS2), which comprises the (R/K)-(L/V/I)-X_5-(Q/H)-(L/A) (where X can be any amino acid) consensus sequence placed near to the N-terminus (Rachubinski and Subramani, 1995). More recent analysis of functional PTS2 sequences has suggested that the consensus sequence should be redefined as – R(L/V/I/Q)XX(L/V/I/H)(L/S/G/A)X(H/Q)(L/A) which represents the most common variant of the PTS2, whereas (R/K) (L/V/I/Q)XX(L/V/I/H/Q) (L/S/G/A/K)X(H/Q) (L/A/F) sequences characterize essentially all variants of PTS2 (Petriv et al., 2004). The import of peroxisomal matrix proteins based on using either the PTS1 or PTS2 pathway differs among organisms. For example, in plants the number of matrix proteins using the PTS2 pathway is greater than in mammals and yeast (Reumann et al., 2009). However, the nematode *Caenorhabditis elegans* uses only the PTS1 pathway (Motley et al., 2000).

In the cytosol the newly synthesised proteins with a PTS1 or a PTS2 need a receptors to transfer them into the peroxisomal matrix. There are two soluble cytosolic receptors termed Pex5 and Pex7 that recognise PTS1- and PTS2-containing proteins respectively (Fujiki, 2000, Rachubinski and Subramani, 1995). Pex5 has a C-terminal domain (six tetratricopeptide repeats TPRs) providing the proper direct PTS1- binding site (Stanley et al., 2006). By contrast, Pex7 needs to be associated with other cytosolic co-receptors to allow import of the PTS2-containg proteins into the peroxisome. These co-receptors vary between different organisms. In *S.cerevisiae* they are Pex18 and Pex21, in fungi, Pex20. The co-receptor in mammals is the long version of Pex5 (Pex5pL) (Purdue et al., 1998, Titorenko et al., 1998, Otera et al., 2000).

Once the PTS-receptors have bound to their targets in the cytosol they interact with different complexes of peroxisomal membrane proteins, comprising the docking-complex and the RING (finger)-complex. The docking-complex includes three proteins Pex13, Pex14 and, in *S. cervisiae,* Pex17.

Pex13 is described as a peroxisomal integral membrane protein having a C-terminus Src-homology-3 (SH3) domain which interacts with pex5 in the cytosol (Erdmann and Blobel, 1996, Rayapuram and Subramani, 2006). The N-terminal domain of Pex13 also faces the cytosol and interacts with Pex7 and Pex14 (Stein et al., 2002). Pex14 can also bind Pex5, Pex7 and Pex17. In cells of higher eukaryotes, Pex17 is absent. However, it has been suggested that Pex17 cooperates in the docking process due to its interaction with Pex14. Thus, the role of Pex17 remains to be elucidated (Kiel et al., 2006, Rucktaschel et al., 2011). The docking complex interacts with the RING-complex, comprising Pex2, Pex10 and Pex12, by the intra peroxisomal protein Pex8 in order to form a multi-proteins- complex termed the importomer (Agne et al., 2003).

Following the docking process, the peroxisomal matrix protein must have to cross the peroxisomal membrane. However, the machinery by which the proteins translocate into the peroxisomal matrix is not fully understood. Interestingly, although Pex5 is known as a soluble cytosolic protein, it can behave also as integral membrane protein upon interaction with the peroxisomal membrane (Gouveia et al., 2000). In this context, three hypotheses have been suggested to

describe the protein translocation machinery. First, the shuttle hypothesis proposes that the PTS-receptor is associated with the peroxisomal membrane surface and delivers its cargo without entering into the peroxisomal matrix (Dammai and Subramani, 2001, Nair et al., 2004). Secondly, the extended shuttle hypothesis suggests that the whole PTS-receptor complex reaches the peroxisomal matrix and then releases the cargo (Kunau, 2001, Smith and Schnell, 2001). The third hypothesis claims that the PTS-receptors join together with the co-receptors to form an import pore in order to open the membrane upon loading the cargo (transient pore hypothesis) (Erdmann and Schliebs, 2005).

The mechanism by which the PTS-receptor releases its cargo into the peroxisomal matrix is still not clear. However, it has been suggested that Pex8 has a role in this event (Rehling et al., 2000). Following release of the cargo Pex5, Pex7 and Pex20 need to be recycled back to the cytosol to interact again with a new target (Dammai and Subramani, 2001, Nair et al., 2004, Rucktaschel et al., 2011). Unlike the import machinery which has been proposed to be ATP-independent, both export and the ubiquitination machineries require a source of energy. In this context, Pex1 and Pex6 which are members of the AAA-ATPases family and can hydrolyse the ATP providing energy to pull the receptor out of the membrane (Miyata and Fujiki, 2005, Platta et al., 2005). These two AAA-peroxins are associated partially with the peroxisomal membrane via an interaction with the integral peroxisomal membrane Pex15 in yeast or Pex26 in mammals (Birschmann et al., 2003, Matsumoto et al., 2003).

Generally, ubiquitination refers to the labelling of a selected protein with the 76 amino acid ubiquitin in order for it to be degraded. It has been demonstrated that Pex5 is mono- and polyubiqitinated. The mono-ubiquitination of Pex5 is facilitated by E2-enzyme Pex4 (Platta et al., 2007). In addition, it was found that Pex12 from the RING-complex is involved in the Pex5 mono-ubiquitination (Platta et al., 2009). In *pexΔ* mutants, (e.g. *pex1Δ*, *pex4Δ*, *pex6Δ* or *pex15Δ*), Pex5 is polyubiquitinated by two members of the RING- complex (Pex2 and Pex10) for proteasomal degradation (Williams et al., 2008, Platta et al., 2009).

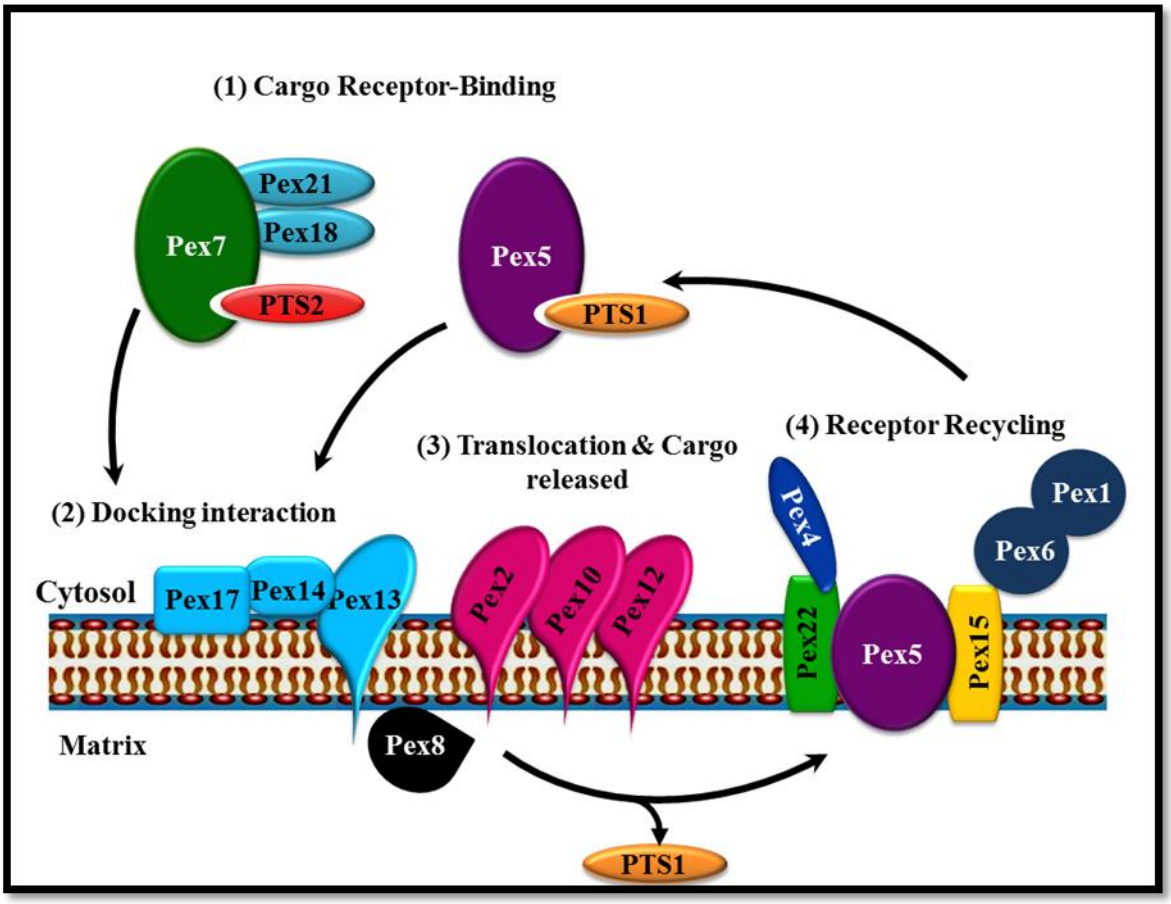

Figure 1.1: Model for peroxisomsal matrix protein import in *S.cerevisiae*.

The peroxisomal matrix protein import pathway can be divided into four steps: (1) Cargo recognition in the cytosol (2) Cargo- receptor docking (3) Translocation and disassembly of the receptor-cargo (4) Return of the receptor to the cytosol. Peroxisomal matrix proteins with either a PTS1 or a PTS2 are recognized by the soluble receptor Pex5 or Pex7 respectively. Pex7 also requires co-receptors Pex18 and Pex21 in *S.cerevisiae.* The receptor-cargo then associates with the peroxisomal membrane via the docking complex (Pex13, Pex14 and Pex17). The PTS receptor cargo is translocated across the peroxisomal membrane via a not well understood mechanism. Following cargo release the PTS-receptors are recycled back to the cytosol. This process requires the AAA-ATPase activities (Pex1 and Pex6), along with Pex4 and its membrane anchor Pex22. Some organisms have specific adaptations to this model (adapted from Rucktäschel et al, 2011).

1.6 Peroxisomal membrane proteins

Peroxisomal membrane proteins (PMPs) are similar to the matrix proteins that both are encoded in the nuclear genome and synthesized via free cytosolic polyribosomes (Lazarow and Fujiki, 1985). However, the first indications that the import machinery for peroxisomal membrane proteins and for peroxisomal matrix proteins are entirely different came in the late 1980s when immunofluorescence microscopy studies of cells from Zellweger patients indicated that the peroxisomal matrix proteins are absent from the peroxisomal structures which are referred to as "ghosts" (Santos et al., 1988). Thus, two different mechanisms for sorting the peroxisomal membrane and matrix proteins have been considered.

Out of the 32 known peroxins, Pex3, Pex19 and Pex16 can be classified as crucial peroxins for peroxisomal membrane biogenesis. In *S. cerevisiae,* Pex3 and Pex19 have been identified as fundamental components for peroxisome formation (Gotte et al., 1998, Hettema et al., 2000). Furthermore, it has been shown that among 16 different (*pex*) mutants in *S. cerevisiae*, there were only two mutants, *pex3* and *pex19,* that resulted in a complete absence of peroxisomal membrane structures and mislocalisation of the PMPs into the cytosol where they break down rapidly (Hettema et al., 2000). In mammals, Pex16 is considered as an essential peroxin for peroxisomal membrane assembly (Honsho et al., 1998). Although Pex16 has been suggested to play an important role in peroxisomal biogenesis, this role seems to be species-specific because in some organisms lacking a functional copy of Pex16 such as *Yarrowia lipolytica* peroxisomal structure was observed (Eitzen et al., 1997).

1.7 Targeting of peroxisomal membrane proteins

Peroxisomal membrane proteins can be targeted to the peroxisomes via two separate pathways. Proteins in the first category are synthesised in the cytosol and imported subsequently into the peroxisomal membrane post-translationally. These insertions of the PMPs depend on a peroxisomal membrane protein targeting sequences (mPTS). The other group of the PMPs is targeted to the peroxisome via an uncharacterized area of the ER (Platta and Erdmann, 2007a).

The PMPs require a peroxisomal targeting sequence (mPTS) for correct targeting to the peroxisome. This mPTS has been identified recently in several PMPs and comprises combinations of hydrophobic and basic amino acid residues which provide a binding platform for Pex19. Furthermore, in the case of peripheral membrane proteins these residues are followed by a protein binding site but, in the case of integral membrane proteins, by a single transmembrane domain (Rottensteiner et al., 2004, Girzalsky et al., 2006).

In addition, the PMPs also require the peroxins Pex19, Pex3 and, in some organisms, Pex16 for their sorting pathway. Pex19 is a hydrophilic and acidic protein that is present predominantly in the cytosol but interacts partially with the peroxisomal membrane (Gotte et al., 1998, Sacksteder et al., 2000). Pex19 has been characterized as a multi-functional protein due to its ability to bind most peroxisomal membrane proteins and import newly synthesized PMPs into the peroxisome (Snyder et al., 2000, Sacksteder et al., 2000). Therefore, Pex19 can act as a chaperon and a cytosolic receptor for the PMPs (Jones et al., 2004). Pex3 has been identified as an integral peroxisomal membrane protein and it has been shown to act as a docking factor for Pex19-PMP complexes (Matsuzono et al., 2006). Pex16 also has a role in the PMPs' sorting pathway by acting as a receptor for Pex3-Pex19 complexes and it thus facilitates the targeting of the PMPs into the mature peroxisomes (Schliebs and Kunau, 2004, Matsuzaki and Fujiki, 2008).
Only a few PMPs are imported into peroxisomes without assistance from Pex19, Pex3 and Pex16. These are directed to the ER before being imported into the peroxisome. Pex3 and Pex16 are the well known peroxins that are believed to follow an ER to peroxisome sorting pathway. However, the mechanism by which

these PMPs are inserted into the ER remains be identified.

1.8 The mevalonate pathway of isoprenoid

The mevalonate pathway (MVA) of isoprenoid biosynthesis has been studied extensively for a long time (Goldstein and Brown, 1990). This pathway exists in all mammals, higher plants, archaebacteria, algae (except chlorophytes) and in some protozoa (Trypanosome and Leishmania). Spurgeon and Proter (1981) have pointed out that Conrad Bloch (1958) and Feodor Lynen (1958) first described the mevalonate pathway in animals and yeast cells. In eukaryotic cells, the seven enzymes of the MVA pathway play a vital role in providing precursors that are essential for numerous cellular processes. For example, farnesyl diphosphate (FDP) mainly serves as a precursor for sterol biosynthesis but it is also used for protein prenylation (covalent attachment of a hydrophobic farnesyl or geranylgeranyl group to the C-terminus of some proteins) (Goldstein and Brown, 1990). In addition, isopentenyl diphosphate is a precursor of the side-chain of ubiquinone (an electron carrier which is essential for the mitochondrial respiratory chain). Furthermore, the mevalonate pathway also supplies precursors for the side-chain of haem A; the synthesis of dolichol (an isoprenoid lipid which is involved in glycoprotein synthesis) and for tRNA prenylation. In plants, the MVA pathway provides FDP as a precursor for the synthesis of sesquiterpenes and triterpenes (Bouvier et al., 2005, Sapir-Mir et al., 2008).

The five carbon isoprenoids isopentenyl diphosphate (IDP) and its allylic isomer dimethylallyl diphosphate (DMAPP) were, for several decades, considered to be synthesised only by the reactions of the mevalonate pathway (McGarvey and Croteau, 1995). Several decades, the mevalonate pathway was considered to be the only source of the IDP and DMAPP. However, it has been shown that the biosynthesis of IDP and DMAPP occurs via two pathways in higher plants: the non-mevalonate methylerythritl phosphate pathway (MEP) and the mevalonate pathway (MVA) (Lichtenthaler, 1999). The subcelluar location of the MEP pathway enzymes has been found to be entirely within the plastids (Hsieh et al., 2008) whereas the subcellular distribution of the MVA pathway enzymes remains to be elucidated.

The mevalonate pathway is started with two molecules of acetyl CoA which are converted into acetoacetyl CoA by a thiolase (Figure 1.2). The second reaction catalysed by HMG-CoA synthase produces 3-hydroxy-3-methylglutaryl-CoA (HMG-CoA) from the condensation of acetyl-CoA with acetoacetyl-CoA. HMG-CoA reductase, the rate-limiting enzyme of the mevalonate pathway, then catalyzes the conversion of HMG-CoA to mevalonate (MVA). Subsequently, the MVA is phosphorylated to form mevalonic acid-5- diphosphomevalonate by mevalonate and phosphomevalonate kinases. Next, the diphosphate is decarboxylated by diphosphomevalonate decarboxylase to produce isopentenyl diphosphate (IDP). The IDP is then converted to dimethylallyl diphosphate (DMAPP) by IDP-isomerase. IDP and DMAPP serve as substrates for farnesyl diphosphate synthase (FDP-synthase) to form geranyl diphosphate. The latter is then converted into the final product of the mevalonate pathway, farnesyl diphosphate, by FDP-synthase.

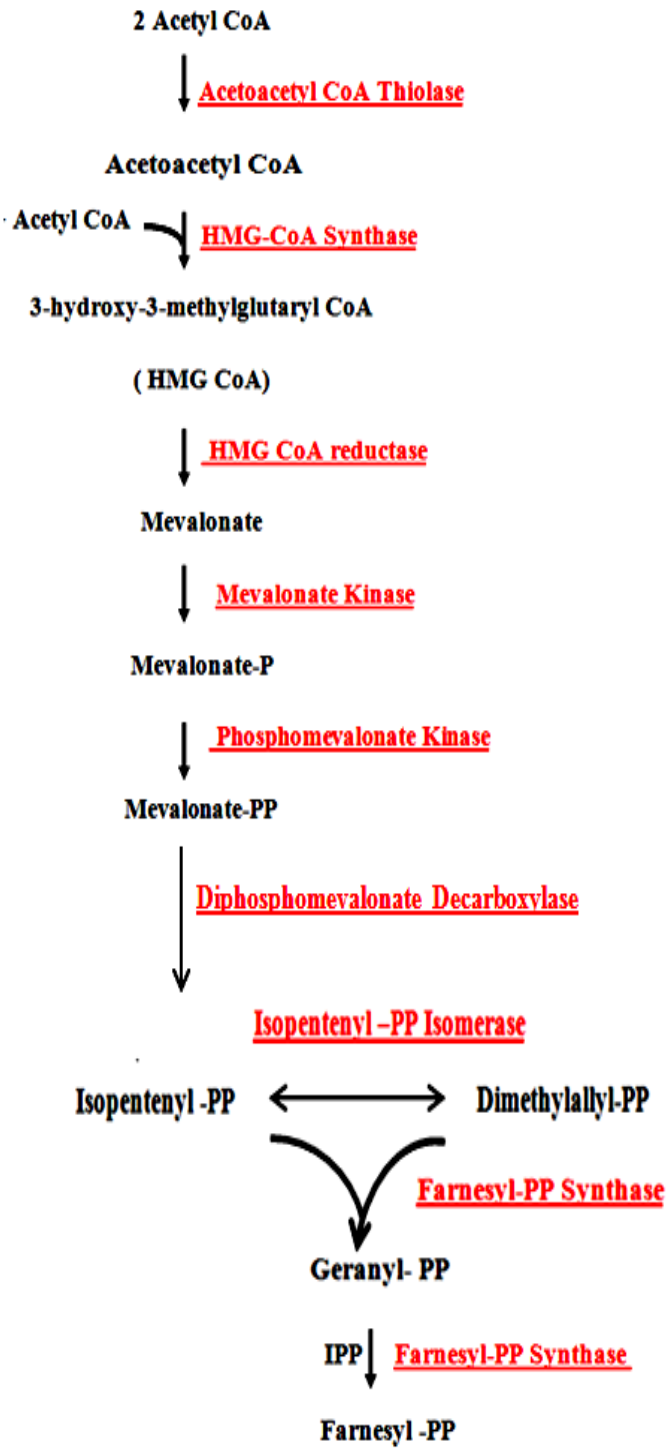

Figure 1.2: The mevalonate pathway of isoprenoid biosynthesis

1.9 The subcellular distribution of the mevalonate pathway enzymes among different organisms

Although the reactions on the mevalonate pathway are well known, the subcellular distribution of the pathway enzymes is still a matter of debate. In mammals, the subcellular location of the MVA pathway enzymes was, for a long time, considered to be in the cytosol. However, this view changed in 1994 as a result of an electron microscopy study to determine the subcelluar location of two enzymes of the mevlaonate pathway, mevalonate kinase and farnesyl diphosphate synthase , which were both found to be peroxisomal (Biardi et al., 1994, Krisans et al., 1994).

Furthermore, the observation that the activity of the MVA pathway enzymes decreased in tissue from Zellweger's syndrome patients, a peroxisomal-deficiency disease, also suggested that the mevalonate pathway might operate in the peroxisomes (Krisans et al., 1994). Later on, a peroxisomal location was reported for most of the other pathway enzymes. For example, acetoacetyl-CoA thiolase was identified as a peroxisomal enzyme in mammals (Olivier et al., 2000). In addaition, immunofluorrescence studies demonstrated that overexpressing hamster IDP-isomerase tagged with a hemagglutinin epitope was directed to the peroxisomes (Paton et al., 1997). A GFP fusion protein of human phosphomevalonate kinase was also reported as a peroxisomal enzyme (Kovacs et al., 2007). Nevertheless, HMG-CoA reductase was an exception and found to be associated with the endoplasmic reticulum (Goldfarb, 1972, Liscum et al., 1985).

By contrast, contradictory results have been reported that cast doubt on the peroxisomal location for mevalonate kinase; phosphomevalonate kinase and diphosphomevalonate decarboxylase in mammals (Gupta et al., 1999, Wanders and Waterham, 2006, Hogenboom et al., 2004b, Hogenboom et al., 2004c, Hogenboom et al., 2004a, Michihara et al., 2001). Thus, the subcellular location of the MVA pathway enzymes remains unclear.

In plants, investigation the subcellular location of the mevalonate pathway enzymes has had less attention. However, it has been shown that some of the MVA pathway enzymes are localized to the peroxisomes (Table 1.2).

A bioinformatics approach has identified acetoacetyl-CoA thiolase as a peroxisomal enzyme (Reumann et al., 2007). In addition, HMG-CoA reductase has a dual localization and is in the endoplasmic reticulum and within uncharacterized spherical structures (Leivar et al., 2005). Phosphomevalonate kinase and diphosphomevalonate decarboxylase also were found in the peroxisomes (Simkin et al., 2011). Nevertheless, some debate regarding the subcellular distribution of the MVA pathway enzymes in plant persists. For example, the GFP-fusion protein of the short version of *Arabidopsis* IDP-isomerase was considered to be a cytosolic enzyme (Nakamura et al., 2001, Okada et al., 2008). However, Sapir-Mir et al, (2008) found that an internal GFP fusion protein of *Arabidopsis* IDP-isomerase is localized to the peroxisomes.

Overall, the results are so contradictory that some of them must be incorrect. It is difficult to know which we can believe. On some enzymes there is no PTS or, at best, a very weak PTS. Therefore, one could conclude that the subcellular location of the MVA pathway enzymes needs further investigation.

Protein name	PTS1 motif	Organism	Peroxisomal location	Other subcellular location	References
Acetoacetyl CoA Thiolase	QKL	*Hs*	√	Mitochondria	(Kovacs et al., 2007)
	SAL	*At*	√	_	(Reumann et al., 2007)
Phosphomeval-onate Kinase	SRL	*Hs*	√		(Kovacs et al., 2007)
				Cytosol	(Hogenboom et al., 2004c)
Isopentenyl –PP Isomerase	YRM	*Hs*	√		(Clizbe et al., 2007)
	HRV	*Hs*	√		
	HRM	*Rn*	√		(Kovacs et al., 2007)
	HKL	*At*	√		(Sapir-Mir et al., 2008)
				Cytosol	(Nakamura et al., 2001)
				Cytosol	(Okada et al., 2008)
				Cytosol	(Phillips et al., 2008)
Consensus PTS1			(S/ C / A) (K/R/H) (L/M)		
		PTS2 motif			
HMG-CoA Synthase	SVKSNLMQL	*Rn*	√		(Olivier et al., 2000)
				Cytosol	(Ayte et al., 1990)
Mevalonate Kinase	KVILHGEHA	*Hs*	√		(Kovacs et al., 2007)
				Cytosol	(Hogenboom et al., 2004b)
	KVIILAGEHA	*At*	_	Cytosol	(Simkin et al., 2011)
Diphosphomevalonate Decarboxylase	SVTLHQDQL	*Hs*	√		(Kovacs et al., 2007)
				Cytosol	(Hogenboom et al., 2004a)
	SVTLDPDHL	*At*	√	_	(Simkin et al., 2011)
Farnesyl-PP Synthase	NSDVYAQE	*Hs*	√		(Krisans et al., 1994)
Consensus PTS2			(R/K) (L/V/I) X_5(H/Q) (L/A)		

Table 1.2: Compartmentalization of the mevalonate pathway enzymes from different organsimes. *Homo sapiens* (*Hs*); *Mus musculus* (*Mm*); *Rattus norvegicus* (*Rn*); *Arabidopsis thaliana* (*At*).

1.10 The biosynthesis of sterols

Sterols are fundamental membrane components of all eukaryotic cells because they regulate membrane fluidity and permeability. Sterols can also interact with proteins and lipid within the membrane (Darnet and Rahier, 2004). In addition, sterol biosynthesis can supply the eukaryotic cells with various precursors that are important for many cellular and development processes (Clouse, 2002). For example, cholesterol is the major sterol in animals and serves as a precursor for the formation of many important compounds such as steroid hormones, bile acids and vitamin D (Nes, 2011). In plants, a mixture of sterols exists supplying plant growth and development (e.g. growth hormone brassinosteroids and triterpenoids).

The biosynthesis of plant sterols is similar to the cholesterol biosynthetic pathway in that both have the isoprenoid farnesyl diphosphate as the precursor. The first step unique to biosynthesis of sterols is the formation of squalene from two molecules of farnesyl diphosphate. Squalene is then converted to squalene epoxide which is then folded to give a sterol - lanosterol in mammals and fungi but the lanosterol isomer, cycloartenol in vascular green plants. The chemical structure of lanosterol resembles that of cycloartenol except that the latter possesses an additional cyclopropane ring (Figure 1.3). Furthermore, it has been reported that mutated forms of cycloartenol synthase from *Dictyostelium discoideum* and *Arabidopsis thaliana* will synthesis lansterol instead of cycloartenol (Segura et al., 2003).

By contrast, the subsequent steps of sterol biosynthesis are different in plants from those in mammals and fungi. Cholesterol (mammals) or ergosterol (fungi) synthesis requires the removal of the two C-4 methyl groups from lanosterol and this occurs early in the biosynthetic pathway. In plants, conversion of cycloartenol to phytosterols also requires removal of both C-4 methyl groups but, although the first methyl group is removed early in the pathway, the second group is not removed until many steps later (Figure 1.3). Furthermore, removal of both methyl groups at C-4 is essential for the sterol molecule to be functional in the plasma membrane. In *D.discoideum* the biosynthesis of dictysterol, the major sterol that is produced by growing amoebae, requires conversion of squalene into cycloartenol

(Nes et al., 1990). This implies that the pathway of sterol biosynthesis in *D.discoideum* is the same as that in plants.

In general, the enzymes catalysing sterol biosynthesis from squalene are believed to be located in the endoplasmic reticulum (Nes, 2011). For example, squalene synthase, the first committed enzyme of the sterol biosynthesis, has been identified as an ER enzyme in various organisms (Stamellos et al., 1993, Busquets et al., 2008). However, in *D.discoideum*, sterol biosynthesis enzymes that catalyze the initial steps on the pathway have a putative PTS which implies that part of the sterol biosynthesis pathway may take place in the peroxsiomes. The intracellular locations of the sterol biosynthesis enzymes in *D.discoideum* will be discussed in more detail in Chapter 4.

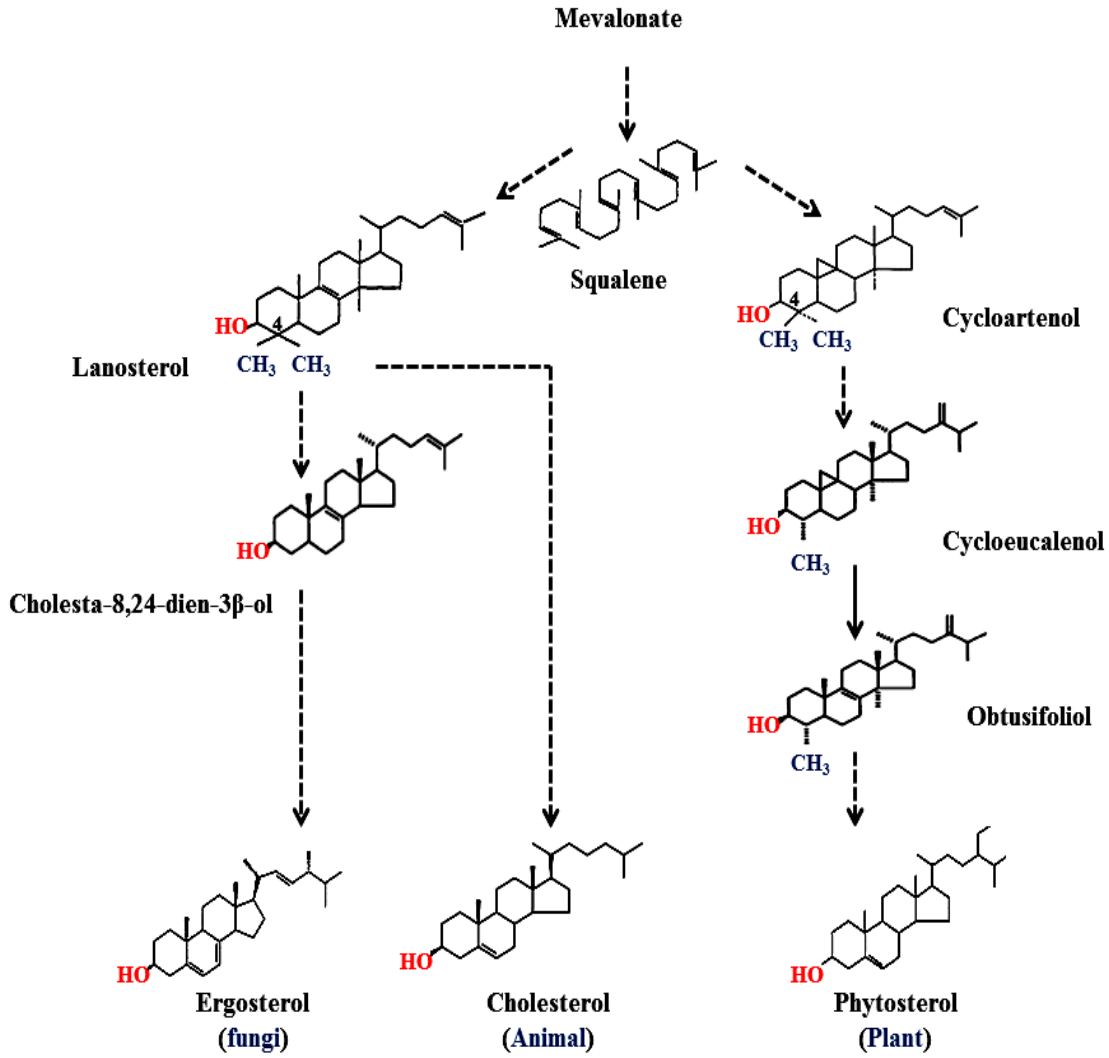

Figure 1.3: The biosynthesis of sterols in animals, fungi and plants. Sterols are derived initially from mevalonate. In plants, squalene is cyclised to form cycloartenol while in animals and fungi lanosterol is produced. Production of the final products of sterol biosynthesis from mevalonate requires more than 30 enzyme-catalysed reactions. Multiple biosynthetic steps are indicated by broken arrows (adapted from Hartmann, 1998).

1.11 *Dictyostelium discoideum* cellular and genetic aspects

In 1935, *Dictyostelium discoideum* was first discovered by Raper in North Carolina deciduous forests. The life cycle of *D. discoideum* consist of two separate phases. In the vegetative (growth) phase, the amoeba exists as motile unicellular amoebae using bacteria as a food source. The second phase, termed development, is entered when the food supply is depleted. In this phase *D. discoideum* can differentiate into a multicellular organism by forming aggregates which develop in several stages to produce a fruiting body consisting of a stalk and spores. Based upon that the term 'social amoeba' was proposed.

D. discoideum amoebae are eukaryotic cells because they contain a nucleus, nucleolus, ER, mitochondria, peroxisomes, microtubules, osmoregulatory vacuoles, microfibrils and other vacuoles that are bounded by a plasma membrane.

The free-living *D. discoideum* amoebae feed naturally on bacterial cells using a process termed phagocytosis. However, several mutations have been generated to enable the amoeba to grow in a semi-defined liquid medium without any source of bacteria (axenic culture) (Watts and Ashworth, 1970). The amoebae can take up nutrients from the liquid medium by macropinocytosis. Growing amoebae axenically facilitates performing biochemical experiments and imaging live cells.

D. discoideum is a haploid genome consisting of 34 Mb and arranged within six chromosomes. Most genes, expressed in both vegetative and the development phase, are present as a single copy in the genome. The genome of *D. discoideum* is rich in adenine and thymine nucleotides (77.57%) and has simple sequence repeats (SSRs) more than any other known sequenced genome (Eichinger et al., 2005).

1.12 Aim of the project

As we discussed before, the compartmentalization of the mevalonate pathway enzymes is still a matter of debate. Furthermore, in *Dictyostelium discoideum* the intracellular locations of the MVA pathway enzymes are unknown. Thus, the aim of this study was to characterize the intracellular locations of both the MVA pathway and the sterol biosynthesis pathway enzymes in *D. discoideum*. I used a fusion protein approach that allowed for monitoring the localisation of the enzymes in vivo. For those proteins that were predicted to be integral to the membrane we tested this by membrane association studies.

Chapter 2

Materials and Methods

2.1 Media, chemicals and enzymes

Components for making HL5 medium for growth of *Dictyostelium discoideum* bacteriological peptone LP 0037, yeast extract LP 0021 were supplied by Oxoid. *Escherichia coli* and yeast growth media components were supplied by Difco Supplies.

All buffers for PCR and DNA polymerases were obtained from Bioline. New England Biolabs supplied restriction enzymes and buffers. Qiagen supplied the Miniprep Kit, the Gel Extraction Kit and the QIAamp DNA Mini Kit.

Unless otherwise stated in the Method section, all other chemicals and buffers were obtained from either BDH, Fisher or Sigma-Aldrich (UK).

2.2 Strains and plasmids

2.2.1 Strains

Table 2.1: *Dictyostelium discoideum, Escherichia coli* and *Saccharomyces cerevisiae* strains.

Strain	Genotype	Use	Source
***Dictyostelium discoideum* strains**			
Dictyostelium discoideum Ax-2 strain		Expression of fusion proteins and source of genomic DNA	Watts and) Ashworth, 1970)
***Escherichia coli* strains**			
Electroporation competent DH5α	*supE44ΔlacU196 ((ϕ80 lacZ (ϕ80M15) hsdR17 recA1 endA1 gyrA96 thi-1 relA1*	Cloning constructs and recovery of plasmid DNA from *Saccharomyces cerevisiae*	(Hanahan, 1983)
Chemically competent DH5*α*	*supE44ΔlacU196 ((ϕ80 lacZ (ϕ80M15) hsdR17 recA1 endA1 gyrA96 thi-1 relA1*	Cloning constructs and expression of plasmid DNA	(Hanahan, 1983)
***Saccharomyces cerevisiae* strains**			
Saccharomyces cerevisiae BY4742	*Mat a; his3Δ1, leu2Δ0, lys2Δ0, ura3Δ0*	Cloning constructs and source of genomic DNA.	EUROSCARF, Johann Wolfgang Goethe-University, Frankfurt, Germany
Saccharomyces cerevisiae *erg6* mutant strain	*BY4741;Mat a;his3Δ1;leu2Δ0 ;met15Δ0;ura3Δ 0;YML008::kan MX4*	Yeast complementation assay	EUROSCARF

2.2.2 Plasmids

Table 2.2: Plasmids used in this study

Description	Promoter	Parental plasmid	Lab reference	Source
HMG-CoA synthase (isozyme A) - GFP	A15P	pMAA-1	pMA01	This study
GFP- HMG-CoA synthase (isozyme B)	A15P	pDXA3C-MA	pMA02	This study
HMG-CoA reductase (isozyme 1) - GFP	A15P	pMAA-1	pMA03	This study
HMG-CoA reductase (isozyme 2)- GFP	A15P	pMAA-1	pMA04	This study
Mevalonate kinase-GFP	A15P	pGFP	pMA05	This study
GFP-Mevalonate kinase	A15P	pDXA3C-MA	pMA06	This study
GFP-phosphomevalonate kinase	A15P	pDXA3C-MA	pMA07	This study
GFP-PTS1 (PKL)	A15P	pDXA3C-MA	pMA08	This study
GFP- phosphomevalonate kinase **(**Δ PKL)	A15P	pDXA3C-MA	pMA09	This study
GFP- phosphomevalonate decarboxylase	A15P	pDXA3C-MA	pMA10	This study
Phosphomevalonate decarboxylase-GFP	A15P	pGFP	pMA11	This study
GFP-IDP isomerase	A15P	pDXA3C-MA	pMA12	This study
IDP isomerase-GFP	A15P	pGFP	pMA13	This study
IDP isomerase internal GFP	A15P	pDXA3C	pMA14	This study
mRFP- PTS1 (HRY)	A15P	p339-3mRFPmars	pmRFP	Nuttall et al.,(2012)
mRFP-squalene synthase	A15P	p339-3MA	pMA15	This study
GFP-squalene synthase	A15P	pDXA3C-MA	pMA16	This study

Squalene epoxidase-GFP	A15P	pGFP	pMA17	This study
mRFP-oxidosqualene cyclase	A15P	p339-3MA	pMA18	This study
GFP- oxidosqualene cyclase	A15P	pMAA-2	pMA19	This study
GFP- cycloartenol-C-24-methyltransferase	A15P	pDXA3C-MA	pMA20	This study
Cycloartenol-C-24-methyltransferase-GFP-SKL	TPI	pEH012	pMA21	This study
Cycloartenol-C-24-methyltransferase **(**Δ PTS1)	TPI1	pEH116	pMA22	This study
HcRed-SKL	His	pEW319	pAS63	Lab stock
Methylsterol monooxygenase (isozyme 1) -GFP	A15P	pGFP	pMA23	This study
Methylsterol monooxygenase (isozyme 2) -GFP	A15P	pGFP	pMA24	This study
GFP-PTS1	A15P	pDXA3C	pGFP	Nuttall et al, (2012)
mRFP-PTS1	A15P	p339-3mRFPmars	pmRFP-PTS1	Nuttall et al, (2012)
*Dd*PDI-mRFP	A15P	P339-MA	pMA25	This study
*Dd*Calnexin-mRFP	A15P	p339-3mRFPmars	pMA26	This study
GFP-*Dd*SQS-ΔPTS1	A15	pDXA3C-MA	pMA27	This study
GFP-*Dd*OSC-ΔPTS1	A15	pMAA-2	pMA28	This study
GFP-*Dd*SMT-ΔPTS1	A15	pDXA3C-MA	pMA29	This study
*Dd*Top2-isomerase-mRFP	A15	P339-MA	pMA30	This study

2.2.3 Plasmid design

2.2.4 *Dictyostelium discoideum* plasmids

All *Dictyostelium discoideum* plasmids were based on the parental plasmids pDXA3C (Manstein et al., 1995) and p339-3mRFPmars (Fischer et al., 2004). pDXA3C-MA was generated by amplifying the open reading frame (ORF) for GFP by PCR (section 2.8.5) using pGFP as a template and VIP 1265 + VIP 1266 as primers (Table 2.3). After digestion with HindIII and BamHI the fragment encoding GFP was ligated into pDXA3C that had also been digested with HindIII and BamHI as indicated below:

Oligonucleotides VIP1890 and VIP 1891 (Table 2.3) were annealed and ligated into BamHI-XbaI digested pDXA3C-MA to generate pMAA-2. The oligonucleotides encode an Ala-Gly-Ala-Gly linker sequence plus the restriction sites (Rs) for BamHI, XhoI, KpnI, NsiI, EcoRI, SacI, XbaI. This destroyed the original BamHI site.

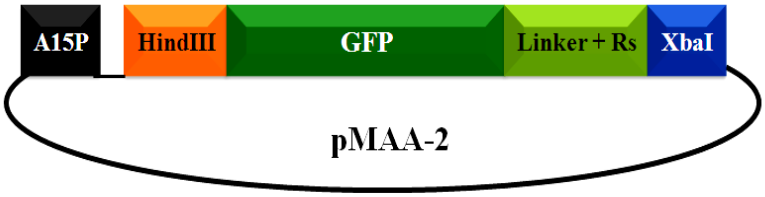

Similarly, oligonucleotides VIP 1405 and VIP 1406 (Table 2.3), consisting of restriction sites (Rs) for XhoI, EcoRI, NsiI, KpnI, BamHI and SacI, were annealed

and ligated into pGFP (Nuttall et al., 2012) that had been digested with HindIII and BamHI. Again, the original BamHI site was destroyed. The resulting plasmid was named pMAA-1.

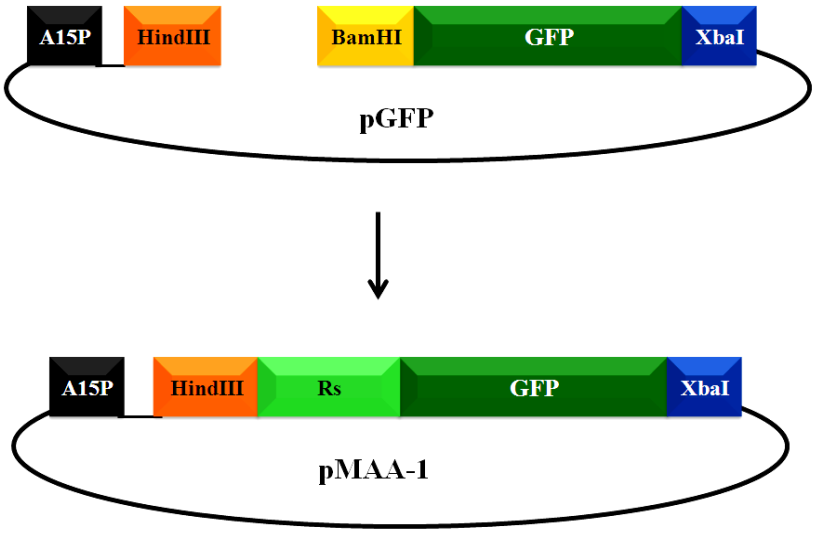

p339-3MA was generated by annealing and inserting the oligonucleotides VIP 1046 and VIP 1047 (Table 2.3) into BamHI- ClaI digested p339-3mRFPmars. The oligonucleotides encode the amino acid linker sequence Gly-Ser-Gly-Ala and restriction sites (Rs) BamHI, XbaI, SaII, PstI, SphI, EcoRI as shown below:

2.2.5 Plasmid design for homologous recombination in *S. cerevisiae*

pMA22 encoding cycloartenol-C-24-methyltransferase **(**Δ PTS1) was generated by homologous recombination in yeast. First, plasmid pEH116 was linearised with *SacI* and *PstI*. The open reading frame (ORF) of *D. discoideum* cycloartenol-C-24-methyltransferase Δ PTS1 (*Dd*SMT Δ PTS1) was then amplified by PCR using primers VIP 1590, VIP 1591 (Table 2.3) and the DNA template pMA20. The 5`end of the product was complementary to the final 18 nucleotides at the *SacI* – digested end of plasmid pEH116 (Figure 2.1). Similarly, the 3`end of the PCR product was complementary to the 18 nucleotides at the *PstI* digested end of the plasmid. When *S. cerevisiae* **(**BY4742) was transformed with the PCR product and the linearised pEH116, the gapped plasmid was repaired by homologous recombination. Plasmid pMA21encoding *Dd* SMT-GFP-PTS1 was obtained similarly. Initially, primers VIP 049 and VIP 272 (Table 2.3) were used in amplification of *Dd* SMT from pMA22. The plasmid pEH012 was digested with *SacI* and *BamHI* and the PCR product was inserted into the linearised pEH012 by homologous recombination.

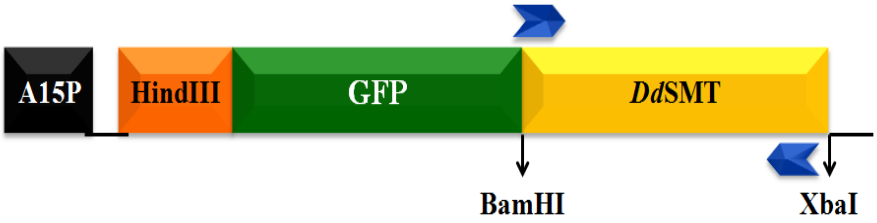

pMA20

A) PCR reaction used to amplify the ORF of *Dd*SMT from pMA20

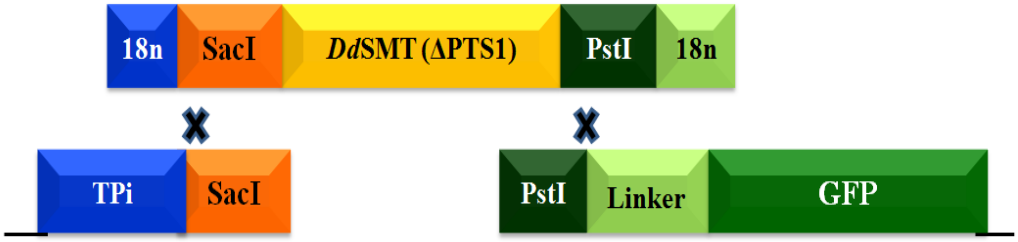

pEH116

B) Homologous recombination between *Dd*SMT(ΔPTS1) and linearised pEH116

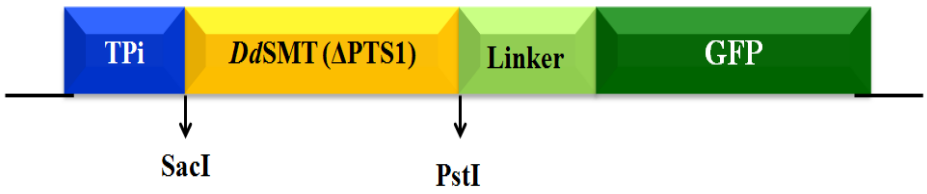

pMA22

C) The recombinant vector (pMA22) encoding the *Dd*SMT(ΔPTS1)

Figure 0.1: Generating the pMA22 construct using homologous recombination.

2. 3 Primers

Table 2.3: Primers used in this study

Name	Sequence (5'-3')	Application
VIP 1958	GACCTCGAGAAAAAATGACAAAA CCAGAAAATATCGG	(F) primer to amplify HMG-CoA synthase (A)
VIP 1959	GCAGGATCCAGCACCAGCACC TTTTTTTAAAATTGATAAAACTGA TTTAG	(R) primer to amplify HMG-CoA synthase (A)
VIP 1960	GACGGATCCAGCACCAGCACC ATGAAAAAAACAAAAGATATT GGA	(F) primer to amplify HMG-CoA synthase (B)
VIP 1961	GCATCTAGATTACAATTTTGAAGA TATAATTGGCT	(R) primer to amplify HMG-CoA synthase (B)
VIP 1753	GACCTCGAGAAAAAATGCTATTC GCTCCACCAAATTTAGAAACT AAAGAGTTATTTTGGATTATATAT ATTTTAATCCTTATACCAAAAGTA TTCGC	(F) primer to amplify HMG-CoA reductase (A)
VIP 1408	GCAGGATCCAGCACCAGCACC ATTTGTTTTTGCTCTATTATATTG AAG	(R) primer to amplify HMG-CoA reductase (A)
VIP 1409	GACCTCGAGAAAAAATGATTAGA ATTGGTTCAAATTTA	(F) primer to amplify HMG-CoA reductase (B)
VIP 1410	GCAGGATCCAGCACCAGCACC ATCAGAATGTGGTAAATTATGAG	(R) primer to amplify HMG-CoA reductase (B)
VIP 1269	GACAAGCTTAAAAAATGATATCA AACCAAGACAATATC	(F) primer to amplify mevalonate kinase, to clone it at the N-terminus of GFP
VIP 1270	GCAGGATCCAGCACCAGCACC TTTTTGAATTGGTAAAATATTAATAG	(R) primer to amplify mevalonate kinase, to clone it at the N-terminus of GFP
VIP 1361	GACGGATCCAGCACCAGCACCATG ATATCAAACCAAGACAATATC	(F) primer to amplify mevalonate kinase, to clone it downstream of the GFP
VIP 1362	GCATCTAGATTATTTTTGAATTGGTAA	(R) primer to amplify mevalonate kinase, to clone

	AATATTAATAG	it downstream of the GFP
VIP 1267	GACGGATCCAGCACCAGCACCATG GAAAGAGTTGTTTGTTCAGC	(F) primer to amplify phosphomevalonate kinase
VIP 1268	GCATCTAGATTATAATTTTGGAGT AATATGAGA	(R) primer to amplify phosphomevalonate kinase
VIP 1369	GCATCTAGATTAGGAGTAATATGA GACATATCAATTG	(R) primer to amplify phosphomevalonate kinase Δ PTS1(-PKL)
VIP 1253	GACAAGCTTAAAAAATGGTTTTA GCATCAGTTACATG	(F) primer to amplify phosphomevalonate decarboxylase, to clone it at the N-terminus of GFP
VIP 1254	GCAGGATCCAGCACCAGCACCATT TAATTGTTTTGGTAAACCAGTTG	(R) primer to amplify phosphomevalonate decarboxylase, to clone it at the N-terminus of GFP
VIP 1323	GACGGATCCAGCACCAGCACCATG GTTTTAGCATCAGTTACATG	(F) primer to amplify phosphomevalonate decarboxylase, to clone it downstream of the GFP
VIP 1324	GCATCTAGATTAATTTAATTGTTT TGGTAAACCAG	(R) primer to amplify phosphomevalonate decarboxylase, to clone it downstream of the GFP
VIP 1328	GACAAGCTTAAAAAATGGCAACAAAA TCAAATGAAGAG	(F) primer to amplify IDP-isomerase, to clone it at the N-terminus of GFP
VIP 1329	GCAGGATCCAGCACCAGCACCATA TCTATGAATTGTATTTGTTGG	(R) primer to amplify IDP-isomerase, to clone it at the N-terminus of GFP
VIP 1288	GACGGATCCAGCACCAGCACCATG GCAACAAAATCAAATGAAGAG	(F) primer to amplify IDP-isomerase, to clone it downstream of the GFP
VIP 1289	GCATCTAGATTAATATCTATGAATTGT ATTTGTTGG	(R) primer to amplify IDP-isomerase, to clone it downstream of the GFP

VIP 1418	GACAAGCTTAAAAAATGGCAACAAAA TCAAATGAAGAG	(F) primer to generate internal GFP-fusion protein of the IDP-isomerase
VIP 1419	GCAGGTACCAGCACCAGCACCATA TCTATGAATTGTATTTGTTGG	(R) primer to generate internal GFP-fusion protein of the IDP-isomerase
VIP 1420	GACGAGCTCATGAGTAAAGGAGAA GAACTTTTC	(F) primer to amplify GFP
VIP 1421	GCACTCGAGTTTGTATAGTTCATCCAT GCC	(R) primer to amplify GFP
VIP 1200	GGTGCTGGATCCATGCAATATATG AAATCACTTGCT C	(F) primer to amplify squalene synthase, to generate mRFP fusion protein
VIP 1201	GCTAATCGAT TTATAATTTCGAAAA AAAGTT TGGACC	(R) primer to amplify squalene synthase, to generate mRFP fusion protein
VIP 1892	GACGGATCCAGCACCAGCACCATG CAATATATGAAATCACTTGCTC	(F) primer to amplify squalene synthase, to clone it downstream of the GFP
VIP 1893	GCATCTAGATTATAATTTCGAAAA AAAGTTTGGACC	(R) primer to amplify squalene synthase, to clone it downstream of the GFP
VIP 2184	GCATCTAGATTAAAAAAAGTTTGG ACCATGACG	(R) primer to amplify squalene synthase ΔPTS1
VIP 1309	GACAAGCTTAAAAAATGGAAGATATT CAATTTGAAAATG	(F) primer to amplify squalene epoxidase
VIP 1310	GCAGGATCCAGCACCAGCACCTTT TGTTAATCTTAAAATAATACA	(R) primer to amplify squalene epoxidase
VIP 1377	GGTGCTGGATCCATGACAACTACT AATTGGAGT	(F) primer to amplify oxidosqualene cyclase
VIP 1378	GCTAGAATTCTTAAATTTTAGATTT TAAATATAATTG	(R) primer to amplify oxidosqualene cyclase

VIP 2105	GACGGATCCATGACAACTACTAAT TGGAGT	(F) primer to amplify oxidosqualene cyclase ΔPTS1
VIP 2185	GCAGAATTCTTATTTTAAATATAA TTGATTATATCTAG	(R) primer to amplify oxidosqualene cyclase ΔPTS1
VIP 1453	GACGGATCCAGCACCAGCACCATG GTATTAATTCAAACTAATCATC	(F) primer to amplify Cycloartenol-C-24-methyltransferase
VIP 1454	GCATCTAGATTAAAGTTTAGCAGC ATTTGG	(R) primer to amplify Cycloartenol-C-24-methyltransferase
VIP 2186	GCATCTAGATTAAGCATTTGGTTT TGAAGATAAGAATC	(R) primer to amplify Cycloartenol-C-24-methyltransferase ΔPTS1
VIP 1590	AAAAACACATACATAAACGAGCTC AAAATGGTATTAATTCAAACTAAT CATC	(F) primer to clone Cycloartenol-C-24-methyltransferase into a yeast vector
VIP 1591	TGCACCCGCCCCTGCTCCCTGCAG AGCATTTGGTTTTGAAGATAAG	(R) primer to amplify Cycloartenol-C-24-methyltransferase, to clone it into a yeast vector
VIP 049	GTTTTCCCAGTCACGACG	(F) primer to amplify Cycloartenol-C-24-methyltransferase, to clone it into a yeast vector
VIP 272	CCCATTAACATCACCATC	(R) primer to amplify Cycloartenol-C-24-methyltransferase, to clone it into a yeast vector
VIP 1461	GACAAGCTTAAAAAATGGAATCACTT TCATTAAAATTTATTG	(F) primer to amplify Methylsterol monooxygenase (1)
VIP 1462	GCAGGATCCAGCACCAGCACCTTC AGATTTATTAATTGATTTTTTTTC	(R) primer to amplify Methylsterol monooxygenase (1)

VIP 1808	GCAGGATCCAGCACCAGCACCTTC AGATTTACCAGCAGCAAG	(R) primer to amplify Methylsterol monooxygenase (Wada et al.)
VIP 1749	GACAAGCTTATGAATAAATTAATT TTATTATTAATTTTATC	(F) primer to amplify Calnexin
VIP 1750	GCAGGATCCAGCACCAGCACCTTT AACTTTATTAGTTCTTTTTGTAAC	(R) primer to amplify Calnexin
VIP 1575	GACAAGCTTATGAAAATATTATTATTT GTTACATTA	(F) primer to amplify PDI
VIP 1576	GCAGGATCCAGCACCAGCACCTTT TGATTTGAAAGATTCTAAAATATTG	(R) primer to amplify PDI
VIP 1265	GACAAGCTTAAAAAATGAGTAAAGGA GAAGAACTTTTC	(F) primer to amplify GFP
VIP 1266	GCAGGATCCTTTGTATAGTTCATCCAT GCC	(R) primer to amplify GFP
VIP 1890	GATCTGCTGGTGCTGGTGGATCCCTC GAGGGTACCATGCATGAATTCGAG CTCT	Oligonucleotides used to generate pMAA-2
VIP 1891	ACGACCACGACCACCTAGGGAGCTC CCATGGTACGTACTTAAGCTCGAG AGATC	Oligonucleotides used to generate pMAA-2
VIP 1405	AGCTTCTCGAGGAATTCATGCAT GGTACCGGATCCGAGCTCA	Oligonucleotides used to generate pMAA-1
VIP 1406	AGAGCTCCTTAAGTACGTACCATGG CCTAGGCTCGAGTCTAG	Oligonucleotides used to generate pMAA-1
VIP 1372	GATCCGTTGCAATTGATATGTCTCAT ATTACTCCAAAATTATAAT	Oligonucleotides used to generate pMA08
VIP 1373	GCAACGTTAACTATACAGAGTATAA TGAGGTTTTAATATTAGATC	Oligonucleotides used to generate pMA08

VIP 1447	TCGAGCCATTAGTTGAACCAACAAAT ACAATTCATAGATATTAAT	Oligonucleotides encoding the 12 amino acids at the C-terminus of IDP-isomerase
VIP 1448	CGGTAATCAACTTGGTTGT TTATGTTAA GTATCTATAATTAGATC	Oligonucleotides encoding the 12 amino acids at the C-terminus of IDP-isomerase

2.4 Cell Culture

Table 2.4: Culture media

Culture media	Description
Bacterial medium (2TY)	1.6% Bacto tryptone, 1% yeast extract, 0.5% NaCl
HL5 glucose medium for growing *D. discoideum* amoebae	1.43 % bacteriological peptone, 0.715% yeast extract, 1.54 % D-glucose, 0.128 % Na_2HPO_4 $12H_2O$, 0.0486 % KH_2PO_4
Yeast medium (YPD)	1% peptone, 1% yeast extract, 2% glucose
Yeast minimal medium 2 (ym2)	0.17% yeast nitrogen base (without amino acids and ammonium sulphate), 0.17% ammonium sulphate, 1% casaminoacids, 2% glucose or galactose as required. Leucine and tryptophan were added from stocks to the autoclaved media, as required.
All the above media were dissolved in distilled water and sterilised by autoclaving at121°C for 15-20 minutes. If required, antibiotics were added to appropriate concentrations after the media had been autoclaved and cooled to ~ 50 (Table 2.5). For preparation of solid medium, 2% Bacto-agar was added to the liquid medium which was then autoclaved. After cooling (~50°C) and addition of the any antibiotics, the autoclaved medium was poured into sterile Petri dishes and allowed to solidify at room temperature. The plates were then stored at 4 ˚C.	

Table 2.5: Antibiotics used in this study

Antibiotics	Final concentrations
Ampicillin	75 μg/ml
G418	10 μg/ml
Blasticidin	10 μg/ml
Cycloheximide	0.05 μg/ml
BMS181221	4.3μM

2.5 Growth of *Escherichia coli*

2.5.1 Growth and maintenance of *E. coli*

E.coli was obtained from a frozen stock (-80°C) and streaked on a 2TY agar plate for overnight growth at 37°C. Transformed strains that were ampicillin resistant grown on 2TY selective medium. Each plate was kept at 4°C for use for up to a week. For long-term storage, *E.coli* was grown overnight at 37°C in 2TY medium with shaking at 180 rpm. The following day, 0.8 ml culture was mixed with 0.8 ml autoclaved 30% (v/v) glycerol in a 1.8ml cryotube (Nunc) and placed in the -80°C.

2.5.2 Preparing chemical-competent cells of *E.coli* DH5α

Routinely, the preparation of the chemical competent cells was carried out at 0ºC. ml *E.coli* DH5α was streaked on a 2TY plate and incubated at 37ºC overnight. 5 2TY medium was inoculated with a single colony of DH5α and incubated at 37 ºC in a shaking incubator (~ 200 rpm) overnight. Next moring, the cells were diluted into 200ml 2TY to OD = 0.05 at 600nm and incubated at 30 ºC. Once the culture had reached the mid-log phase (OD = 0.5-0.6 at 600nm), the cells were incubated at 0 ºC for 15 minutes. Subsequently, the cells were harvested in pre-cooled 50ml Falcon tube by centrifugation at 3000 rpm for 10 minutes at 4 ºC in the 4×4 place rotor of a Sigma 4-16 K centrifuge. The supernatant was removed and the pellet

was resuspended in 70ml ice-cold RF1 (100mM rubidium chloride, 50mM manganese chloride, 30mM potassium acetate, 10mM calcium chloride, 15% (*v/v*) glycerol adjusted to pH 5.8 with 2M acetic acid).The cells were incubated at 0 ºC for 15-30 minutes and then centrifuged at 3000 rpm for 10 minutes at 4 ºC. The supernatant was removed before the pellet was resuspended in 16ml RF2 (10mM MOPS, 10mM rubidium chloride, 75mM calcium chloride, 15% (*v/v*) glycerol adjusted to pH 6.8 with NaOH) at 0˚C. The suspension of bacteria was then dispensed as aliquots of 200µl or 400µl into 1.5ml pre-cooled Eppendorf tubes and immediately frozen in liquid nitrogen. The bacteria were stored at -80 ºC.

2.5.3 Transformation of chemical-competent *E.coli* by the heat-shock method

A 100µl aliquot of chemical competent *E.coli* (DH5α) for each transformation was placed on ice to thaw. 1µl plasmid DNA (1-2µg DNA) or 10µl ligation reaction was added to the bacteria and then mixed gently before being placed on ice for 30 minutes. The bacteria were heat-shocked in a 42°C water bath for 90 seconds and immediately placed on ice for 1-2 minutes. 400 µl 2TY medium were added to each sample before being incubated for one hour at 37°C. The sample was centrifuged in a micro-centrifuge for 30 seconds at 13,000 rpm. 800 µl of the supernatant was removed and the pellet was resuspended in the residual medium. The bacterial suspension was plated out on a 2TY agar plate with ampicillin and incubated at 37°C overnight.

2.5.4 Transformation of *E.coli* by electroporation

10µl (10x dilution) of yeast genomic DNA (section 2.7.4) was added to a single 40µl aliquot of thawed electrocompetent *E.coli* and mixed. The bacteria were incubated on ice for 1 minute and transferred to a pre-cooled 2mm electroporation cuvette (Cell Projects). A 5 msec pulse was applied at 2,5 kV, 201Ω, 25µF and the cells were mixed with 600 µl of 2TY medium before being transferred to a 1.5ml Eppendorf tube. The bacteria were incubated at 37°C for 30 minutes and then centrifuged in a micro-centrifuge for 5 minutes at 5,000 rpm. The pellet was re-suspended in 100µl of the supernatant. The bacterial suspension was streaked on a 2TY ampicillin plate and incubated at 37°C overnight.

2.6 Axenic growth of *Dictyostelium discoideum*

2.6.1 Growth and maintenance of *D.discoideum*

Routinely, amoebae of *D.discoideum* strain Ax-2 were grown axenically in HL5 glucose medium at 22°C with shaking at 160 rpm (Watts and Ashworth, 1970). Stocks of amoebae were stored in a 22°C incubator without shaking for a maximum of 2 weeks, before being sub-cultured into fresh HL5 glucose medium. For long-term storage, 10^8 cells were harvested by centrifugation for 5 minutes at 1000 rpm at 4°C. The supernatant was removed and the pellet was resuspended in chilled horse serum (Sigma) containing 7.5% (v/v) DMSO and mixed thoroughly. The mixture was dispensed as 1ml samples into 1.8ml cryotubes (Nunc). The tubes were kept in a pre-cooled polystyrene container at -80°C overnight, before being stored at -80°C.

2.6.2 Isolation of *D. discoideum* genomic DNA by using a QIAamp DNA Mini Kit

D. discoideum genomic DNA was isolated by using a QIAamp DNA Mini Kit. Amoebae were cultured in 70ml HL5 glucose medium at 22°C with shaking at 160 rpm for 3 days. 2×10^7 amoebae were centrifuged for 5 minutes at 1000 rpm and the supernatant was removed. The pellet was resuspended in 10ml PBS buffer and subsequently centrifuged for 5 minutes at 1000 rpm. The supernatant was removed and 200 µl PBS buffer were added and mixed thoroughly. 20 µl protenase K was then added and mixed gently. Following steps were carried out according to the manufacturer's instructions.

2.6.3 Isolation of *D. discoideum* cDNA by using a QIAamp DNA Mini Kit

A QIAamp DNA Mini Kit was also used according to the manufacturer's instructions to isolate cDNA from a cDNA library (200µl) constructed by Stratagene in λzap by use of mRNA prepared from *D. discoideum* strain Ax-2 amoebae harvested during exponential axenically growth.

2.6.4 Transformation of *D. discoideum* by electroporation

Great care was taken to keep the suspensions of amoebae sterile and as many steps as possible were carried out in a lamina flow cabinet.

Transformation of amoebae by electroporation was performed according to the method of (Pang et al., 1999). 5×10^6 amoebae were harvested by centrifugation in a sterile pre-cooled 15ml Falcon tube for 5 minutes at 1000rpm and at 4˚C. The supernatant was removed aseptically. 8 ml sterile ice-cold H50 medium (10mM NaCl, 5mM $NaHCO_3$, 1mM $MgSO_4$, 1mM NaH_2PO_4, 20mM HEPES, 50mM KCl, adjusted to pH 7.0 with KOH) were added to the cells and vortexed thoroughly. The cells were centrifuged and the supernatant was removed. The pellet was resuspended again in 8 ml H50 medium and centrifuged. Following centrifugation, the last residual supernatant was removed with a sterile pipette and the pellet was resuspended in 100µl H50 medium. 10 µl plasmid DNA were added and mixed gently. The mixture then was transferred to a chilled electoporation cuvette (1mm gap). Two pulses were applied at 0.65 kV and 25Ω (using a Bio-Rad Gene Pulser) and the cuvette then was incubated on ice for 5 minutes. The cells then were transferred into a sterile Petri dish containing 10 ml HL5 glucose medium and incubated at 22 ˚C overnight. Next day, appropriate antibiotic was added to the cells before incubation at 22 ˚C for approximately 2 weeks.

2.6.5 Fluorescence microscopy (*D.discoideum*)

Unfixed amoebae were analysed using a Zeiss Axiovert 200M microscope (Carl Zeiss Microimaging, Inc.) equipped with an Exfo X-cite 120 excitation light source, band pass filters (Carl Zeiss Microimaging, Inc. and Chroma Technology Corp.), an α plan-Fluar 100X/1.45 NA or a Neofluar 40 ×/1.3 NA (numerical aperture) oil Ph3 objective lens (Carl Zeiss MicroImaging, Inc.) and a digital CCD camera (Orca ER, Hamamatsu). Image acquisition was performed using Openlab software (Improvision). Live cells were imaged in 0.7% NaCl at room temperature.

Unless otherwise stated, fluorescence images were collected as 1 µm Z-stacks, merged into one plane after contrast enhancing in Velocity, and processed further in Photoshop (Adobe). Bright field images were collected in one plane and added into the blue channel in Photoshop (Adobe).

For each transformant many fields were examined under the microscope but essentially all cells had the same appearance. However, the fluorescence intensity varied. Probably this is because some cells contain more copies of the plasmid encoding the fluorescent protein than others.

2.7 Growth of Saccharomyces *cerevisiae*

2.7.1 Growth and maintenance of *S.cerevisiae*

The *S.cerevisiae* strains were plated out on a YPD plate containing 2% glucose and incubated at 30 ^{o}C for 2 days. Yeast was stored at room temperature for up to 1 week. For long-term storage, the strains were cultured in 3ml liquid medium at 30 ^{o}C with shaking at 180 rpm overnight. Next day, 0.8 ml of culture was mixed with 0.8 ml 30% glycerol in a 1.8ml cryotube (Nunc) and stored at -80°C.

2.7.2 Yeast high efficiency transformation procedure

The yeast high efficiency transformation protocol was based on the method of Gietz et al., 1992. Yeast were grown in 3 ml liquid medium at 30°C overnight. The overnight culture was diluted to OD_{600}=0.05-0.1 in 10 ml fresh culture medium for each required transformation and the cultures were grown to mid-log phase (OD_{600}=0.5-0.6). The cells were harvested by centrifugation for 5 minutes at 5000 rpm, and the pellet was resuspended in sterile Millipore water. The cells were centrifuged again (5 minutes at 5000 rpm) and the supernatant was removed. The pellet then was resuspended in 1ml TE/LiAc buffer (10mM Tris-Cl pH 7.5, 0.1 mM DTT, 0.1 M LiAc pH 7.5). The cells were centrifuged for 1 minute at 9000 rpm, the supernatant was taken off and the pellet was resuspended in a 50 µl TE/LiAc. 2 µl plasmid (0.5µg-1µg), 5µl single stranded DNA (`Salmon testes) and 300 µl 40% PEG 4000 solution (50% PEG 4000, 10mM Tris-Cl pH 7.4, 0.1mM EDTA pH 8.0, 0.1M LiAc pH 7.5) were added to the samples and mixed thoroughly. The cells were incubated at 30°C for 30 minutes and heat-shocked in a 42°C water bath for 15 minutes. The cells were centrifuged for 1 minute at 7000 rpm and the supernatant was removed. The pellet was resuspended in 100µl TE (10mM Tris-Cl pH 7.5, 0.1 mM EDTA). The cells were streaked on a selective agar plate and incubated at 30° C for 2 days.

2.7.3 Yeast one step transformation procedure

The yeast one step transformation was performed according to Chen et al., 1992. *S.cerevisiae* strains were grown in 3ml YPD at 30° C overnight. 200µl of the cultures were centrifuged in a micro-centrifuge for 1 minute at 13,000 rpm and the supernatant was removed. The pellet was resuspended in 2 µl (0.5 µg-1 µg) of the appropriate plasmid by vortexing. 5µl (50µg) single stranded DNA and 50µl one-step buffer (0.2M LiAc pH 5.0, 40% (w/v) PEG4000, 0.1M DTT) were added. The cells were incubated at room temperature for 3-4 hours with vortexing intermittently. The cells then were heat-shocked in a water bath at 42 °C for 30 minutes. They were then plated out on solid minimal medium and incubated at 30 ºC for two days.

2.7.4 Isolation of yeast total DNA

Yeast cells were grown in 6ml of appropriate culture medium (YPD or minimal medium) at 30 ºC overnight. The cells then were harvested by centrifugation in a 2ml screw-cap tube for 1minute at 13,000 rpm and the supernatant was removed. The pellet was resuspended in 1ml sterile water and the cell suspension was centrifuged for 1 minute at 13,000rpm. The supernatant was removed. 200µl TENTS (20mM Tris-HCl pH 8.0, 1mM EDTA, 100mM NaCl, 2% (v/v) Triton X-100, 1% (w/v) SDS), 200µl of 452-600µm glass beads and 200µl phenol:chloroform:isoamyl alcohol (25:24:1) were added to the pellet and mixed. A mini bead beater (Biospec Products) was used at full speed for 45 seconds to break open the cells and the mixture was subsequently centrifuged for 30 seconds at 12,000rpm. 200µl of TENTS was added to the sample and vortexed thoroughly. The sample was centrifuged for 5 minutes at 12,000rpm and 350µl of the supernatant were transferred into an Eppendrof tube. 200µl phenol: chloroform: isoamyl alcohol was added to the sample which was vortexed thoroughly. The sample was centrifuged for 5 minutes at 12,000rpm and subsequently 200µl of the supernatant were transferred into an Eppendrof tube. 15µl 3M sodium acetate pH 5.2 and 2.5x the volume of the sample of 100% ethanol were added to the sample and vortexed. The sample was incubated at -20 ºC for 2 hours or overnight. The sample was then centrifuged for 15 minutes at 12,000rpm and the supernatant was removed. The pellet was resuspended in 500µl 70% ethanol and the suspension

centrifuged for 1 minute at 12,000rpm. The supernatant was removed and the pellet was resuspended in 200µl TE pH 8.0 with 2µl RNAse (10µg/ml). The sample then was incubated at room temperature for 10 minutes. 20µl 3M sodium acetate pH 5.2 and 2.5x the sample volume of 100% ethanol were added, before the sample was incubated at -20 ºC for 1 hour or overnight. The sample was centrifuged for 15 minutes at 12,000 rpm and the pellet was resuspended in 500µl 70% ethanol. The suspension was centrifuged for 1 minute at 12,000 rpm and the supernatant was removed. The sample was incubated at 30 ºC in order to evaporate the last trace of the ethanol. The pellet was resuspended in 50µl TE pH 7.5.

2.7.5 Fluorescence microscopy (*S.cerevisiae*)

Yeast cultures were grown to log phase and images captured on a Zeiss Axiovert 200M microscope (described in 2.5.5**).** Fluorescence images were routinely collected as 0.5 µm Z-stacks.

2.8 Molecular cloning

2.8.1 Preperation of plasmid DNA

A single colony of transformed *E.coli* was inoculated into 5ml 2TY medium containing the appropriate selection antibiotic. The cells were grown at 37º C with shaking at ~ 200 rpm overnight. Next day, the plasmid DNA was purified using the QIAprep Spin Miniprep Kit (Qiagen), according to the manufacturer's instructions (the protocol was obtained from www.qiagen.com).

2.8.2 Restriction enzyme digestion of plasmid DNA

Plasmid DNA was digested by using appropriate restriction endonucleases (New England Biolabs). Each reaction was carried out in a final volume of 20µl, consisting of plasmid DNA (0.5µg-1µg), 5 units restriction enzyme per 1µg DNA, 2 µl 10x compatible restriction buffer and the volume was made up to 20µl using sterile Millipore water. The mixture was incubated at 37ºC for 2 hours. For multiple restriction enzyme digestion when the restriction endonucleases shared the same buffer, the double digestion was set up with both enzymes. If the restriction endonucleases needed different buffers, the digestion reaction was carried out with one enzyme using its appropriate buffer. Subsequently, the first buffer was removed using a QIAquick Gel Extraction Kit (Qiagen) according to the manufacturer's instructions and the second digestion reaction was set up using the compatible buffer.

2.8.3 DNA electorophoresis on agarose gels

Agarose gel electrophoresis was used to analyse digested DNA fragments. A 1% agarose gel was prepared by adding Bio-Rad Ultra Pure DNA Grade agarose to the TBE buffer (0.04M Tris-acetate, 0.04M boric acid, 0.001M EDTA) and the mixture was heated in a microwave until the agarose had melted. The mixture was cooled down to ~50 ˚C and ethidium bromide (0.5µg/ml, final concentration) was added. Subsequently, the mixture was poured into a gel tray containing a comb and allowed to set at room temperature. The gel then was placed in the electrophoresis tank and covered with TBE buffer. The DNA was mixed with 6× loading dye (0.25% bromophenol blue, 0.25% xylene cyanol FF, 30% glycerol in distilled water) and loaded onto the gel. A DNA marker (Hyperladder I, Bioline

Ltd.) was run alongside the DNA sample in order to determine the size of DNA fragments. The electrophoresis gel was run at a constant voltage of ~ 100 V. The DNA fragments were analysed using an ultraviolet transilluminator imaging system (Gene Genius) and a photograph recorded digitally using Genesnap software (SynGene).

2.8.4 DNA elution from agarose gels

The required DNA fragment was extracted from the agarose gel by using a QIAquick Gel Extraction Kit, following the manufacturer's instructions (the protocol was obtained from www.qiagen.com).

2.8.5 Amplification of DNA by the polymerase chain reaction (PCR)

The polymerase chain reaction (PCR) was used to amplify specific regions of DNA. The reaction was carried out in a PCR tube in a final volume of 50 µl, comprising template DNA (~ 300 ng) , 1.5mM $MgCl_2$, 0.15mM dNTP mix (consisting of dATP, dCTP, dTTP, dGTP), 1mM forward primer, 1 mM reverse primer, 1x Taq buffer and 2.5 units Taq DNA polymerase (Bioline). The reaction was then run in a thermocycler (Biometra). The temperature of the thermocycler lid was set to 100˚C in order to prevent condensation on the lid of the PCR tube. The thermocycler was programmed as indicated below:

Table 2.6: PCR cycling conditions when using Taq polymerase

Temperature	Step	Time	Cycles
95°C	initial denaturation	5 minutes	1
95°C	Denaturation	30 seconds	25-35
56°C	annealing	30 seconds	
74°C	Extension	1min/1Kb DNA to be amplified	
74°C	Final extension step	10 minutes	

The annealing temperature was varied depending on the Tm of each primer. Tm was calculated using the equation: (annealing temperature) = 4 x (#G + #C) + 2 x (#A + #T). The PRC product was routinely analysed on a 1% agarose gel to confirm the presence of the product.

2.8.6 Proofreading PCR

Proofreading PCR was carried out using either the ACCUZYME^{TM} or Velocity proofreading DNA polymerase (supplied by Bioline) as follows:

Table 2.7: PCR reaction for ACCUZYME and Velocity polymerases

Velocity	ACCUZYME	PCR reaction
~300 ng	~300 ng	Template DNA
—	1.5mM	$MgCl_2$
0.25mM	0.3mM	dNTP mix
2mM	1mM	Forward primer
2mM	1mM	Reverse primer
1x Velocity buffer which contains $MgCl_2$	1x ACCUZYME buffer	DNA polymerase buffer
2 units of Velocity	2.5 units of ACCUZYME	DNA polymerase
50µl	50µl	Final volume

The PCR reaction (using ACCUZYME) was carried out with the same cycle programme described in table 2.6, but with an extension time of 2min/Kb DNA. For the reaction mixture using Velocity, the thermocycler was programmed slightly differently. The temperature of the initial denaturation step and the following denaturation steps was set at 98˚C and the extension time of the reaction was reduced to 30sec/Kb DNA.

2.8.7 DNA ligation by T4 ligase

The DNA ligation mixture was assembled on ice. The components were added together in a total volume of 21µl, comprising 2 µl of 10 x ligation buffer , 1µl T4 ligase (3 units) and varying ratios of double- digested PCR product/linearised vector (~0.5 µg). For a negative control, the same protocol was followed in parallel with the exception that the PCR product was omitted. For a positive control, the plasmid DNA was linearised with only one restriction endonuclease and no PCR product was added. The reactions were placed in ice-cold water and left at room temperature overnight. (T4 DNA ligase was obtained from Promega).

2.8.8 Sequencing of constructs

The sequencing of cloned constructs was performed by Beckman Coulter Genomics. This was performed on plasmid DNA prepared as described in section 2.7.1.

2.9 Protein procedures

2.9.1 Preparation of the samples of mevalonat pathway enzymes

2×10^7 amoebae were harvested by centrifugation at 1000rpm for 5minutes at room temperature. The supernatant was discarded and the pellet was resuspended in 10ml cold distilled water. The sample was then centrifuged (1000rpm, 5minutes). The supernatant was discarded and the pellet resuspended in 1ml cold water. Protein samples were mixed with protein loading buffer (1:3) and heated at 95ºC for ~5minutes.

2.9.2 Preparation of *D. discoideum* cell lysates for investigations of the sterol biosynthesis enzymes

Throughout the procedure, great care was taken to keep the samples at 0˚C. 2×10^8 amoebae were centrifuged in a sterile pre-cooled 50 ml Falcon tube. All centrifugation steps were performed for 5 minutes at 1000 rpm and 4˚C. The supernatant was removed; the cells were washed in 40 ml of ice-cold distilled water and centrifuged. The supernatant was removed and the pellet was

resuspended in 10ml 50mM HEPES pH 7.5 at 0˚C. Subsequently, the cells were centrifuged again and the supernatant removed before, the cells were resuspended in 8ml 50mM HEPES pH 7.5. The suspension was transferred to a pre-cooled 10ml beaker and sonicated on ice for 10 seconds at 10 amplitude microns in a Sanyo sonicater. Amoebal homogenates were kept on ice until used or stored at -80˚C.

2.9.3 Treatment of peroxisomal membranes with sodium carbonate

The protocol for extracting the peroxisomal membranes with sodium carbonate was adapted from (Fujiki et al., 1982, Elgersma et al., 1997). This method allows distinction between integral and peripheral membrane proteins by diluting the membranes in 0.1M Na_2CO_3 pH 11.4 at 0˚C. The amoebal homogenate (described in section 2.8.1) was centrifuged in a 10ml polycarbonate tube at 4˚C for 1 hour at 50,000 rpm (~ 233,000 g_{max}) using a Beckman 50 Ti rotor. The supernatant was gently pipetted off and kept at 0˚C, until analyzed by SDS-PAGE or stored at -80˚C. The pellet was resuspended in 100ml 0.1M $Na_2 CO_3$ pH 11.4 at 0˚C and incubated on ice for 30 minutes in order to dilute it to less than 10mg/ml protein. In these conditions, closed vesicles are converted into open sheets of membrane. 8 ml of the suspension were centrifuged in a polycarbonate tube at 4˚C for 1 hour at 50,000 rpm using a Beckman 50 Ti rotor. The supernatant was retained and 0.5 ml of it was concentrated by centrifugation using Millipore tube, with a 30 K cut-out, in a micro-centrifuge (13,000 rpm, 30 minutes, 4˚C). The final volume was made up to 0.04 ml with 50 mM HEPES pH 7.5 at 0˚C. The pellet was resuspended in 0.64 ml 50 mM HEPES/ 1% Triton. Equivalent amounts (i.e. derived from the same number of cells) of each fraction were analysed on 10 % SDS-PAGE and Western blot analysis.

2.9.4 Treatment of peroxisomal membranes with 1M NaCl

Peripheral membrane proteins can be released from peroxisomal membranes by diluting the membranes in a high salt concentrations followed by high-speed centrifugation. Amoebal homogenate (described in 2.9.2) was centrifuged in a polycarbonate tube at 4˚C for 1 hour at 50,000 rpm using a Beckman 50 Ti rotor. All subsequent steps were carried out at 0˚C. The supernatant was separated from the pellet and was analysed on SDS-PAGE. The pellet was resuspended in 8 ml

1M NaCl in HEPES (50mM pH7.5) and incubated on ice for 30 minutes. The resulting suspension was centrifuged in a polycarbonate tube at 4 ˚C for 1 hour at 50,000 rpm (Beckman 50 Ti rotor). The supernatant was pippeted off. 0.25 ml 40% TCA (trichloroacetic acid) was added to a 0.75ml sample of supernatant in an Eppendrof tube to precipitate protein. The sample then was incubated on ice for 30 minutes and subsequently centrifuged in a micro-centrifuge (13,000 rpm, 5 minutes, 4˚C). The supernatant was removed and the pellet was mixed with10µl 1M Tris pH 10.9. The mixture was diluted (×10) in protein loading buffer (250 mM Tris-Cl pH 6.8, 9.2 % (w/v) SDS, 40 % (v/v) glycerol, 0.2 % (w/v) bromophenol blue, 0.1 M DTT). The membrane pellet was resuspended in 8 ml 50 mM HEPES/1% (*v/v*) Triton. The samples were examined by 10 % SDS-PAGE and Western blot analysis.

2.9.5 Protein separation by sodium dodecyl sulphate-polyacrylamid gel electrophoresis (SDS-PAGE)

Proteins were analysed by SDS-PAGE according to the metod of (Lamemmli et al, 1970). A 10% resolving gel was made from a stock solution consisting of the following:

Table 2.8: Composition of the resolving gel

Stock solution	10% Resolving gel
Protogel (polyacrylamide 30 % (w/v)/ 0.8 % (w/v) bis-acrylamide)	6.6 ml
Resolving gel buffer (1.5 M Tris-HCl, 0.4% SDS, pH 8.8)	5.2 ml
Distilled water	8.2 ml
10 % (*w/v*) ammonium persulphate (APS)	200 µl
N,*N*,*N'*,*N'*-tetramethylethylenediamine (TEMED)	20 µl

The above components were mixd and poured between 1.5mm glass plates. The resolving gel surface was overlaid with isopropanol and allowed to polymerize. Once, the resolving gel had set, the isopropanol was removed. Subsequently, a stacking gel was added and a 1.5mm comb immediately inserted. The stacking gel consisted of the following:

Table 2.9: Composition of the stacking gel

Stock solution	Stacking gel
Protogel (polyacrylamide 30 % (w/v)/ 0.8 % (w/v) bis-acrylamide)	2.6 ml
Stacking gel buffer (0.5 M Tris-HCl, 0.4% SDS, pH 6.8)	5 ml
Distilled water	12.2 ml
10 % (*w/v*) ammonium persulphate (APS)	200 µl
N,*N*,*N'*,*N'*-tetramethylethylenediamine (TEMED)	20 µl

When the stacking gel had polymerized, the plates containing the gel were placed into an electrophoresis tank (Bio-Rad Mini-PROTEAN®) which was filled with 1x running buffer (25mM Tris; 250mM glycine; 0.1% (w/v) SDS). Protein samples were mixed with protein loading buffer (250 mM Tris-Cl pH 6.8, 9.2 % (w/v) SDS, 40 % (v/v) glycerol, 0.2 % (w/v) bromophenol blue, 0.1 M DTT) and heated at 95ºC for ~5minutes. The samples were loaded onto the gel alongside a pre-stained protein marker (BioRad). Electophoresis was performed at constant voltage (150 V) and was continued until the marker dye had migrated to the bottom of the resolving gel.

2.9.6 Western Analysis

Protein samples, separated by SDS-PAGE, were transferred to a nitrocellulose membrane to allow detection of the desired proteins using specific antibodies. The transfer process was carried out in pre-cooled transfer buffer (25 mM Tris; 150 mM glycine, pH 8.3; 40% (v/v) methanol) for 2 hours at constant current (200 mA), using a Mini Trans Blot Electrophoretic Transfer Cell (Bio-Rad), as described in the Bio-Rad manual. In order to confirm that the proteins had been transferred successfully, the membrane was soaked in Ponceau S staining solution (0.1 % (*w/v*) Ponceau S in 5 % (*v/v*) acetic acid) for ~5 minutes. Alternatively, the pre-stained protein marker can give a visual indication of the success of the transfer.

2.9.7 Detection of proteins on western blots

Once the nitrocellulose membrane had been blotted, the membrane was soaked in blocking buffer (2 % (w/v) skimmed milk in 1×TBS from a stock solution comprising 50 mM Tris, 150 mM NaCl, pH 7.4) and placed on a shaking table at room temperature for 1hour. Next, the membrane was incubated in fresh blocking buffer containing an appropriate dilution of the primary antibody (determined experimentally) for 1hour. The previous mixture was removed and the membrane was washed three times in 1×TBS/ 0.1% (v/v) Polysorbate 20 (Tween 20) with each wash lasting 10 minutes. The membrane was then incubated in fresh blocking buffer containing an appropriate dilution of the secondary antibody for 1hour. The membrane was washed with distilled water and the proteins detected by using the EZ-ECL Chemiluminescence detection kit (Biological Industries), according to the manufacturer's instructions.

2.9.8 Sources of antibodies

Monoclonal primary antibody against GFP (Anti_GFP IgG) used in section 2.9.7 was obtained from Roche. Horseraddish peroxidase (HRP)-conjugated goat anti-mouse IgG (Sigma-Aldrich, UK) was used as the secondary antibody.

Chapter 3

Investigations of the intracelluar locations of the mevalonate pathway enzymes in *Dictyostelium discoideum*

3.1 Introduction

In *Dictyostelium discoideum* a number of the mevalonate pathway enzymes possess a PTS. This implies that part of the mevalonate pathway may take place in the peroxisomes. Furthermore, it was found previously that *D. discoideum* FDP-synthase, which catalyzes the final two steps of the mevalonate pathway, is directed to the peroxisomes by making use of the PTS2-dependent pathway (Nuttall et al., 2012). This enzyme is of particular interest because it is the target of nitrogen –containing bisphosphonates drugs (NBPs) (Grove et al., 2000). The therapeutic application of these drugs is to inhibit osteoclast-mediated bone resorption and therefore the drugs are used to treat metabolic bone diseases such as osteoporosis, tumoral bone disease and Paget's disease in which bone resorption is excessive (Fleisch., 1995). The observation that FDP-synthase is the target of the NBPs was originally made in the cellular slime mould *D. discoideum*. This organism was used as a model system for investigating the mechanism of action of NBPs because the drugs inhibit its growth apparently in the same way that they inhibit osteoclast-mediated bone resorption (Rogers et al., 1994, Rogers et al., 1995).

The peroxisomal localization of *D.discoideum* FDP-synthase was identified successfully by transforming *D.discoideum* amoebae to express a fusion protein between the FDP-synthase and GFP, the GFP fluorescence then being localized to the peroxisomes. Furthermore, it was found that the fusion protein was catalytically active and this proved that the enzyme was folded properly in the amoebae (Nuttall et al., 2012).

By contrast, in mammalian cells, attempts to determine the intracellular location of the mevalonate pathway enzymes by expressing each as a GFP-fusion protein were largely unsuccessful (Kovacs et al., 2007, Hogenboom et al., 2004c).

These results were obtained probably because the tagged enzymes could not fold properly and as a result formed aggregates in the cytosol. Thus, identification of the intracellular location of the pathway enzymes had to rely on use of antibodies. Despite the frequent use of immunochemical methods, they can be unreliable because the antibodies are not sufficiently specific for their antigen. In addition, a further difficulty of using immunochemical methods is that the antibodies can only bind to their target when it is present in a sufficiently high concentration (i.e. antibodies usually cannot detect cytosolic enzymes because they are at too low a concentration).

Since the GFP-tagged FDP-synthase folded correctly in *D.discoideum*, it seemed possible that the intracellular location of the other mevalonate pathway enzymes in *D. discoideum* amoebae might be established by transforming amoebae to express each enzyme fused to GFP. I used GFP as this is a bright and stable fluorescent protein that is widely used for subcellular localization studies in living cells. For double labeling we used a *D. discoideum* optimised red fluorescent protein (mRFP) (Fischer et al., 2004). Thus, the aim of this chapter is to describe investigations of the intracellular locations of the pathway enzymes in *D. discoideum* by generating GFP fusion proteins and analyzing the intracellular distribution of the transformed amoebae by fluorescence microscopy.

Tagging of proteins with GFP or mRFP may affect their localization. However, if fusion proteins are targeted to peroxisomes, we will conclude that the enzyme has the targeting information for this organelle. No examples have been reported where a fusion protein is mistargetted to peroxisomes. If fusion proteins are localized to the cytosol, the interpretation is more difficult since the tags might interfere with localization to peroxisomes or other places in the cell.

3.2 Results

3.2.1 The intracellular location of 3-Hydroxy-3-Methylglutaryl-Coenzyme A Synthase

HMG-CoA synthase catalyzes the second reaction in the biosynthesis of isoprenoids by adding acetyl-CoA to acetoacetyl CoA to form HMG-CoA. In mammalian cells, there are two genes encoding HMG-CoA synthase. One gene was identified as a mitochondrial enzyme required for ketogenesis (Hegardt, 1999). The other enzyme was believed to be localized to the cytosol (Ayte et al., 1990). However, it has been reported that HMGS is directed to the peroxisomes by use of PTS2-dependent pathway (Olivier et al., 2000).

D. discoideum amoebae possess two different HMG-CoA synthase genes HMGS (A) and HMGS (B). HMG-CoA synthase (A) has neither a PTS1 nor a PTS2. In order to determine the subcellular location of the enzyme, a GFP-fusion protein was generated with the GFP at the C-terminus. The 1449bp DNA fragment was amplified by PCR from the *D. discoideum* cDNA library by using VIP 1958 and 1959 as primers (section 2.3 in the materials and methods). After digestion with XhoI and BamHI, the DNA fragment of *Dd* HMGS (A) was ligated into XhoI-BamHI digested pMAA1to give pMA01. Amoebae transformed with pMA01 expressed *Dd*HMGS (A)–GFP and the fluorescence was in the cytosol (Figure 3.1) indicating that this enzyme is cytosolic.

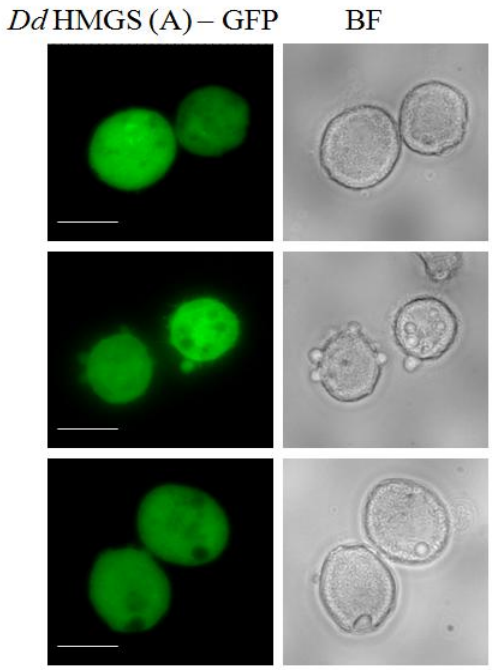

Figure 3.1: The intracellular localization of *D.discoideum* HMG-CoA synthase (A). Amoebae overexpressing the full-length *Dd*HMG-CoA synthase (A)-GFP show a distribution of green fluorescence in the cytosol. Bright field (BF) shows cell morphology. Scale bars 5µm.

In *D. discoideum*, HMG-CoA synthase (B) contains a consensus PTS1 (-Ser-Lys-Leu_{COOH}) located at the C-terminus. The GFP-fusion protein was generated without masking the amino acid triplet at the carboxy terminus. The open reading frame of *Dd* HMGS (B) was amplified by PCR from the *D. discoideum* cDNA library using VIP 1960 and VIP 1961. The resulting fragment (1407bp) was ligated into BamHI-Xbal digested pDXA3C-MA to produce pMA02. When amoebae co-expressing pMA02 (encoding GFP- *Dd* HMGS (B)) and the peroxisomal marker mRFP-PTS1 the pattern of GFP fluorescence was punctate and superimposable on the fluorescence pattern of mRFP (Figure 3.2). Therefore, it appeared that HMGS (B) is a peroxisomal enzyme in *D. discoideum*.

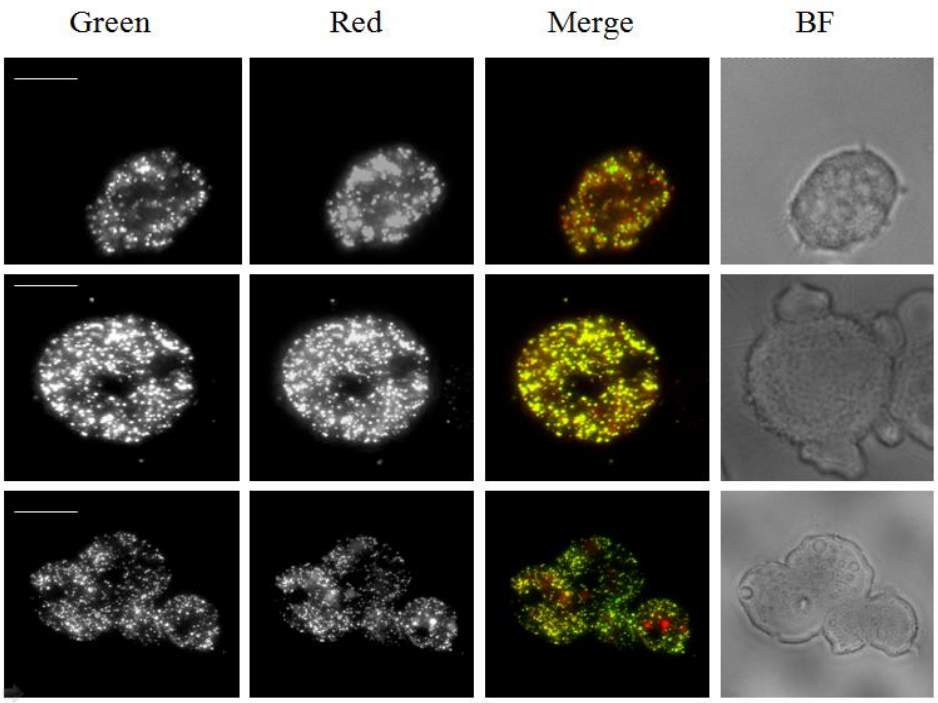

Figure 3.2: Demonstration of the peroxisomal location of *Dd*HMG-CoA synthase (B). Amoebae were expressing both GFP- *Dd*HMG-CoA synthase (B) (green) and a peroxisomal marker mRFP-PTS1 (red). The green fluorescence of *Dd*HMG-CoA synthase (B) is co-localized with the red fluorescence of the peroxisomal marker (mRFP-PTS1). Since peroxisomes have a tendency to move during the imaging it appeared that the patterns of green and red fluorescence are not completely co-localized. Scale bars 5µm.

3.2.2 Hydroxy-3-Methylglutaryl-Coenzyme A Reductase is localized to the endoplasmic reticulum

In *D. discoideum* there are two different genes encoding HMG-CoA reductase (HMGR1 and HMGR2). The amino terminus of each gene comprises hydrophobic and charged amino acids resembling a signal peptide. In mammalian cells it has been shown that HMG-CoA reductase is localized to the endoplasmic reticulum (Goldfarb, 1972, Liscum et al., 1985) although it has been suggested that the human enzyme is also peroxisomal (Kovacs et al., 2007, Keller et al., 1986, Krisans, 1996). A dual localization of *Arabidopsis* HMG-CoA reductase has also been observed (Leivar et al., 2005). Although *Arabidopsis* HMGR is localized to the ER, it is also clearly within spherical vesicular structures which are located in the cytoplasm and within the vacuole.

To verify the intracellular location of *D. discoideum* HMGR1 and HMGR2, we generated a C-terminal GFP-fusion protein for each isozyme as N-terminal fusions are likely to interfere with targeting to the ER. The full length of *Dd*HMGR2 was amplified by PCR from the cDNA by use of primers VIP 1409 and VIP 1410. The 1581bp DNA fragment was digested with XhoI and BamHI and ligated into linearised pMAA-1 to obtain pMA04. The resulting plasmid encoded HMGR2 joined to GFP by a linker sequence comprising Ser-Thr-Ser-Thr. In amoebae expressing *Dd*HMGR2-GFP a punctate distribution of fluorescence was observed (Figure 3.3). However, in amoebae co-expressing *Dd*HMGR2-GFP and the peroxisomal marker mRFP-PTS1 (monomeric red fluorescent protein having –SKL at the C-terminus), the pattern of GFP fluorescence was different from the pattern given by the mRFP (Figure 3.4). Thus, it was apparent that HMGR2 is not a peroxisomal enzyme.

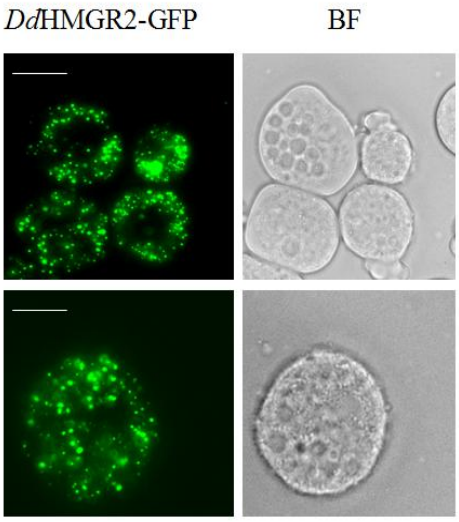

Figure 3.3: Analysis of the *Dd*HMGR2-GFP in *D.discoideum*. The green fluorescence in amoebae expressing the fusion protein DdHMGR-2-GFP was punctate. Scale bars 5µm.

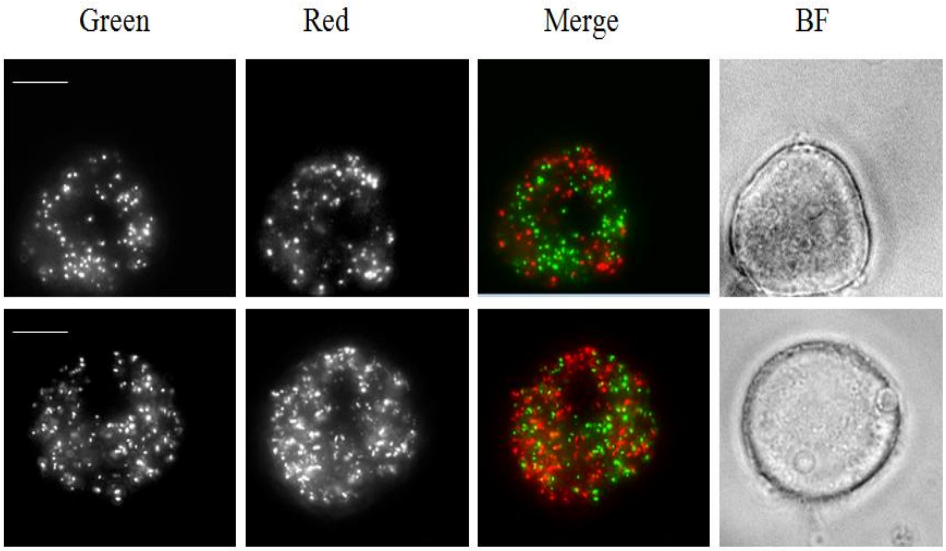

Figure 3.4: *Dd*HMGR2-GFP is not a peroxisomal enzyme in *D.discoideum*. Amoebae co-expressing *Dd*HMGR2-GFP and the peroxisomal marker mRFP-PTS1 showed two entirely different patterns of fluorescence. Scale bars 5µm.

In order to investigate further the location of *Dd*HMGR2, we generated an ER marker pMA25 encoding protein disulfide isomerase (PDI) tagged at its C-terminus with mRFP. The PDI had been identified as an endoplasmic reticulum resident enzyme in *D. discoideum* despite its lacking an ER-retrieval signal (Monnat et al., 1997). Amoebae co-expressing *Dd*HMGR2-GFP and PDI-mRFP showed a punctate distribution of GFP fluorescence which was superimposable on the fluorescence pattern of the ER marker (Figure 3.5). Thus, *Dd*HMGR2-GFP is localized to the ER in *D. discoideum.*

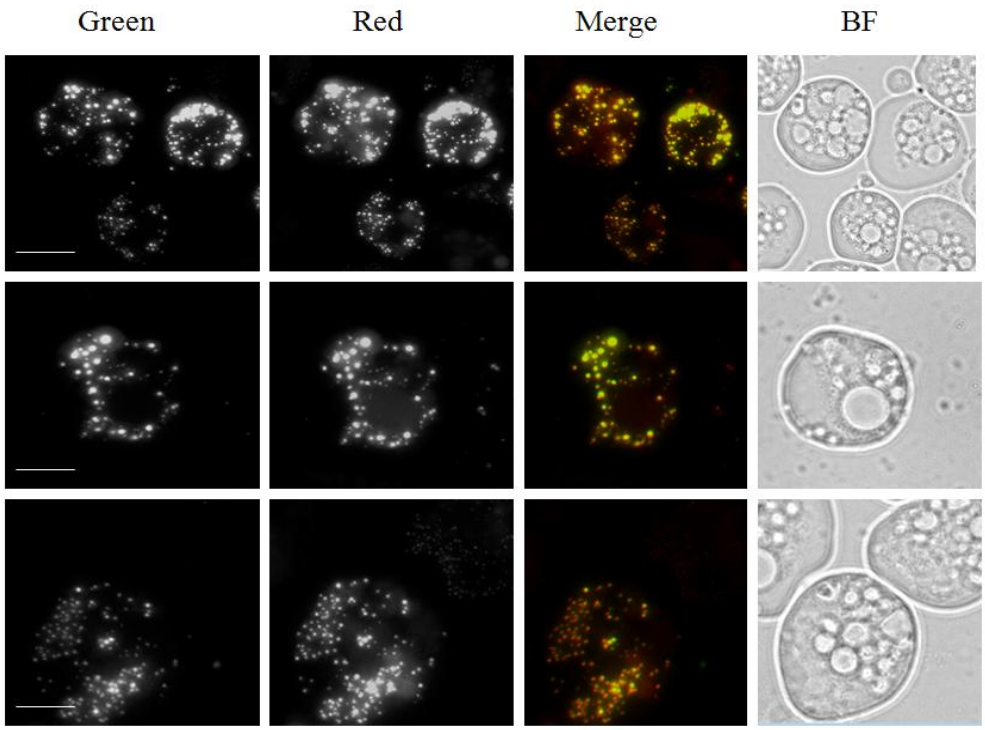

Figure 3.5: Demonstration of the ER localization of *Dd*HMGR2. When amoebae co-expressed *Dd*HMGR2-GFP and the ER marker PDI-mRFP, there was complete co-localization of the GFP and mRFP fluorescence. Scale bars 5µm.

Similarly, we investigated the intracellular location of *Dd*HMGR1 by generating a GFP-fusion protein. It was found that the initial part of the 5´ end (approximately 62 nucleotides) of the *Dd*HMGR1 cDNA was missing from the cDNA in two separate *D. discoideum* cDNA libraries. Therefore, the full length *Dd*HMGR1 cDNA was obtained by using oligonucleotide VIP 1753, comprising the first 83 nucleotides and VIP 1408. The DNA fragment was digested with XhoI and BamHI and ligated into XhoI-BamHI digested pMAA-1 to give pMA03. When amoebae expressed *Dd*HMGR1-GFP, a punctate pattern of fluorescence was observed (Figure 3.6). In amoebae co-expressing *Dd*HMGR1-GFP and PDI-mRFP the patterns of GFP and mRFP fluorescence were superimposable (Figure 3.7). Furthermore, the PDI-mRFP fluorescence was in the form of variably-sized spots exactly matching the *Dd*HMGR1-GFP fluorescence. It was therefore concluded that *Dd*HMGR1 is also associated with the ER.

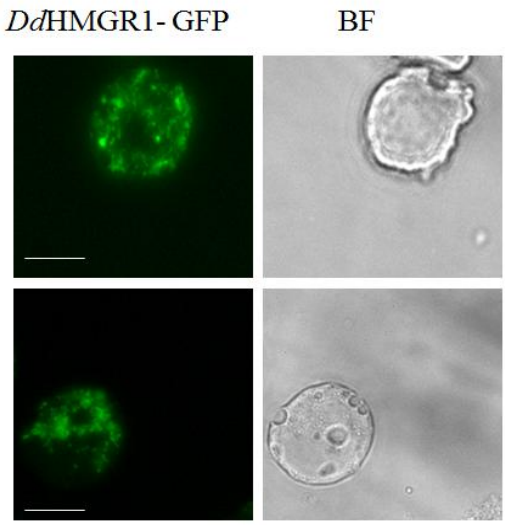

Figure 3.6: Analysis of the *Dd*HMGR1-GFP fusion protein in *D.discoideum*. Amoebae expressing the fusion protein *Dd*HMGR1-GFP exhibited a punctate pattern of GFP fluorescence. Scale bars 5µm.

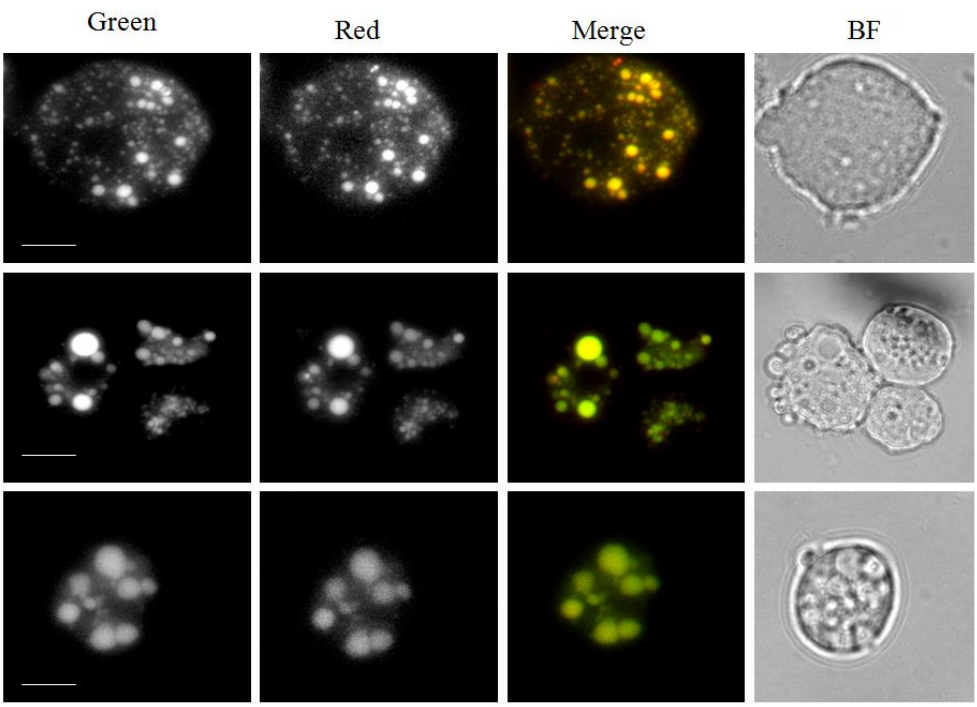

Figure 3.7: The intracellular localization of *D.discoideum* HMGR1. Amoebae expressing *Dd*HMGR1-GFP contained fluorescent vesicles of different sizes. The GFP fluorescence co-localized with the fluorescence of an ER marker (mRFP-PDI). Scale bars 5µm.

In the plant *Arabidopsis*, spindle-shaped (fusiform) organelles were observed after overexpressing ER-targeted GFP and it had been suggested that this structure arises owing to inclusion of so much enzyme within the lumen of the ER (Gunning 1998, Hawes et al., 2001). In addition, it has been reported that overexpressed membrane-targeted GFP fusion proteins cause formation of organelle aggregates (Lisenbee et al., 2003). Since *D. discoideum* immunoblots indicated that *Dd*HMGR1 seems to behave as an integral membrane protein (see section 3.2.3 below), it is difficult to explain the observed pattern of fluorescence given by *Dd*HMGR1-GFP but, possibly as suggested by Lisenbee et al, 2003, it is caused by organelle aggregation.

3.2.3 The membrane association of HMG-CoA Reductase in *D. discoideum*

In *D.discoideum* HMGR1 possesses three predicted transmembrane domains (TMD) as predicted by phyre2. Two of them located near the N-terminus extending from residues 18-33 and 52-66. The third TMD is located near to the C-terminus (amino acid residues 517-533). However, *Dd*HMGR2 does not seem to have a predicted TMD. In order to investigate the membrane association of *Dd*HMGR1 and *Dd*HMGR2, amoebae were disrupted by sonication and the suspension centrifuged at ~233,000 g_{max} for 1 hour. The pellet was then treated with 100mM sodium carbonate followed by high speed centrifugation ~ 233,000 g_{max} (section 2.9.3 Materials and Methods), a treatment that is believed to separate the lumenal proteins, which are found in the supernatant from the integral membrane proteins which remain associated with the membrane fraction (Fujiki *et al.*, 1982). It was found that *Dd*HMGR2 was released into the supernatant after the treatment with carbonate, whereas the *Dd*HMGR1 could not be extracted with Na_2CO_3 pH 11.4. These results suggested that *Dd*HMGR1 is very strongly associated with the ER membrane and could be an integral membrane protein (Figure 3.8). By contrast, *Dd*HMGR2 behaves as a luminal protein but it is possible that it is loosely bound to the ER membrane (Figure 3.8). These results are in agreement with the bioinoformatic predictions.

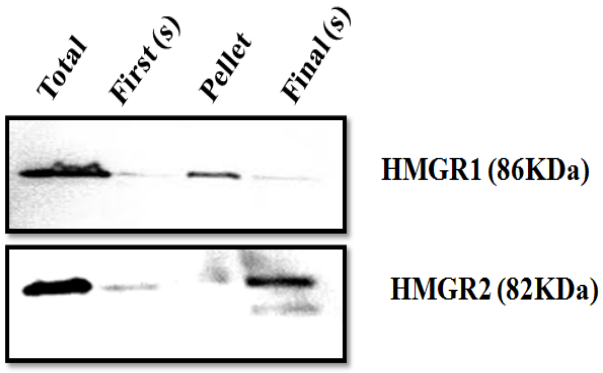

Figure 3.8: Association of *D. discoideum* HMG-CoA Reductases with the ER membrane. Amoebal homogenate was centrifuged at 4 ˚C for 1 hour at 50,000 rpm using a Beckman 50 Ti rotor. The supernatant (first s) was separated from the pellet and subjected to SDS- PAGE and western blot analyses using an anti-GFP antibody. The pellet fraction was extracted with 100mM Na_2CO_3 pH 11.4. Extracted proteins were separated from the membrane by high speed

centrifugation (~ 233,000 g_{max}). Samples of the pellet and supernatant (final s) fractions were analyzed by immunoblot analyses using the anti-GFP antibody. Each sample on the immunoblot was derived from the same number of cells.

3.2.4 Mevalonate kinase fusion proteins are localized to the cytosol

The amino-terminal region of *D. discoideum* mevalonate kinase (*Dd*MVK) contains a putative PTS2 (KIILFGEHA) (Table 3.1). We generated two GFP fusion proteins to determine the intracellular location of *Dd*MVK. The first comprised *Dd*MVK linked to the amino-terminus of GFP. The DNA fragment amplified from the *D. discoideum* cDNA library by using primers VIP 1269 and VIP 1270 (section 2.3 in the Materials and Methods) encoded *Dd*MVK with the addition of the carboxy-terminal amino acids sequence Ser-Thr-Ser-Thr. This DNA fragment was digested with HindIII and BamHI and inserted into HindIII-BamHI digested pGFP. The resulting plasmid was named pMA05.

The second construct, which comprised *Dd*MVK joined to the C-terminus of GFP, was generated similarly. A *Dd*MVK cDNA, with the addition of the N-terminal amino acids sequence Ser-Thr-Ser-Thr, was amplified by PCR using pMA05 as the DNA template and VIP 1361 plus VIP 1362 as primers and ligated as a BamHI-XbaI fragment into the PDXA3C-MA vector to give pMA06. Fluorescence in amoebae transformed with either of the two constructs was in the cytosol (Figure 3.9). Hence, it appears that the putative PTS2 does not direct *Dd*MVK to the peroxisomes.

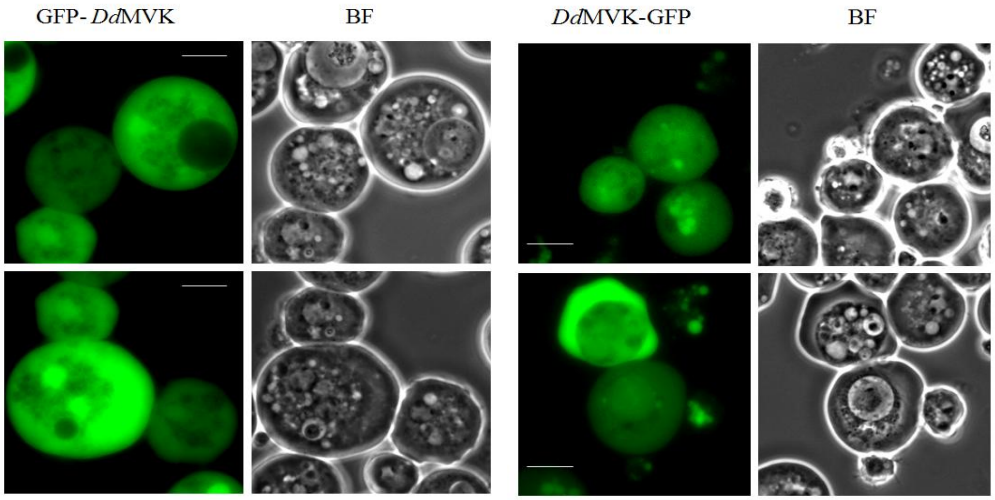

Figure 3.9: Localization of *D. discoideum* mevalonate kinase. A) Amoebae transformed to express the GFP-*Dd*MVK fusion protein. B) Amoebae transformed to express the *Dd*MVK-GFP fusion protein. In both case a cytosolic distribution of green fluorescence was observed. Scale bars 5µm.

Organism	The putative PTS2	Position	Localization	References
D. discoidium	KIILFGEHA	16-24	Cytosol	This study
C.roseus	KIILAGEHA	10-18	Cytosol	Simkin et al., 2011
A.thaliana	KIILAGEHA	10-18	Cytosol	Simkin et al., 2011
R.norvegicus	KVILHGEHA	13-21	Peroxisomes	Kovacs et al., 2007
H. sapiens	KVILHGEHA	13-21	Cytosol	Hogenboom et al., 2004
Consensus PTS2				**(R/K) (L/V/I) X_5(H/Q) (L/A)**

Table 3.1: Sequence of the putative PTS2 within mevalonate kinases from different organisms.

In mammals, MVK contains a consensus PTS2 (e.g. KVILHGEHA in the rat enzyme) which was found to target the enzyme into the peroxisomes (Kovacs et al., 2007). However, the cytosolic localization of *Dd*MVK is in agreement with the previous studies identifying the localization of *Catharanthus roseus* and *Arabidopsis thaliana* MVK to the cytosol (Simkin et al., 2011). Furthermore, five proteins in mice, apparently possessing a consensus PTS2, have been identified by a bioinformatics approach but none of them is directed to the peroxisome (Mizuno et al., 2008). A consensus PTS2 sequence is present near to the amino-terminus of some archaebacteria and eubacteria MVK even though bacteria lack peroxisomes (Houten et al., 2000). This evidence would imply that a putative PTS2 sequence does not necessarily direct a protein into the peroxisomes, as appears to be the case for the *Dd*MVK.

3.2.5 The GFP-Phosphomevalonate kinase fusion protein is localized to the peroxisome

The *D. discoideum* phosphomevalonate kinase (*Dd*PMK) contains a putative PTS1 (-Pro-Lys-Leu_{COOH}) at the C-terminus whereas the N-terminus of *Dd*PMK does not seem to contain any putative targeting signal. Therefore, the intracellular location of *Dd*PMK was determined by generating a GFP fusion protein without masking the putative PTS1 at the carboxy-terminus. The open reading frame of *Dd*PMK was amplified by PCR from the cDNA library using VIP 1267 and VIP 1268. This DNA fragment encodes *Dd*PMK, with the addition of the N-terminal amino acid linker sequence Ser-Thr-Ser-Thr, was digested and ligated into BamHI-XbaI digested pDXA3C-MA. The resulting plasmid, pMA07, encoded GFP-*Dd*PMK. In amoebae expressing pMA07 a punctate distribution of fluorescence was observed suggesting that *Dd*PMK is peroxisomal (Figure 3.10).

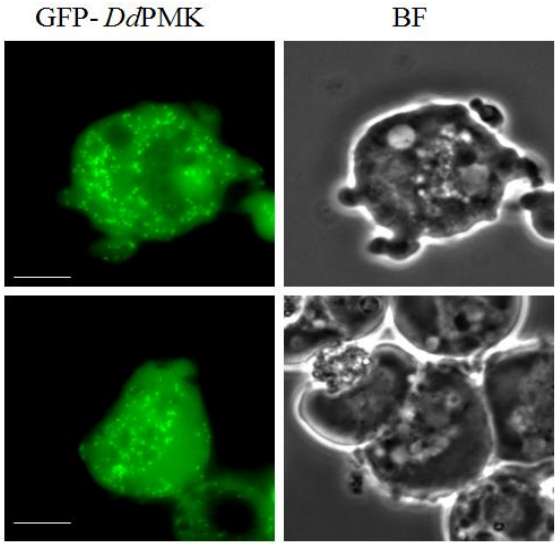

Figure 3.10: Analysis of the GFP-*Dd*PMK fusion protein in *D.discoideum*. Amoebae transformed to express GFP-*Dd*PMK show a punctate pattern of GFP fluorescence**.** Scale bars 5µm.

To confirm the peroxisomal location, the amoebae were re-transformed to express the peroxisomal marker mRFP-PTS1. The punctate fluorescence of *Dd*PMK and the peroxisomal marker co-localized (Figure 3.11). Thus, it could be concluded that *Dd*PMK is localized to peroxisomes.

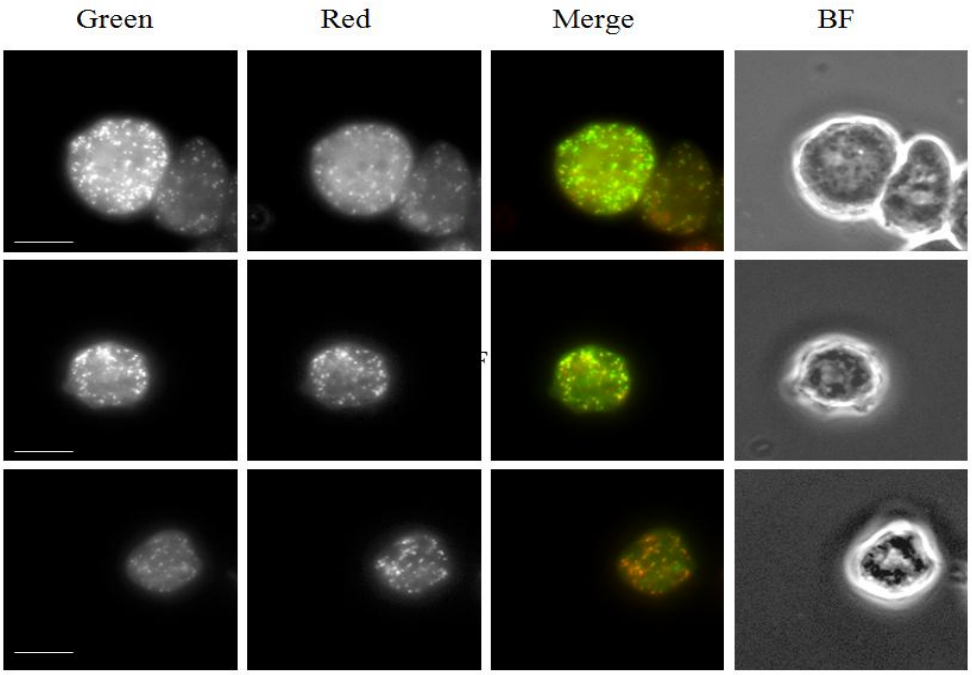

Figure 3.11: Demonstration of the peroxisomal localization of *Dd*PMK. Amoebae were transformed with two plasmids to express both GFP-*Dd*PMK (green) and the peroxisomal marker mRFP-PTS1 (red). Co-localization of the GFP and mRFP fluorescence in the peroxisomes was observed. Scale bars 5µm.

3.2.6 *D. discoideum* phosphomevalonate kinase is imported into the peroxisomes by use of its PTS1 (-PKL)

To investigate whether the putative PTS1 is essential for *Dd*PMK localization to peroxisomes, two constructs were generated. The first construct (PMA09) was generated to encode a GFP-*Dd*PMK fusion protein in which the last three amino acids corresponding to the PTS1 of *Dd*PMK had been removed. When amoebae were transformed with this construct, the fluorescence indicated that the *Dd*PMKΔPTS1 was cytosolic (Figure 3.12).

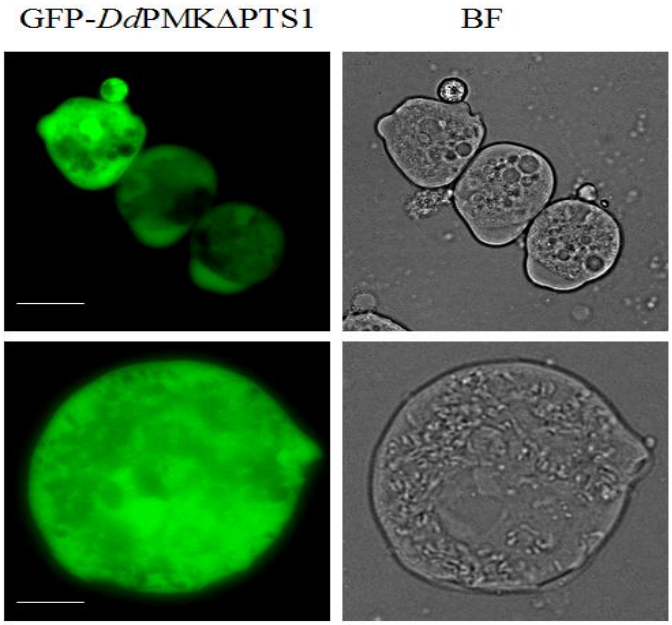

Figure 3.12: Analysis of the GFP-*Dd*PMKΔPTS1 fusion protein in *D. discoideum*. Amoebae transformed to express GFP-*Dd*PMKΔPTS1 showed green fluorescence throughout the cytosol. Scale bars 5µm.

In the second construct, oligonucleotides VIP 1372 and VIP 1373, encoding the last 12 amino acids of *Dd*PMK including the putative PTS1 (VAIDMSHITPKL$_{COOH}$), were annealed and ligated into BamHI and XbaI digested pDXA3C-MA to give pMA08 (Figure 3.13). When amoebae were transformed with this construct, a typical punctate pattern of peroxisomal fluorescence was observed (Figure 3.14). Hence, use of these two constructs confirmed that *Dd*PMK localizes to peroxisomes by making use of a PTS1 (-PKL).

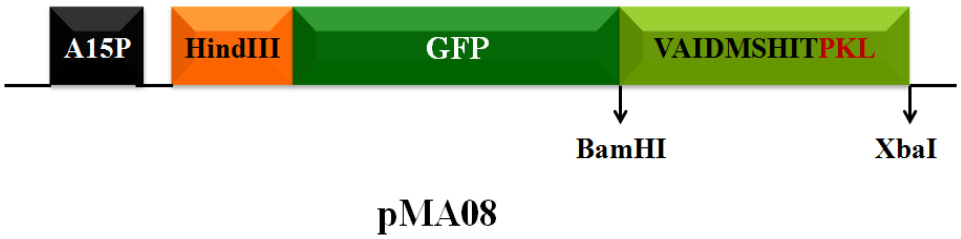

Figure 3.13: Schematic structure of pMA08 which consisted of the putative PTS1 of *Dd*PMK added to the C-terminus of GFP.

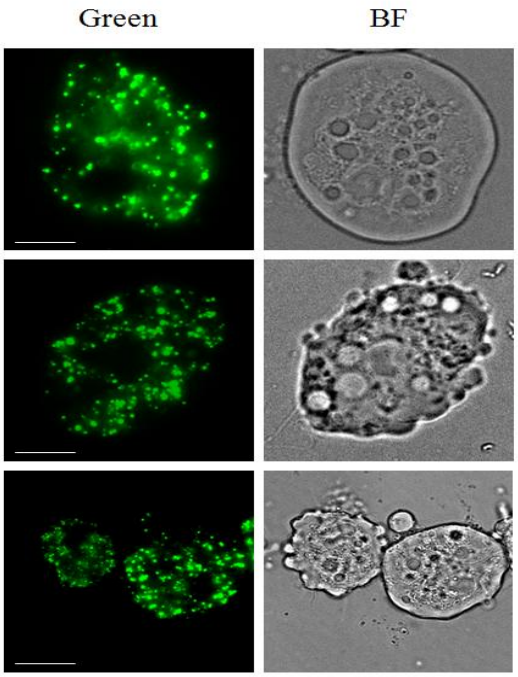

Figure 3.14: The C-terminal PTS1 of *Dd*PMK is responsible for directing the fusion protein into the peroxismes. Amoebae transformed to express the last 12 amino acid residues of *Dd*PMK fused to GFP displayed a typical peroxisomal pattern. Scale bars 5µm.

3.2.7 Diphosphomevalonate Decarboxylase fusion proteins are cytosolic in *D. discoideum*

In *D. discoideum*, diphosphomevalonate decarboxylase (*Dd*DMPD) has neither a PTS1 nor a PTS2. The intracellular location of *Dd*DMPD was investigated by expressing the enzyme, fused C-terminally to GFP, in amoebae. The full length *Dd*DMPD cDNA was amplified by PCR from the cDNA library by using primers VIP 1253 and VIP 1254. This DNA fragment was digested with HindIII and BamHI and ligated into HindIII-BamHI digested pGFP to obtain pMA11. When this construct was expressed in *D discoideum* amoebae, the GFP fluorescence was observed in the cytosol (Figure 3.15 A). pMA10, encoding *Dd*DMPD tagged with GFP at its N-terminus, was generated similarly. The fluorescence of the GFP was again observed in the cytosol (Figure 3.15 B). Thus, these results indicated that *Dd*DMPD is not peroxisomal in *D. discoideum*. This observation is entirely consistent with the absence of a PTS from this enzyme.

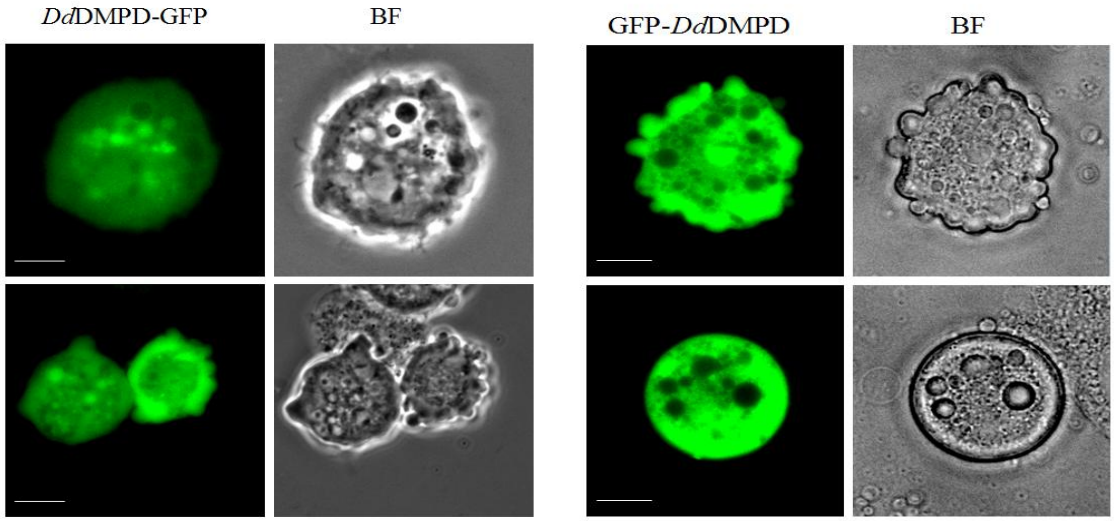

Figure 3.15: The intracellular location of *D. discoideum* diphosphomevalonate decarboxylase. Amoebae were transformed to express either *DdD*MPD-GFP (A) or GFP-*DdD*MPD (B). The pattern of fluorescence indicates a cytosolic distribution for the fusion proteins. Scale bars 5µm.

3.2.8 Isopentenyl Diphosphate: Dimethylallyl Diphosphate (IDP) Isomerase fusion proteins are localized to the cytosol in *Dictyostelium discoideum*

It has been claimed that the hamster (*Mesocricetus auratus*) IDP-isomerase is a peroxisomal enzyme and that it is directed to the peroxisome by an unusual PTS1 (-His-Arg-Met_{COOH}). There is a similar C-terminal triplet (-His-Arg-Tyr_{COOH}) in the *Dictyostelium discoideum* IDP-isomerase. This amino acid triplet of IDP-isomerase is identical in several species of slime mould (Figure 3.16) which implied that the *Dd*IDP-isomerase might also be peroxisomal enzyme.

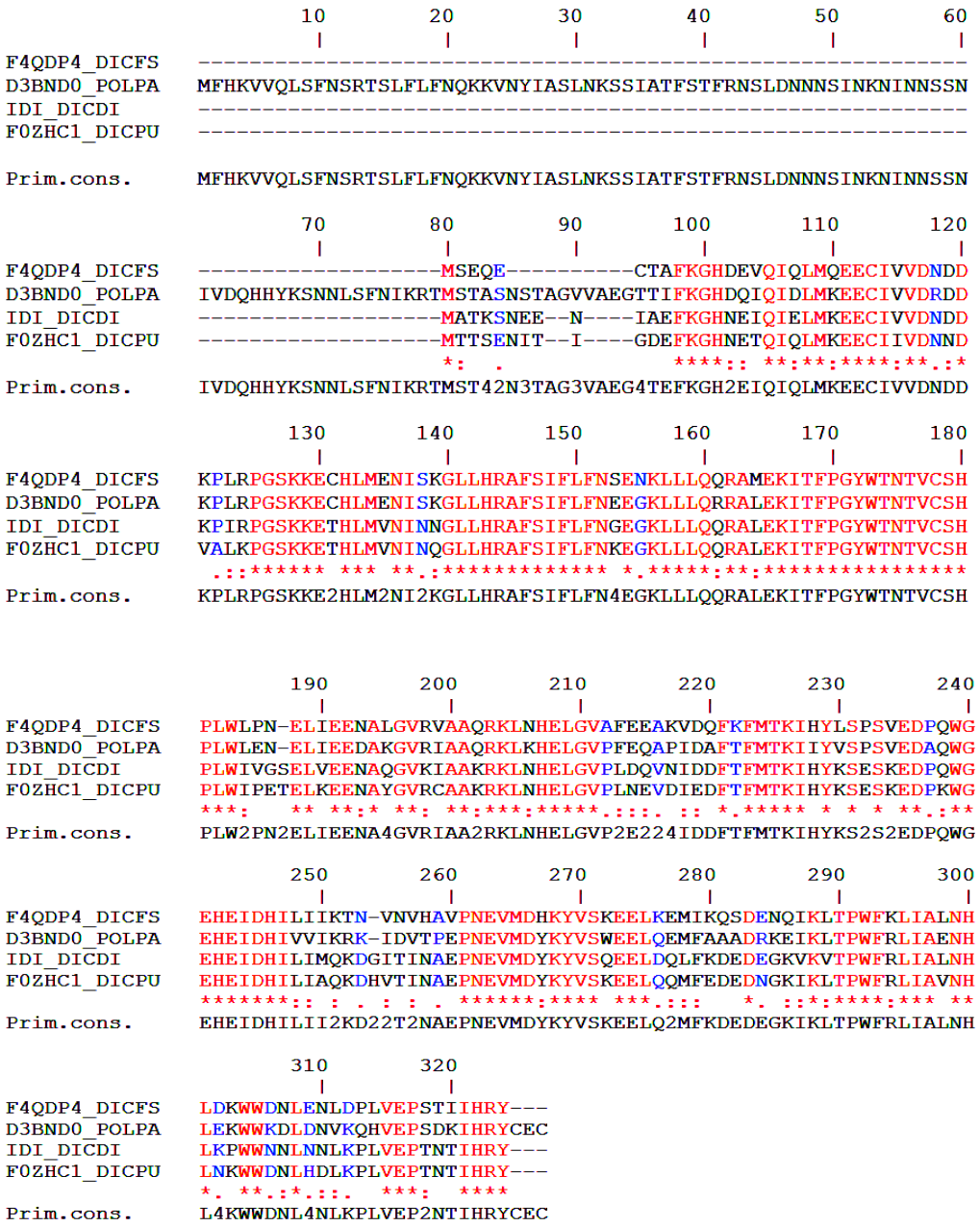

Figure 3.16: Alignment of the amino acid sequences of isopentenyl diphosphate isomerase from related species of slime moulds. (1) *Dictyostelium fasciculatum*. (2) *Polysphondylium pallidum* (3) *Dictyostelium discoideum* (4) *Dictyostelium purpureum*. The isomerase from all four species has a putative PTS1 (-HRY).

The intracellular location of *Dd*IDP-isomerase was first investigated by generating a construct comprising *Dd*IDP-isomerase tagged at its N-terminal end with GFP to avoid masking the putative PTS1. The proof-reading enzyme Accuzyme and the primers VIP 1288 and VIP 1289 were used to amplify the *Dd*IDP-isomerase cDNA from the *D. discoideum* cDNA library. The resulting DNA fragment was ligated into PDXA3C-MA immediately downstream of the sequence encoding GFP by using the BamHI and XbaI restriction sites to obtain pMA12. Wild type amoebae were transformed with the pMA12 to express the GFP-*Dd*IDP isomerase. The fluorescence of the fusion protein was localized to the cytosol (Figure 3.17 A). It thus appeared that the amino acid triplet (–HRY) at the C-terminus of *Dd*IDP-isomerase does not act as a PTS1. Although the N-terminus of IDP-isomerase in *D.discoideum* appears not to contain a putative PTS2, a second construct (pMA13) was generated to encode *Dd*IDP-isomerase-GFP. pMA13 was constructed by ligating the full length *Dd*IDP-isomerase cDNA into HindIII-BamHI digested pGFP. When *D. discoideum* amoebae were transformed with this construct, the GFP fluorescence indicated that the *Dd*IDP-isomerase-GFP fusion protein again remained in the cytosol (Figure 3.17 B).

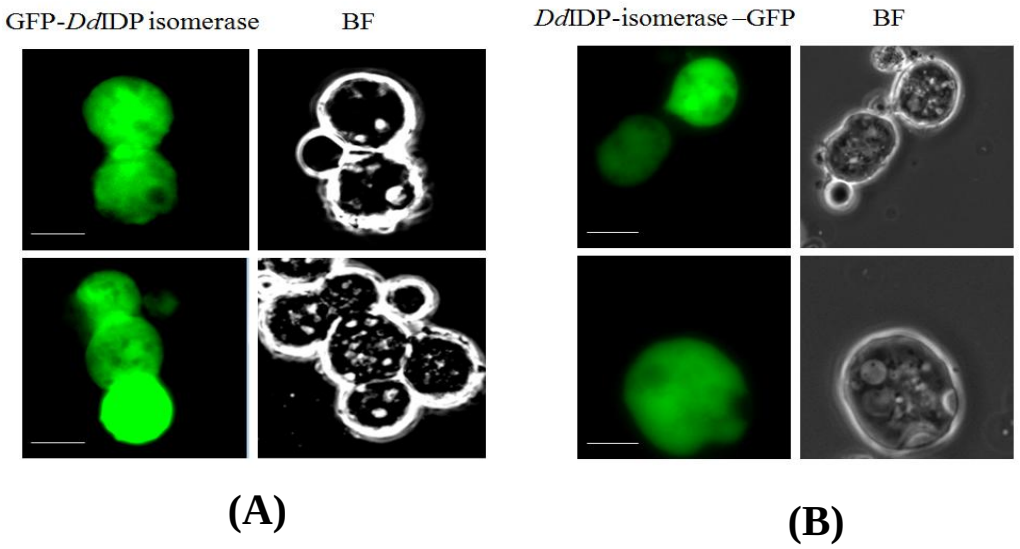

Figure 3.17: The intracellular location of *Dd*IDP-isomerase. Amoebae transformed to express either GFP-*Dd*IDP-isomerase (A) or *Dd*IDP-isomerase-GFP (B) exhibit green fluorescence in the cytosol. Scale bars 5µm.

3.2.9 Generating IDP-isomerase internal GFP fusion protein

In *Arabidopsis* there are two genes for IDP-isomerase and the pre-mRNA transcribed from each gene can be processed to give either a long or short isform. Recent studies have shown that the two short versions of IDP-isomerase are localized to peroxisomes (Sapir-Mir et al., 2008). These have a putative PTS1 (-HKL) at the C-terminus. However, both GFP-IDP isomerase fusion proteins localized to the cytosol. Furthermore, when the short versions of IDP-isomerase were tagged with GFP at the C-terminal end, the fusion proteins again remained in the cytosol (Nakamura et al., 2001, Okada et al., 2008, Phillips et al., 2008). However, a peroxisomal localization for *Arabidopsis* IDP-isomerase was obtained for a fusion protein in which the GFP was placed ten amino acids from the C-terminal end of the IDP-isomerase. It was concluded that sequences at both the N-terminal and C-terminal ends of the short versions of *Arabidopsis* IDP-isomerase are needed to direct the enzymes to the peroxisomes.

To determine whether both C-terminal and N-terminal sequences in the *D. discoideum* IDP-isomerase direct the enzyme to the peroxisomes, an internal GFP fusion was produced. First, the full length IDP-isomerase (700bp) was amplified by PCR from pMA13 by using primers VIP 1418 and VIP 1419. This DNA fragment was ligated between the HindIII and KpnI sites of digested pDXA3C. Then, the full length GFP cDNA was amplified by PCR from pMA13 using primers VIP 1420 and VIP 1421. This DNA fragment was inserted downstream of the IDP-isomerase between the SacI and XhoI restriction sites. Finally, a DNA fragment encoding the final 12 amino acids of the carboxy-terminus of *Dd*IDP-isomerase and containing the potential PTS1 (-HRY) was added between the XhoI and XbaI sites (Figure 3.18). Amoebae were transformed with the final construct (pMA14) to allow expression of the internal GFP fusion protein. The tagged *Dd*IDP-isomerase still remained in the cytosol (Figure 3.19). Hence, IDP-isomerase does not appear to be a peroxisomal enzyme in *D. discoideum*.

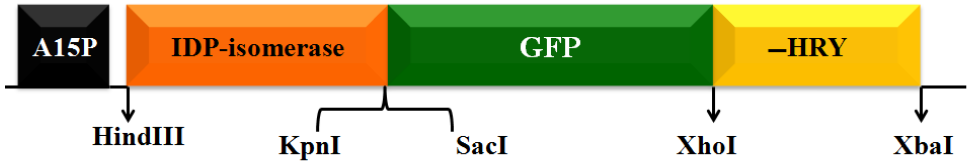

pMA14

Figure 3.18: Schematic structure of pMA14 which encodes *Dd* IDP-isomerase with an internal GFP tag.

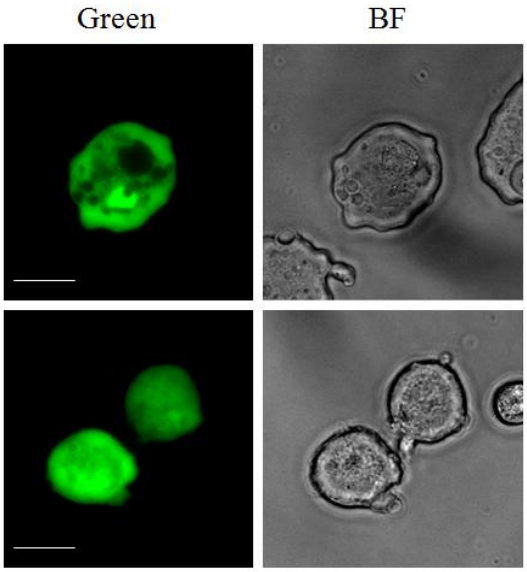

Figure 3.19: Localization of *Dd*IDP-isomerase having an internal GFP tag. Amoebae expressing *Dd*IDP-isomerase with an internal GFP tag exhibited fluorescence indicating that the fusion protein is cytosolic. Scale bars 5µm.

3.2.10 Expression of mRFP terminating in the triplet –HRY

A further experiment was carried out to investigate whether the putative PTS1-sequence (-HRY) is able to target the red fluorescent protein to the peroxisomes. pmRFP (Nuttall *et al*., 2012) was modified so that it encoded mRFP attached to the eight C-terminal amino acids ($PTNTIHRY_{COOH}$) of *Dd*IDP-isomerase. When amoebae were transformed with this plasmid, the mRFP was localized in the cytosol (Figure 3.20). By contrast, it had previously been shown that mRFP having the consensus PTS1 sequence SKL at its C-terminus is peroxisomal (Nuttall *et al*., 2012). Hence, it was apparent that the triplet –HRY is not a functional PTS1 in *D. discoideum*.

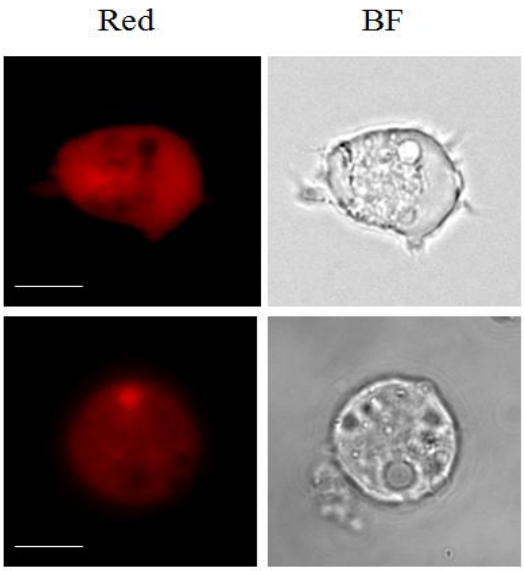

Figure 3.20: The C-terminal PTS1 of *Dd*IDP-isomerase is not functional. Amoebae transformed to express the eight C-terminal amino acid residues of *Dd*IDP-isomerase fused to mRFP exhibited a pattern of fluorescence indicating that the fusion protein is cytosolic. Scale bars 5µm.

3.2.11 Demonstration that the three cytosolic mevalonate pathway enzymes *Dd*MVK, *Dd*MPD and *Dd* IDP-isomerase, expressed as GFP-fusion proteins in *D. discoideum*, were full length

To confirm that these three enzymes were not accumulating in the cytosol owing to partial degradation and loss of peroxisome-directed signal sequences, it was necessary to demonstrate that full length GFP-fusion proteins were accumulating in the cytosol in *D. discoideum* amoebae. Immunoblot analyses were therefore performed. Amoebal extracts (section 2.9.1 in the Materials and Methods) were analyzed by SDS-PAGE and western blotting, the GFP tags being detected by use of a monoclonal antibody. GFP was used as a control protein. In each case, a protein of the expected molecular weight was detected (Figure 3.21). Furthermore, there was little evidence for accumulation of breakdown products. These results indicated that it was the intracellular location of each full-length enzyme in amoebae that had been determined in the previous experiments making use of fluorescence microscopy.

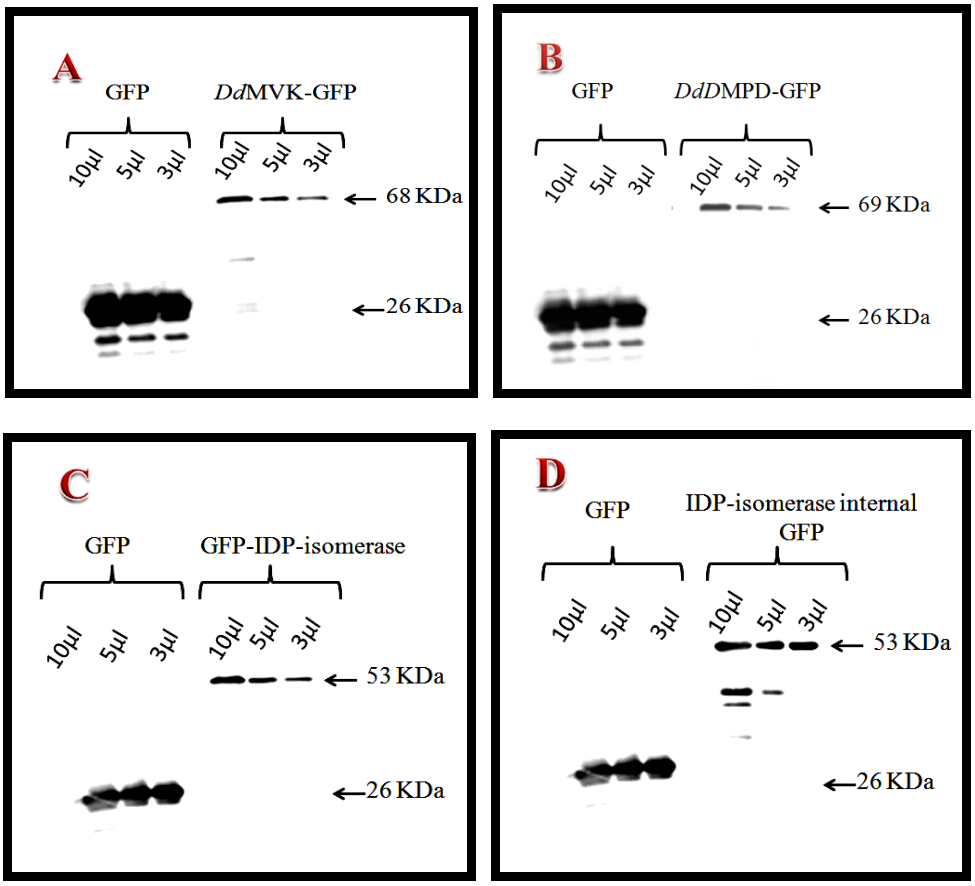

Figure 3.21: Immunoblot analyses of mevalonate pathway enzymes fused to GFP. (A) Mevalonate kinase-GFP (B) Diphosphomevalonate decarboxylase-GFP (C) GFP-IDP-isomerase (D) IDP-isomerase internal GFP.

3.3 Discussion

The use of the GFP/mRFP tagged enzyme approaches allowed us to determine the intracellular locations of the mevalonate pathway enzymes in *Dictyostelium discoideum* amoebae. It has previously been shown that FDP-synthase is a peroxisomal enzyme in *D.discoideum* (Nuttall *et al.,* 2012). Furthermore, in this chapter a peroxisomal location for both the second isozyme of HMG-CoA synthase and phosphomevalonate kinase has been identified. As in other organisms, both HMG-CoA reductases seem to be associated with the ER. Finally, four enzymes of the mevalonate pathway (i.e. HMG-CoA synthase (A), mevalonate kinase, diphosphomevalonate decarboxylase and IDP-isomerase) were appeared to be ctosolic (Table3.2).

Enzyme	N-terminal sequence	C-terminal sequence	The Putative PTS	Enzyme location
HMGS (A)	MTKPENIGIH GIEVYFPSTY VAQEDLEKFD	RATKSVLSIL	NO PTS	**Cytosol**
HMGS (B)	MKKTKDIGIC AIDIYFPQTY VNQSELKKYD	KSKPIISSKL	PTS1	**Peroxisome**
HMGR1	MLFAPPNLET KELFWIIYILIL IPKVFAKV	HLQYNRAKTN	NO PTS	**ER**
HMGR2	MIRIGSNLIK QSIKNTNKSG ISRFFTTGSN	SMTHNLPHSD	NO PTS	**ER**
MVK	MISNQDNIIQ VSAPGKIILF GEHAVVLEKT	VSINILPIQK	PTS2	**Cytosol**
PMK	MERVVCSAPG KVLVTGGYLV LDKKYDGIVF	IDMSHITPKL	PTS1	**Peroxisome**
DPMD	MVLASVTCTA PVNIAVIKYW GKRDENIILP	NTTGLPKQLN	NO PTS	**Cytosol**
IDP- isomerase	MATKSNEENI AEFKGHNEIQ IELMKEECIV	VEPTNTIHRY	PTS1	**Cytosol**
FDP-synthase	MNNQSLQRAA MISEHLAPTS	LSKIYKRDL	PTS2	**Peroxisome**

	ELNMNQTSAP
Consensus PTS1	**(S/ A/ C) (K/R/H) (L/M)**
Consensus PTS2	**(R/K) (L/V/I) X_5(H/Q) (L/A)**

Table 3.2: The intracellular locations of the mevalonate pathway enzymes in *Dictyostelium discoideum* based on fusion protein studies.

Both *Dd*HMGS(B) and phosphomevalonate kinase possess a putative PTS1 SKL and PKL at the C-terminus respectively. The amino acid triplet Ser-Lys-Leu is a highly efficient peroxisomal targeting signal and when GFP tagged at the C-terminus with Ser-Lys-Leu was expressed in amoebae, a typical peroxisomal pattern of fluorescence was observed (Nuttall et al., 2012). The C-terminal tripeptide Pro-Lys-Leu agrees with the consensus PTS1 sequence for two out of the three amino acids and it has previously been predicted as a possibly functional, though minor, PTS1 tripeptide (Reumann, 2004). In addition, it has been shown that both mammalian and plant Δ^3,Δ^2 enoyl CoA isomerases, possessing the amino acid triplet –PKL at the C-terminus, are peroxisomal enzymes (Geisbrecht et al., 1999, Goepfert et al., 2008). In *D.discoideum*, it was found that this sequence acted as a PTS1 when the C-terminus of GFP was joined to the final 12 amino acid residues (VAIDMSHITPKL$_{COOH}$) of *Dd*PMK. Furthermore, *Dd*PMK from which the putative PTS1 (-PKL) was absent was no longer imported into the peroxisomes. Therefore, it is concluded that *Dd*PMK, as well as *Dd*HMGS(B), is a peroxisomal matrix enzyme.

The cytosolic location of *Dd*HMG-CoA synthase A and *Dd*DPMD is not unexpected because neither of these enzymes possesses a PTS. Although it has been proposed that the mammalian HMG-CoA synthase localizes to the cytosol (Ayte et al., 1990), it has also been claimed that it is a peroxisomal matrix protein that makes use of a sequence (SVX_5QL) similar to a PTS2 (Olivier et al., 2000) to gain entry to the peroxisomes.This putative PTS2 is absent from the *Dd*HMG-CoA synthase A.

The cytosolic location of *D.discoideum* diphosphomevalonate decarboxylase conflicts with work by Simkin et al., (2011) on plants. They proposed that *Cr*DPMD (*C.roseus*) and *At*DPMD (*A.thaliana*) are localized to the peroxisomes. This may be due to the presence of a sequence resembling a putative PTS2 (SVTLDP(A/D)HL) present in each enzyme around residue 40. In addition, Kovacs et al., (2007) postulated that mammalian DPMD is imported into the peroxisomes by a similar unusual PTS2 motif (SVX_5QL). Nevertheless, other investigations have not confirmed that the mammalian DPMD is peroxisomal (Hogenboom et al., 2004a, Michihara et al., 2001). The cytosolic location for the *Dd*DPMD is in agreement with the latter observations. Furthermore, the *Dd*DPMD lacks the unusual PTS2 that has been proposed to allow the plant and mammalian DPMDs to enter the peroxisomes (Table3.2).

Although two of the mevalonate pathway enzymes, mevalonate kinase and IDP-isomerase, in *D.discoideum* appear to possess a PTS, neither PTS is functional. The putative PTS2 in *D.discoideum* mevalonate kinase, as in plant and mammalian mevalonate kinases, matches exactly the consensus PTS2 sequence but several observations, discussed previously, support the conclusion that this conserved sequence does not act as a PTS2. Furthermore, the crystal structure of rat MVK revealed that the amino terminal lysine residue of the putative PTS2 is part of the ATP binding site (Fu et al., 2002). Therefore, despite the single investigation that identified a peroxisomal location for the mammalian MVK, it would appear that in *D.discoideum* and also in other organisms, the putative PTS2 is not a functional peroxisomal targeting signal.

By contrast, the putative PTS1 (-HRY) of *D. discoideum* IDP-isomerase matches only poorly the PTS1 consensus sequence. However, it has been shown that the hamster IDP-isomerase is directed into the peroxisomes by use of a similar sequence (-HRM) (Paton et al., 1997) and the second isozyme of human IDP-isomerase (IDI2), containing a putative PTS1 (-HRV), has been identified as a peroxisomal enzyme (Paton et al., 1997, Clizbe et al., 2007). Although the putative PTS1 in the *Dd*IDP-isomerase is only slightly different from the mammalian PTS1s, it does not seem to direct the enzyme into the peroxisomes. However, there is no known example of any PTS1 ending in tyrosine and this

would support the conclusion that the *Dd*IDP-isomerase is not a peroxisomal enzyme but is cytosolic.

Finally, it has been shown previously that the final mevalonate pathway enzyme in *D.discoideum*, FDP-synthase, is peroxisomal. This enzyme has a slightly unusual PTS2 that directs it to the peroxisome (Nuttall et al., 2012).

Taken together, the results presented in this chapter allow us to describe the intracellular locations of the mevalonate pathway enzymes in the same organism *D.discoideum*. However, the reasons for the distribution of the pathway enzymes between different cell compartments (i.e peroxisomes, cytosol and endoplasmic reticulum) are unclear. However, the intracellular location of the enzymes requires that all of the phosphorylated intermediates on the mevalonate pathway have to cross the peroxisomal membrane.

The approach I used allowed us to identify proteins that can be imported into peroxisomes. Since these experiments were based on overexpression and tagging with fluorescent proteins, we can not exclude that the cytosolic localization observed in high expressing cells or in some of the fusions are due to the experimental set up or really reflect localization of these enzymes to the cytosol.

Chapter 4

The initial steps of sterol biosynthesis in *D. discoideum* occur in the peroxisomes

4.1 Introduction

The enzymes catalyzing the reactions involved in sterol biosynthesis are associated with the endoplasmic reticulum (Nes, 2011). However, it was noticed that, *Dd*squalene synthase, which catalyses the first unique step of sterol biosynthesis (Figure 4.1), possesses an apparent PTS1 (Ser-Lys-Leu $_{COOH}$). This sequence is also present in other species of slime mould such as *Dictyostelium fasciculatum* and *Polysphondylium pallidum* (Figure 4.2) but appears to be absent from squalene synthase enzymes in other groups of organisms. Moreover, two of the other enzymes catalyzing early steps of sterol biosynthesis in *D.discoideum* also possess a putative PTS1, i.e. oxidosqualene cyclase and cycloartenol-C-24-methyltransferase (Figure 4.1). This suggested that the peroxisome may uniquely play an important role in the sterol biosynthetic pathway in *D.discoideum*.

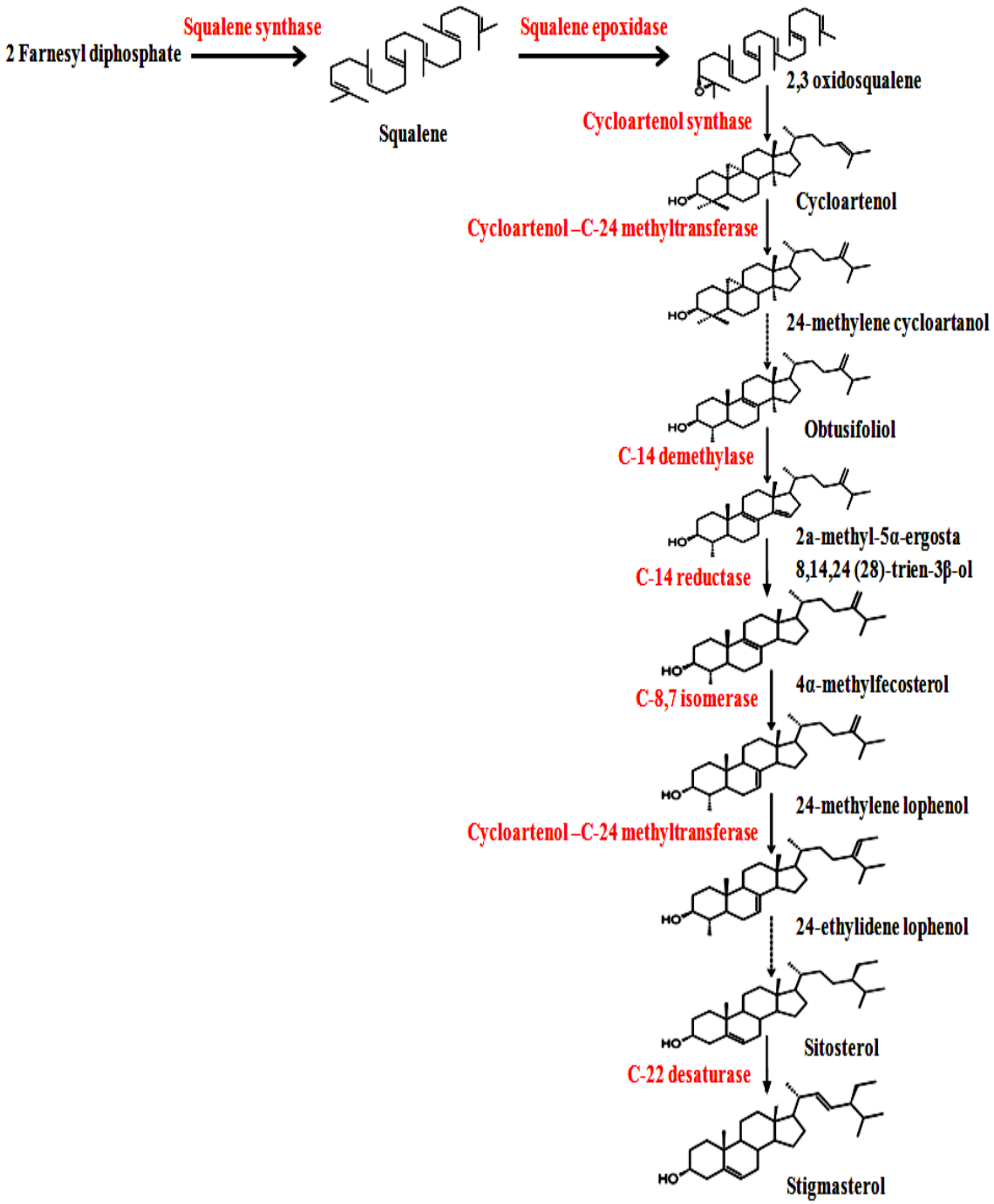

Figure 4.1: Sterol biosynthesis in higher plants. This diagram shows a summary of the sterol biosynthesis pathway of higher plants. Multiple biosynthetic steps are indicated by broken arrows. In *D.discoideum* as in plants squalene is cyclised to form cycloartenol.

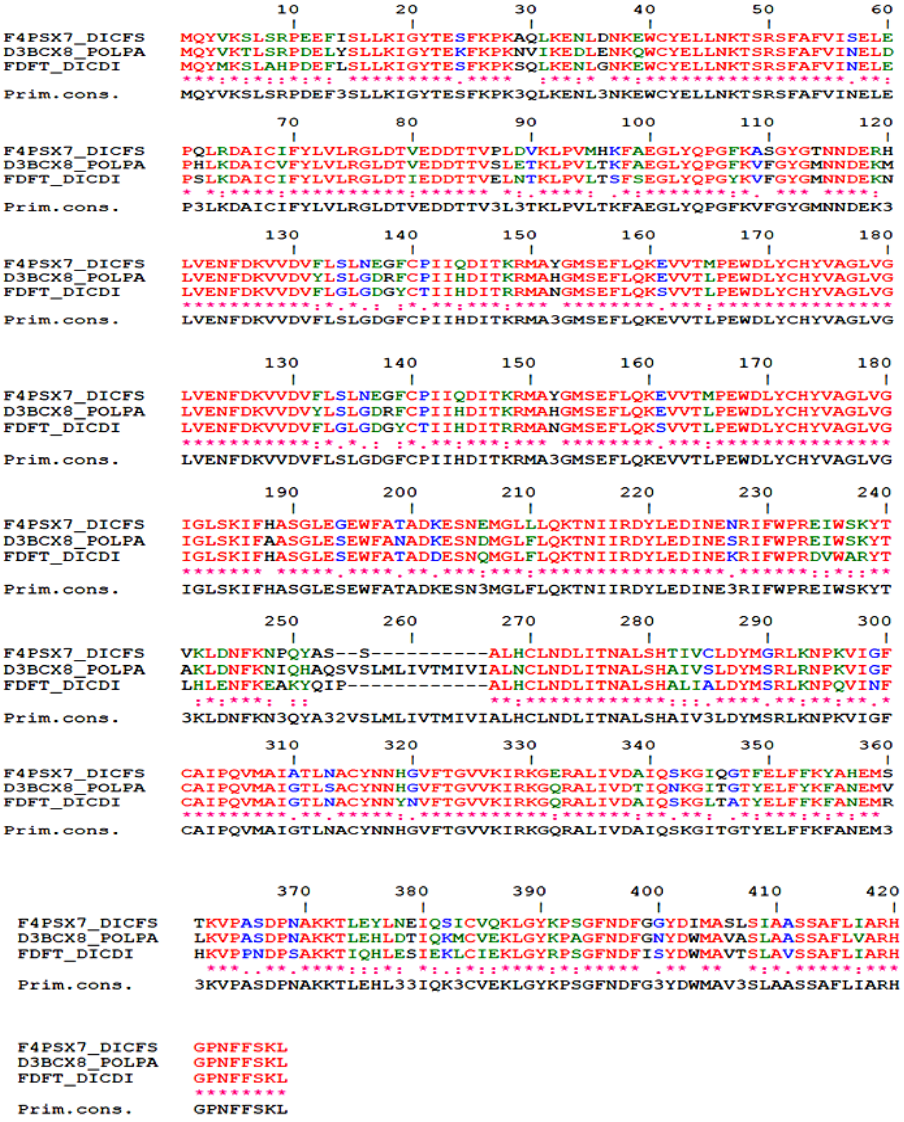

Figure 4.2: The deduced amino acid sequence of *D. discoideum* squalene synthase from related species of slime mould. (1) *Polysphondylium pallidum* (2) *Dictyosteleum fasciculatum* (3) *Dictyostelium discoideum*. These species have the same putative C-terminal PTS1 (-SKL).

As described in chapter 3, the approach using fusion proteins with GFP allowed us to detect successfully the intracellular locations of the mevalonate pathway enzymes in *D.discoideum* and this suggested that it might be possible to determine the intracellular location of the sterol biosynthesis enzymes by using the same technique. Therefore, in order to clarify the possible role of peroxisomes in the sterol biosynthetic pathway in *D.discoideum*, we decided to determine the

intracellular locations of the first five enzymes catalyzing sterol biosynthesis from farnesyl diphosphate.

4.2 Results

4.2.1 Squalene Synthase

Squalene synthase (SQS) catalyses the first unique reaction of the biosynthesis of sterols by converting two molecules of farnesyl diphosphate into squalene. In addition, it has been shown that squalene synthase is generally localized to the endoplasmic reticulum. For example, human and *Arabidopsis thaliana* squalene synthase were found to be targeted to the ER by a C-terminal hydrophobic transmembrane domain (Robinson et al., 1993, Busquets et al., 2008). Furthermore, Stamellos et al., (1993) postulated that the enzymatic activity of rat squalene synthase is localized to the ER. However, in *D.discoideum* the carboxy terminus of squalene synthase has a consensus PTS1 (-Ser-Lys-Leu).

We investigated the intracellular location of *Dd*SQS by producing a GFP- *Dd*SQS fusion protein so that the putative C-terminual PTS1 motif was not masked. The DNA fragment encoding the *D.discoideum* squalene synthase was amplified by PCR, using a proofreading enzyme (Velocity) and primers VIP 1892 and VIP 1893, from the cDNA library. This fragment, encoding *Dd*SQS, with the addition of the amino acids linker sequence Ser-Thr-Ser-Thr, was digested with BamHI and XbaI and ligated into BamHI-XbaI digested pDXA3C-MA to give pMA16. Amoebae transformed with pMA16 displayed a typical peroxisomal pattern of green fluorescence (Figure 4.3).

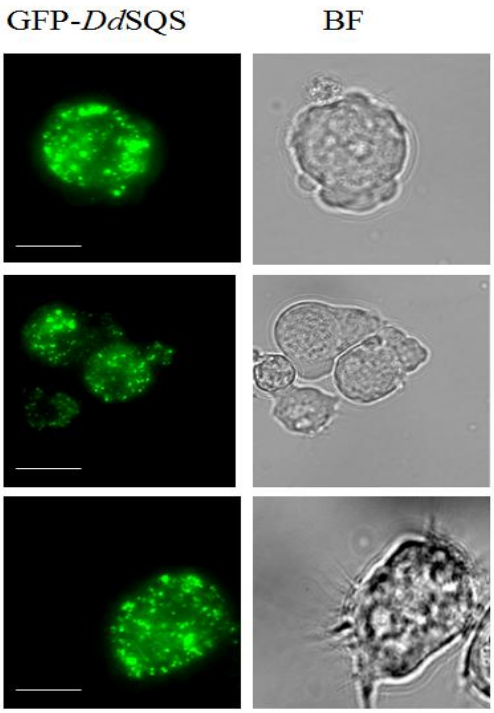

Figure 4.3: Analysis of squalene synthase in *D.discoideum*. The pattern of GFP fluorescence in amoebae expressing the GFP-*Dd*SQS fusion protein was punctate. Scale bars 5µm.

A plasmid pMA15 was also constructed encoding mRFP-*Dd*SQS. In amoebae co-expressing mRFP-*Dd*SQS (pMA15) and the peroxisomal marker pGFP-PTS1, the mRFP and GFP fluorescence overlapped (Figure 4.4). Thus, *Dd*SQS is localized to the peroxisomes.

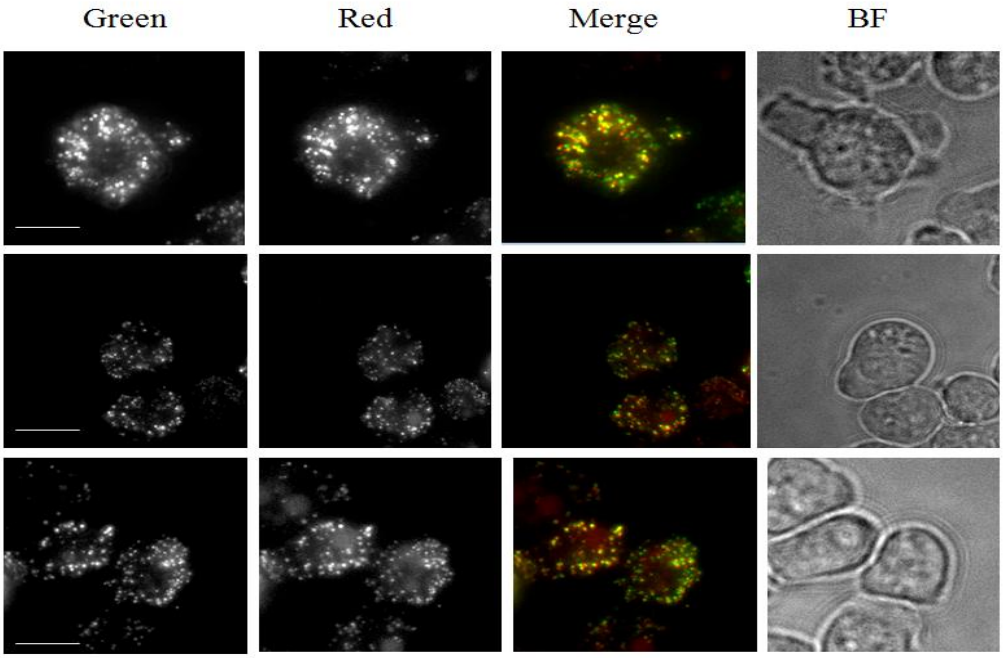

Figure 4.4: Demonstration of the peroxisomal localization of *Dd*SQS. Amoebae were co-expressing mRFP-*Dd*SQS and the peroxisomal marker pGFP-PTS1. Co-localization of the mRFP and GFP fluorescence was observed in the peroxisomes. Scale bars 5µm.

4.2.2 mRFP-*Dd*SQS is catalytically active

In our laboratory, it had been previously found that over-expressing the fusion protein *Dd*FDPS-GFP allowed *D. discoideum* amoebae to grow in the presence of a specific inhibititor of FDP-synthase (the NBP alendronate) at concentrations that would have totally inhibited growth of untransformed amoebae. Thus, it was concluded that the fusion protein is still catalytically active and it is able to fold properly into the active enzyme (Nuttall et al., 2012).

Similarly, attempts were made to determine whether transformants of *D. discoideum* amoebae expressing mRFP-*Dd*SQS are resistant to BMS181221 (Figure 4.5) which is a bisphosphonate that is a specific inhibitor of squalene synthase (Ciosek et al., 1993).

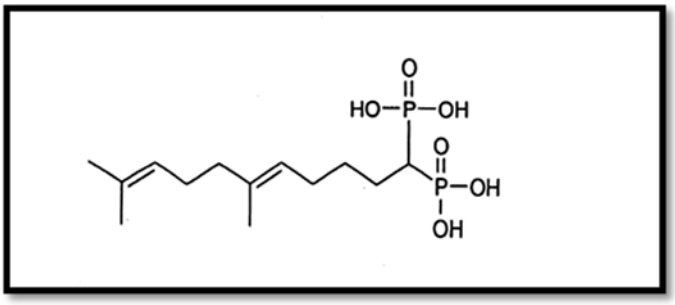

Figure 4.5: Structure of the bisphosphonate BMS181221

D. discoideum amoebae overexpressing mRFP- *Dd*SQS were initially selected in Blasticidin-containing medium before being transferred to medium containing the bisphosphonate BMS181221 (4.3μM). Untransformed amoebae were also grown axenically either in the presence or absence of BMS181221. Each culture (10ml) was inoculated with amoebae to an initial density of 1×10^4 cells/ml and cell proliferation was assessed daily for a week by using a haemocytometer. Amoebae expressing the mRFP- *Dd*SQS fusion protein were able to grow in the presence of BMS181221 whereas the untransformed amoebae failed to grow in the same conditions (Figure 4.6).

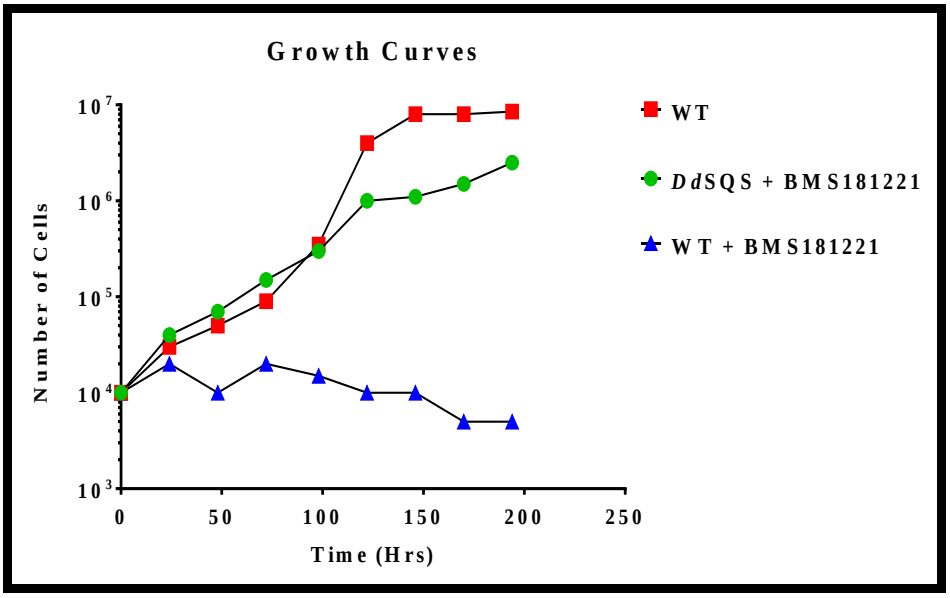

Figure 4.6: Effects of BMS181221 on untransformed amoebae and amoebae transformed to express mRFP-*Dd*SQS.

In addition, analysis by fluorescent microscopy showed that mRFP-*Dd*SQS was expressed at very high levels in amoebae that had been grown in medium containing BMS181221. However, the highly over-expressed fusion protein was still accumulated in the peroxisomes (Figure 4.7).

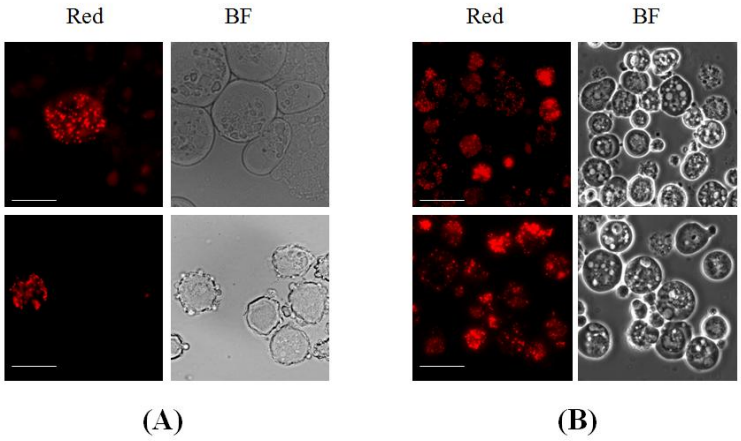

Figure 4.7: Amoebae expressing mRFP-*Dd*SQS become resistant to BMS 181221. (A) Amoebae transformed to express mRFP-*Dd*SQS grown in the presence of 10µg/ml Blasticidin. (B) Amoebae transformed to express mRFP-*Dd*SQS grown in the presence of 4.3µM BMS181221. Scale bars 5µm.

Together, these results suggested that the fusion protein must have been catalytically active and able to fold into its native three dimensional structures. Furthermore, it shows that production of squalene in the peroxisomes promotes *D. discoideum* growth and this is consistent with the conclusion that squalene is also produced in untransformed amoebae in the peroxisomes.

4.2.3 Squalene Epoxidase

The second reaction of sterol biosynthesis from squalene in which the squalene is converted into squalene epoxide is catalysed by squalene epoxidase. There have been few investigations of the intracellular location of squalene epoxidase. Krisans (1996) was unable to detect squalene epoxidase activity in purified peroxisomal fractions incubated with either squalene or dihydrolanosterol. In addition, it has been reported that yeast squalene epoxidase encoded by *ERG1* gene, is localized to both the endoplasmic reticulum and lipid particles (Leber et al., 1998).

In *D. discoideum* there is no obvious PTS sequence at either terminus of squalene epoxidase. However, because we had found that squalene synthase is peroxisomal enzyme we decided to determine the intracellular localization of squalene epoxidase by transforming amoebae to express a s.epoxidase-GFP fusion protein. The 1509bp DNA fragment encoding *Dd*squalene epoxidase was amplified by PCR from the cDNA library by making use of VIP1309 and VIP 1310 primers. This DNA fragment also encoded the additional amino acid linker sequence Ser-Thr-Ser-Thr at the C-terminus. It was digested with HindIII and BamHI and inserted into HindIII-BamHI digested pGFP, to obtain pMA17. There was a punctate pattern of GFP fluorescence, typical of a peroxisomal location, in amoebae transformed to express *Dd*s.epoxidase-GFP (Figure 4.8).

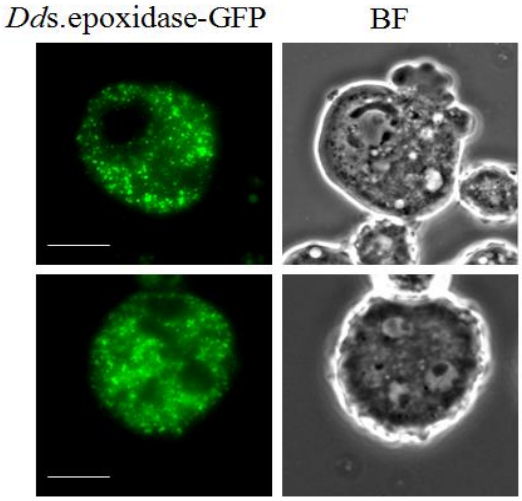

Figure 4.8: Analysis of the expression s.epoxidase-GFP fusion protein in *D. discoideum*. Amoebae expressing *Dd*s.epoxidase-GFP displayed a punctate pattern of green fluorescence. Scale bars 5µm.

When *D.discoideum* amoebae co-expressed pMA17 and the peroxisomal marker mRFP-PTS1, the two fluorescence signals coincided. This confirmed that *Dd*squalene epoxidase is peroxisomal (Figure 4.9).

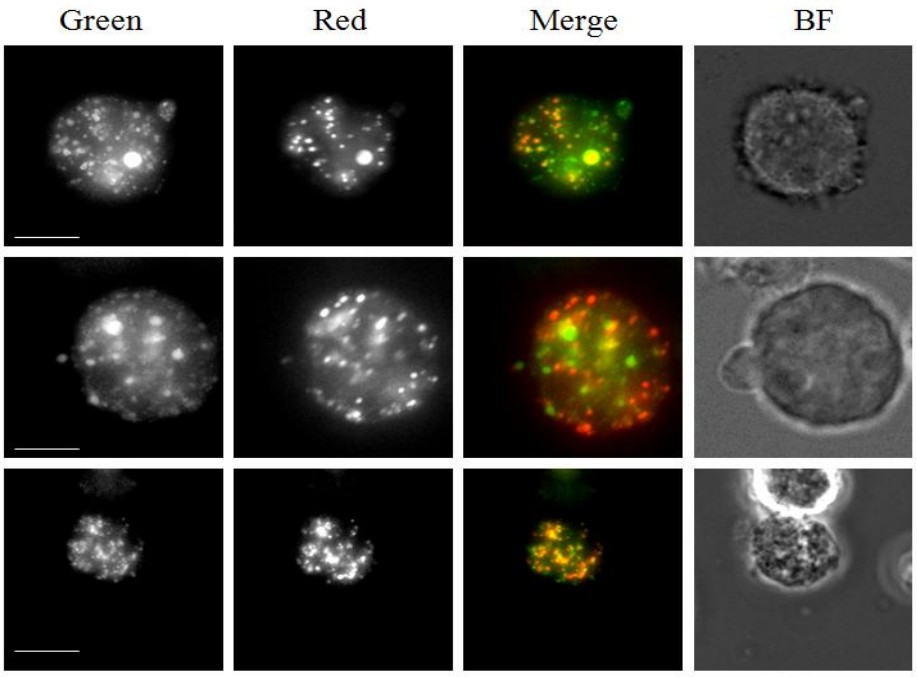

Figure 4.9: Squalene epoxidase is a peroxisomal enzyme in *D. discoideum*. In amoebae co-expressing *Dd*s.epoxidase-GFP and the peroxisomal marker mRFP-PTS1, the GFP and RFP fluorescence co-localised. Scale bars 5µm.

4.2.4 Oxidosqualene Cyclase (Cycloartenol synthase)

*Dd*oxidosqualene cyclase (OSC), as in plants, converts oxidosqualene into cycloartenol. By contrast, in animals and fungi oxidosqualene cyclase produces a different sterol, lanosterol. The C-terminus of *D.discoideum* oxidosqualene cyclase, as in other slime mould species, possesses a putative PTS1 (Figure 4.10). Several studies have shown that the C-terminal tripeptide –Ser-Lys-Ile, which is present on the *Dd*OSC, can act as a PTS and therefore direct an enzyme into the peroxisomes (Recalcati et al., 2001, Purdue and Lazarow, 1994).

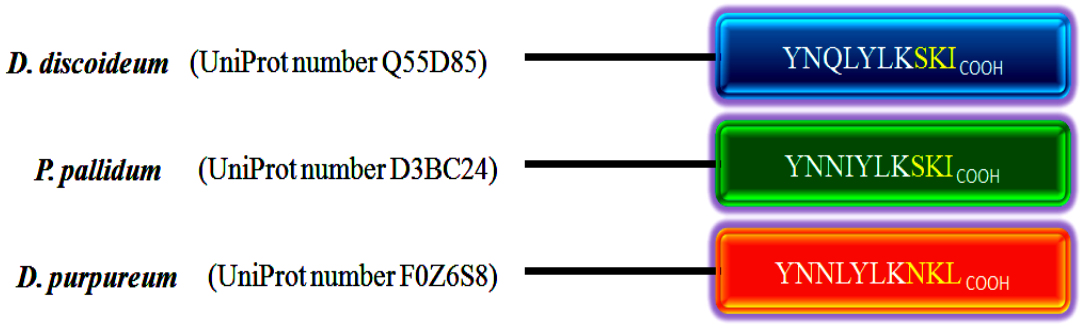

Figure 4.10: Comparison of the amino acid sequences at the carboxy terminus of oxidosqualene cyclases from different slime moulds.

There appear to have been few studies of the intracellular location of oxidosqualene cyclase. However, the human enzyme was purified for determination of its three-dimensional structure from the endoplasmic reticulum (Thoma et al., 2004).

To determine the intracellular location of *Dd*OSC, GFP- *Dd*OSC and mRFP-*Dd*OSC fusion proteins were generated. The ORF of *Dd*OSC was amplified by PCR from the cDNA library using primers VIP 1377 and VIP 1378. The 2112bp DNA fragment was digested with BamHI-EcoRI and ligated into digested p339-3MA with BamHI-EcoRI to obtain pMA18 encoding mRFP-*Dd*OSC. pMA19 encoding GFP- *Dd*OSC was generated similarly. When *D.discoideum* expressed either pMA18 or pMA19, a punctate fluorescence was observed (Figure 4.11).

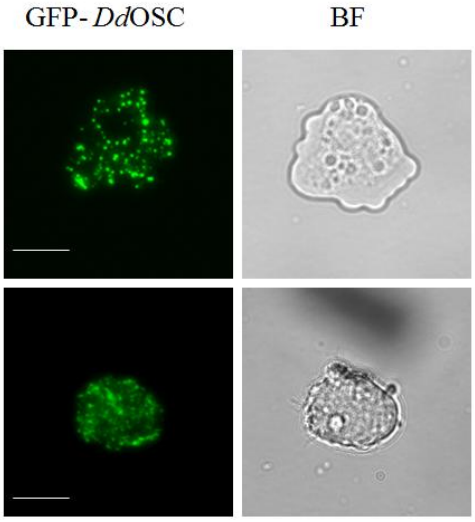

Figure 4.11: Analysis of the expression of the GFP- *Dd*OSC fusion protein in *D.discoideum*. Amoebae expressing GFP- *Dd*OSC showed a punctate distribution of green fluorescence. Scale bars 5µm.

Furthermore, when amoebae co-expressed mRFP-*Dd*OSC and the peroxisomal marker pGFP-PTS1 the punctuate fluorescence of GFP and mRFP overlapped and demonstrated that *Dd*OSC is peroxisomal (Figure 4.12).

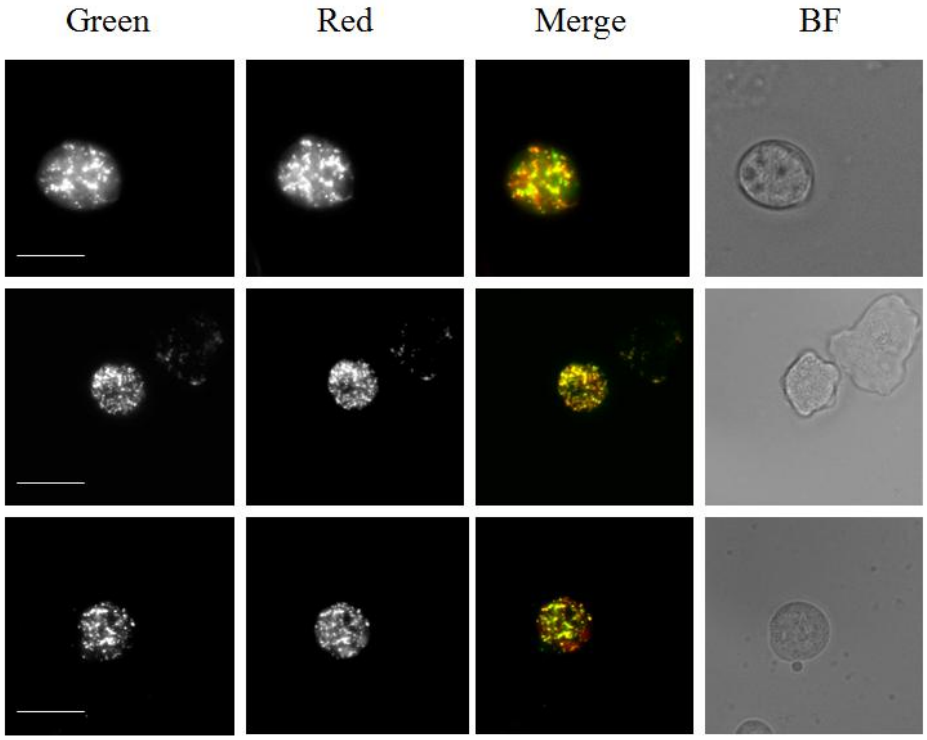

Figure 4.12: Demonstration of the peroxisomal location of *Dd*OSC. Amoebae co-expressing mRFP-*Dd*OSC and the peroxisomal marker pGFP-PTS1. Co-localization of mRFP and GFP fluorescence was observed in the peroxisomes. Scale bars 5µm.

4.2.5 Cycloartenol -C-24-methyltransferase

4.2.5.1 Cycloartenol -C-24-methyltransferase is localized to the peroxisomes

In plants, there are two families of sterol methyltransferases and it has been proposed that one family adds the first methyl group as the first step in cycloartenol modification. The second family adds a further methyl group, to give an ethyl group, near to the end of phytosterol synthesis (Bouvier-Nave et al., 1998). By contrast, because ergosterol has only a single methyl group on C-24, *S.cerevisiae* adds only one methyl group to the C-24 of zymosterol and this is the last step of ergosterol synthesis. In mammalian cells, the transmethylation reaction is entirely absent because cholesterol lacks a C-24 methyl group. Since the major sterol in *D.discoideum* has a C-24 ethyl group, two families of transferases would be expected as in plants. There appear to be only two possible cycloartenol-C-24-methyltransferases (SMT) in the *D.discoideum* genome and, since one has a putative PTS comprising the carboxy-terminal tripeptide –Ala-Lys-Leu, and cycloartenol is in the peroxisome, it seems probable that this enzyme catalyses the first methylation and the other enzyme catalyzed the second methylation to give an ethyl group. The putative PTS1 motif of cycloartenol -C-24-methyltransferases 1 has also been conserved in the other slime mould species (Figure 4.13).

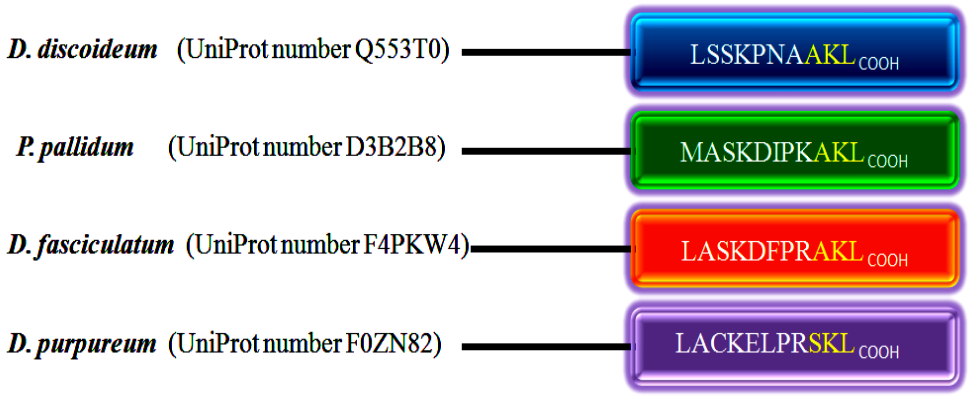

Figure 4.13: Comparison of the C-terminal amino acid sequences of the of cycloartenol -C-24-methyltransferases from different slime moulds.

We investigated the intracellular location of *Dd*SMT1 by generating a GFP-fusion protein. The 1389bp encoding *Dd*SMT was amplified by PCR from the cDNA library using primers VIP 1453 and VIP 1454. The resultant DNA fragment, with the addition of a nucleotide sequence encoding an N-terminal linker sequence Ser-Thr-Ser-Thr, was digested and ligated into BamHI-XbaI digested pDXA3C-MA to obtain pMA20. Wild type *D.discoideum* transformed with pMA20 encoding GFP-*Dd*SMT1displayed a typical peroxisomal punctate pattern of GFP fluorescence (Figure 4.14).

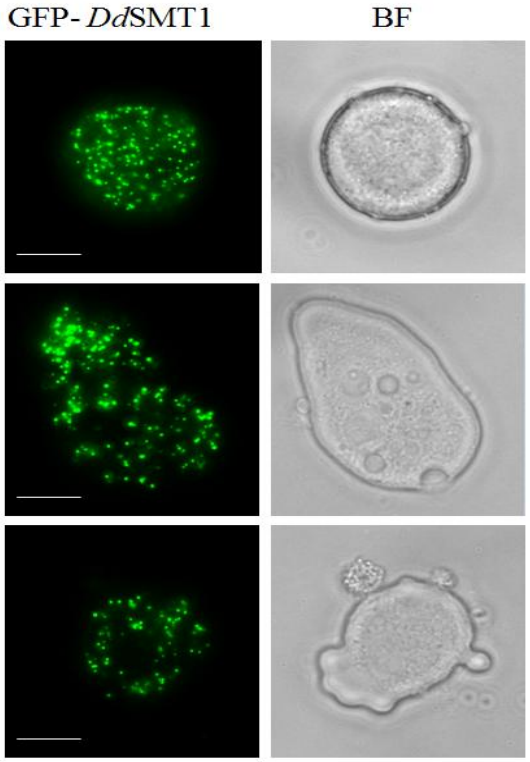

Figure 4.14: Analysis of the expression of the GFP-*Dd*SMT1 fusion protein in *D.discoideum*. Amoebae expressing GFP-*Dd*SMT1 displayed a punctate pattern of green fluorescence. Scale bars 5µm.

In addition, when amoebae co-expressed GFP-*Dd*SMT1 together with the peroxisomal marker mRFP-PTS1, the fluorescence of the two proteins co-localized, indicating that the *Dd*cycloartenol-C-24-methyltransferases 1 is peroxisomal (Figure 4.15).

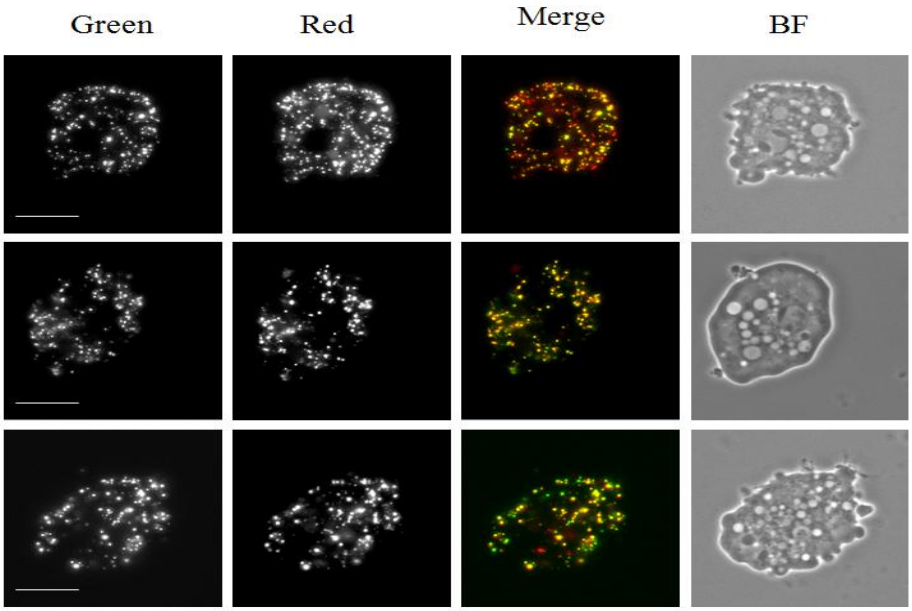

Figure 4.15: Cycloartenol-C-24-methyltransferases 1 is a peroxisomal enzyme in *D.discoideum*. Amoebae expressing both GFP-*Dd*SMT1 and the peroxisomal marker mRFP-PTS1. Co-localization of mRFP and GFP fluorescence was observed in the peroxisomes. Scale bars 5µm.

4.2.5.2 *Dd* cycloartenol-C-24-methyltransferase 1 can complement yeast *erg6*

Although *Dd*SMT1 contains an amino acid sequence that is compatible with its being a sterol C-24 methyltransferase, it also has an N-terminal extension of approximately 114 amino acids (Figure 4.15). The role of the extension is unknown but its presence could indicate that the activity of *Dd*SMT1 is no longer that of a cycloartenol -C-24- methyltransferase. Hence, the function of *Dd*SMT1 (Dictybase reference number DDB_G0275359) is not defined in Dictybase. It therefore appeared essential to determine whether the protein retains sterol methyltransferse activity.

The gene encoding *D.discoideum* cycloartenol-C-24-methyltransferase is homologous to *Saccharomyces cerevisiae ERG6* (Figure 4.16). *ERG6* is the structural gene that encodes the *S.cerevisiae* sterol-C-24-methyltransferase. This enzyme catalyzes addition of a single methyl group to zymosterol to give ergosterol.

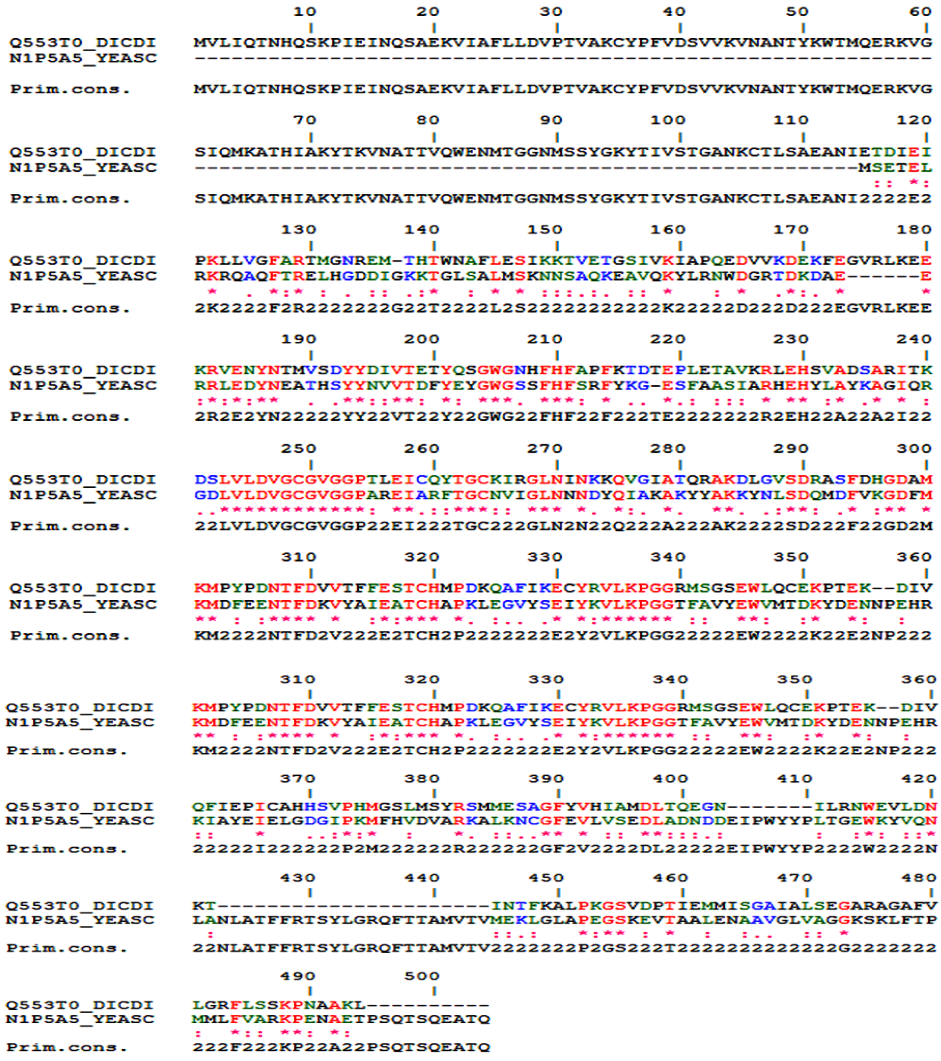

Figure 4.16: The deduced amino acid sequences of *D. discoideum* strain AX-2 cycloartenol -C-24-methyltransferase 1 and *S. cerevisiae ERG6* aligned using CLUSTALW.

An *erg6*Δ strain grows well in standard growth media but the permeability properties of the plasma membrane are changed and an *erg6*Δ strain can take up inhibitors to which the wild-type strain is impermeable. For example, an *erg6*Δ mutant strain exhibits cycloheximide sensitiviy and fails to grow on YNB (Yeast Nitrogen Base) medium containing 0.05µg cycloheximide per ml (Gaber et al., 1989). In order to determine *Dd*SMT fusion protein can complement yeast *erg6*, two constructs were generated. The first construct (pMA22), generated by homologous recombination in yeast (section 2.2.5 in the Material and Methods Chapter), comprises pMA22 encoding cycloartenol-C-24-methyltransferase Δ PTS1. The second construct pMA21 was also generated by homologous

recombination in yeast and encoded *Dd*SMT1-GFP-PTS1. The *erg6* mutant strain was transformed with either pMA21 or pMA22 and it was found that each transformed strain was able to grow in YPD medium containing 0.05 µg per ml cycloheximide. It was also confirmed by fluorescence microscopy analysis that the fusion protein encoded by pMA22 was expressed in the cytosol whereas that encoded by pMA21 was peroxisomal (Figure 4.17).

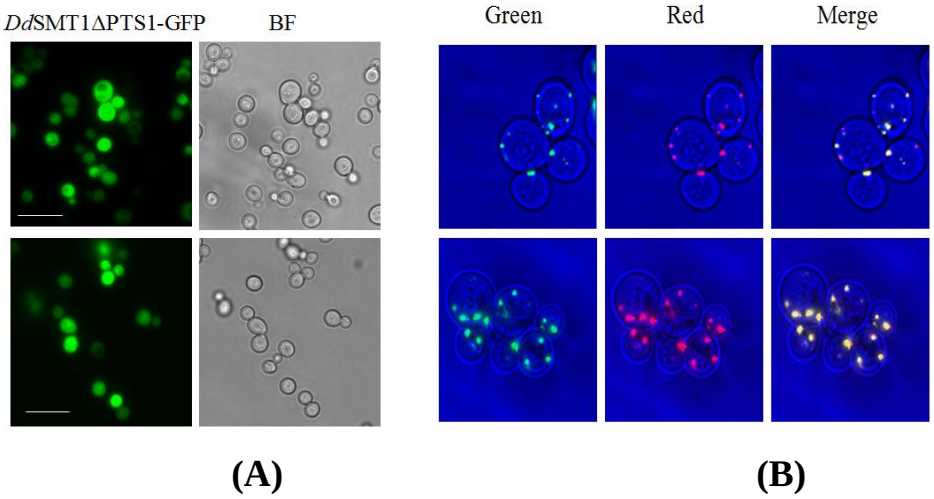

Figure 4.17: Analysis of the expression of *Dd*sterol methyl transferase in an *erg6Δ* strain of *S. cerevisiae*. (A) *erg6*Δ strain expressing *Dd*sterol methyl transferase in the cytosol. The PTS1 had been removed. (B) *erg6*Δ strain co-expressing *Dd*SMT1-GFP-PTS1 and the peroxisomal marker HcRed-SKL. Scale bars 5µm.

By contrast, the *erg6* mutant strain transformed with the empty vector pEH116 remained unable to grow in the cycloheximide-containing medium (Figure 4.18). Because expression of *Dd*SMT1 allowed the *erg6* mutant strain to grow like the wild-type strain in the presence of cycloheximide, it could be concluded that the transformed *erg6* mutant was able to synthesise ergosterol and hence that *Dd*SMT1 must have sterol-C-24-methyltransferase activity.

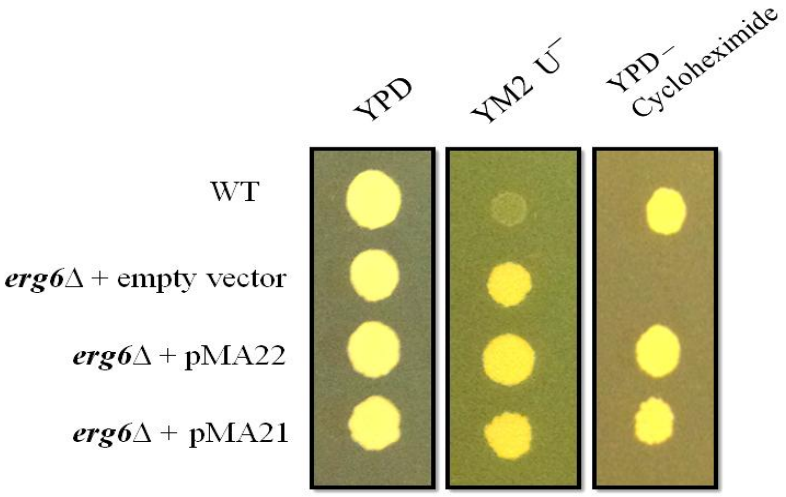

Figure 4.18: Demonstration that the pMA22 and pMA21 plasmids restore wild- type growth to an *erg6* mutant of *S.cerevisiae*. Equivalent dilutions (0.1 OD_{600}) of overnight cultures were spotted on YPD, YM2 without uracil (YM2 U^-) and YPD-cycloheximide medium. Since the WT was a *S. cerevisiae* **(**BY4742) ura^- strain, it could not grow on a YM2 U^-plate. The *erg6Δ* strain of *S.cerevisiae* had been transformed with either the empty vector (pEH116) or pMA22 or PMA21. The plates were left for 2 days at 30ºC before being photographed.

4.2.6 Methylsterol monooxygenase (Sterol 4α-methyl oxidase)

In plants, it has been demonstrated that the two C-4 methyl groups are removed in separate steps by two different families of sterol 4α-methyl oxidase (SMO1 and SMO2) (Darnet and Rahier, 2004). In this context, it has been suggested that one family is responsible for the removal of the first methyl and the other family removes the second methyl group later. Complete removal of each methyl group also needs a C-4 decarboxylase and sterone reductase. In *D.discoideum* there are also two genes encoding methylsterol monooxygenases. The genes are adjacent on the chromosome and encode almost identical proteins. It appears as if they have arisen by a recent gene duplication and it would seem probable that either enzyme can catalyse oxidation of the first and second methyl groups.

In *D.discoideum,* neither of methylsterol monooxygenases has a PTS1 nor a PTS2, whereas the N-terminus of each monooxygenase comprises hydrophobic and charged amino acids which might act as ER-directed signal (Figure 4.19). This suggested that sterol biosynthesis will have moved from the peroxisomes to the ER. Therefore, it seems necessary to determine the intracellular location of the two monooxygenases.

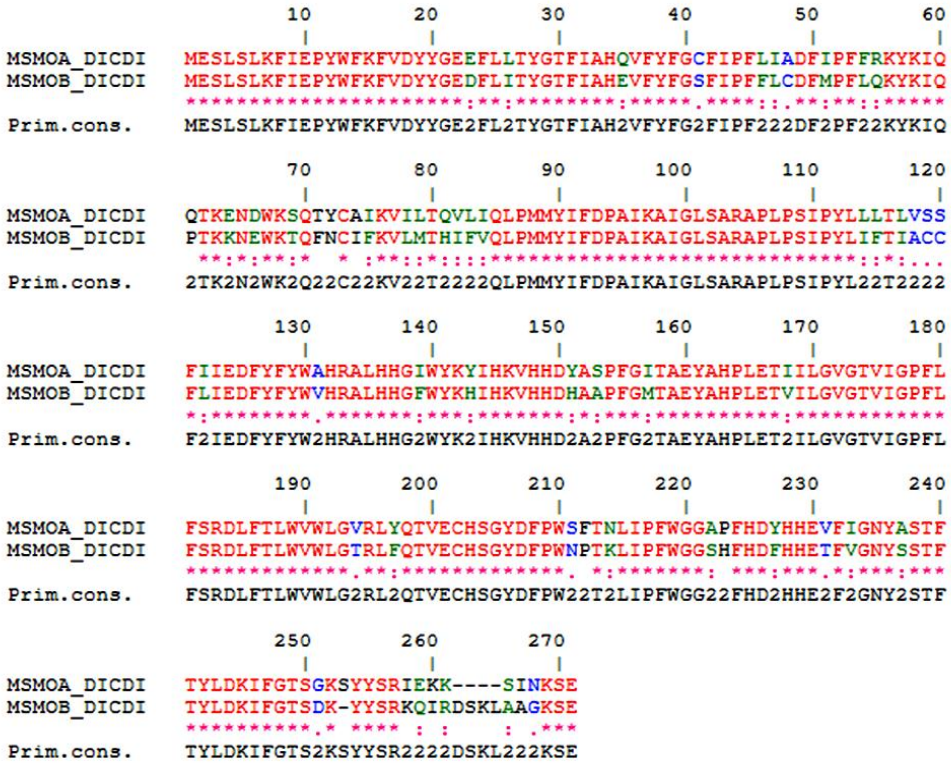

Figure 4.19: The deduced amino acid sequences of *D. discoideum* strain AX-2 methylsterol monooxygenase isoenzymes 1 and 2 aligned using CLUSTALW.

We determined the intracellular location of both methylsterol monooxygenase by generating GFP-fusion proteins. Amoebae transformed with either pMA23 encoding *Dd*methylsterol monooxygenase (isozyme 1)–GFP or pMA24 encoding *Dd*methylsterol monooxygenase (isozyme 2)–GFP had different patterns of GFP fluorescence from the typical peroxisomal pattern (Figure 4.20). This pattern suggested that the two fusion proteins are not peroxisomal but are localized to another cellular compartment which may be the endoplasmic reticulum.

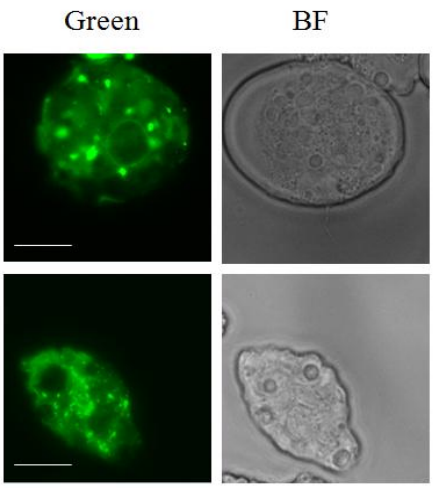

Figure 4.20: Analysis of *Dd*methylsterol monooxygenase (isozyme 1)–GFP expression in *D. discoideum*. Scale bars 5µm.

We therefore decided to re-transform the *D.discoideum* amoebae with two different endoplasmic reticulum markers to confirm the subcellular location of the *Dd*methylsterol monooxygenases. The first marker was protein disulfide isomerase (PDI), a typical ER luminal marker (Monnat et al., 1997). The second maker was calnexin, which is a well- characterized protein in mammals. It has been identified as an ER integral membrane calcium - binding phosphoprotein (Bergeron et al., 1994). Furthermore, it was used recently as a specific ER maker in amoebae of *D.discoideum* (Hervet et al., 2011).

When *D.discoideum* amoebae co-expressing pMA23 with pMA25, encoding *Dd*PDI- mRFP, or pMA26, encoding *Dd*calnexin-mRFP, a complete co-localization was obtained between the monooxygenase and calnexin (Figure 4.20 A and B).

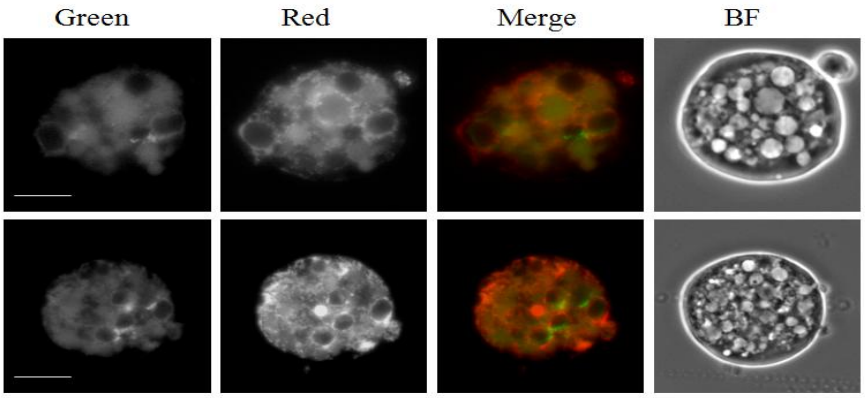

Figure 4.21 (A): The intracellular location of methylsterol monooxygenase isozyme (1) in *D.discoideum*. Amoebae co-expressing *Dd*methylsterol monooxygenase (isozyme 1)–GFP and the ER marker *Dd*PDI-mRFP. The Co-localization of the fluorescence of both fusion proteins was partially observed. Scale bars 5µm.

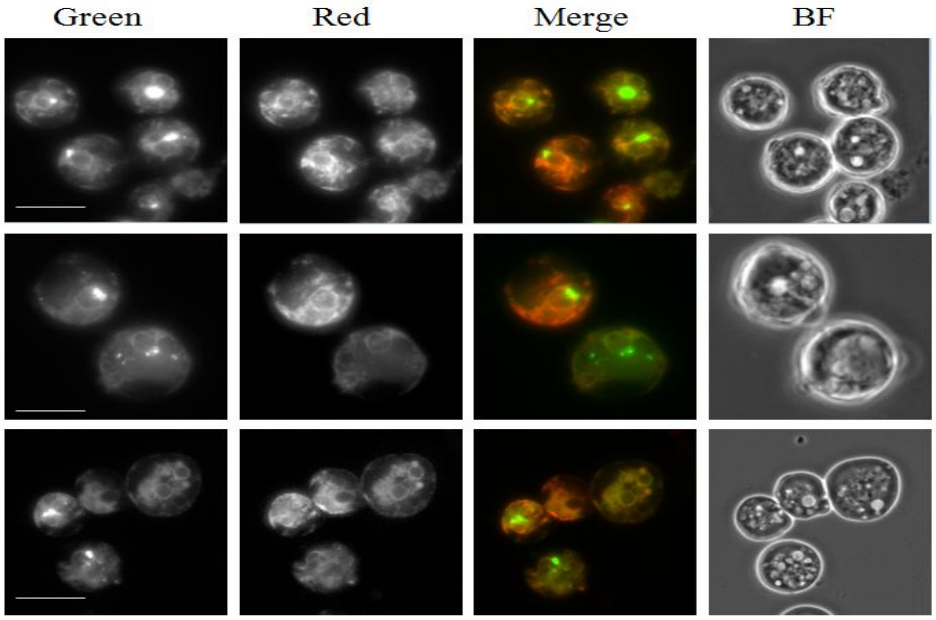

Figure 4.22 (B): The intracellular location of methylsterol monooxygenase isozyme (1) in *D.discoideum*. Amoebae co-expressing *Dd*methylsterol monooxygenase (isozyme 1)–GFP and the ER marker *Dd*calnexin-mRFP. Co-localization of the GFP and mRFP fluorescence was observed. Scale bars 5µm.

A similar result was obtained with the second monooxygenase fusion protein (Figure 4.23) and *Dd*calnexin-mRFP (Figure 4.24). Since both *Dd*methylsterol monooxygenases co-localised with *Dd*calnexin-mRFP and *Dd*methylsterol monooxygenase (isozyme 1) only partially colocalised with *Dd*PDI-mRFP it appeared probable that the monoxygenases are ER membrane proteins.

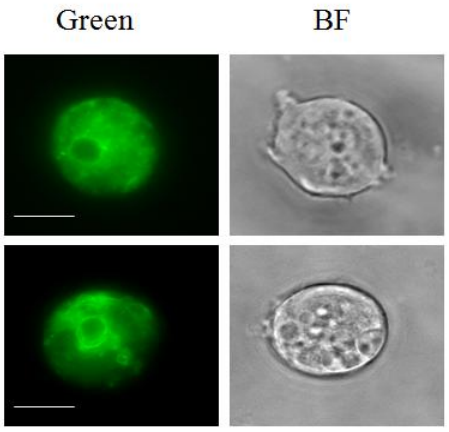

Figure 4.23: Analysis of methylsterol monooxygenase (isozyme 2)–GFP expression in *D. discoideum*. Scale bars 5µm.

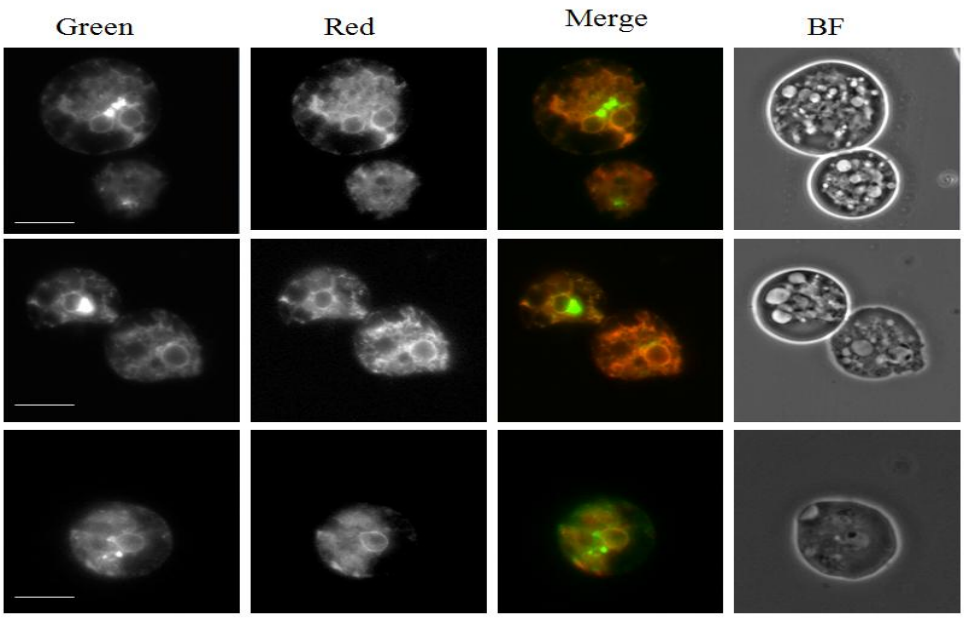

Figure 4.24: Demonstration of an ER localization of *Dd*methylsterol monooxygenase (isozyme 2). Amoebae co-expressing *Dd*methylsterol monooxygenase (isozyme 2)–GFP and the ER marker *Dd*calnexin-mRFP. Co-localization of the GFP and mRFP fluorescence was observed. Scale bars 5µm.

4.3 Discussion

Whereas in other organisms the first four steps on the pathway converting farnesyl diphosphate to sterols are catalyzed by enzymes associated with the endoplasmic reticulum, our data demonstrate that these steps in *D.discoideum* take place in the peroxisomes (Table 4.1).

Enzyme	N-terminal sequence	C-terminal sequence	Putative PTS	Enzyme location
***Dd*SQS**	MQYMKSLAHPD EFLSLLKIGYTES FKPKSQ	GPNFFSKL	PTS1	**Peroxisome**
***Dd*S.epoxidase**	MEDIQFENEVDN KVFDIIVVGAGV AGSAFA	NICIILRLTK	No PTS	**Peroxisome**
***Dd*OSC**	MTTTNWSLKV DRGRQTWEYS QEKKEATDVD	YNQLYLKSKI	PTS1	**Peroxisome**
***Dd*SMT**	MVLIQTNHQ SKPIEINQSA EKVIAFLLDV	LSSKPNAAKL	PTS1	**Peroxisome**
***Dd*MSMA**	MESLSLKFIEPY WFKFVDYYGEE FLLTYGT	IEKKSINKSE	No PTS	**ER**
***Dd*MSMB**	MESLSLKFIEPY WFKFVDYYGED FLITYGT	DSKLAAGKSE	No PTS	**ER**
Consensus PTS1	**(S/ A/ C) (K/R/H) (L/M)**			
Consensus PTS2	**(R/K) (L/V/I) X_5(H/Q) (L/A)**			

Table 4.1: The intracellular locations of six sterol biosynthesis enzymes in *Dictyostelium discoideum* based on fusion proteins studies.

Four of the sterol biosynthetic pathway enzymes are peroxisomal but only three have an obvious PTS1 (Table 4.1). Squalene synthase possesses the most sufficient PTS1 (-SKL_{COOH}) at its C-terminus and the C-terminal triplet of amino acids (-AKL_{COOH}) in cycloartenol-C-24-methyltransferase is known to be an effective PTS1. Similarly, the C-terminal sequence of oxidosqualene synthase (-SKI_{COOH}) has been previously shown to be a functional PTS1 (Recalcati et al., 2001, Purdue and Lazarow, 1994).

Although *D.discoideum* squalene epoxidase was shown to be peroxisomal, it appears not to possess a PTS and the mechanism by which it enters the peroxisome is not clear. Therefore, the process by which the *Dd*squalene epoxidase is imported into the perxisomes requires further investigation. However, it has been suggested that some peroxisomal proteins lacking a PTS may be imported into the perxisomes by using a third type of targeting sequence that has not been identified (van der Klei and Veenhuis, 2006). In addition, other studies have also indicated that some peroxisomal matrix proteins are able to enter the peroxisome, despite lacking a PTS, by still being able to bind to Pex5 or by a piggy-backing process by which the protein binds to another protein containing a PTS sequence (Islinger et al., 2009, Klein et al., 2002).

By contrast, enzymes catalyzing later steps i.e. from the methylsterol monooxygenase onwards appear, as in other organisms, to be associated with the endoplasmic reticulum. These enzymes seem to have an ER- directed signal and do not seem to have a PTS.

Overall, our data showed that the peroxisomes have an important role in the sterol biosynthetic pathway in *D.discoideum* since there are four enzymes of the pathway associated with the peroxisomes. However, no previous studies have detected a peroxisomal location of the sterol biosynthesis enzymes in other organisms. Thus, it seems that a role of the peroxisomes in sterol biosynthesis is a unique aspect in *D.discoideum*.

Chapter 5

Membrane association of the peroxisomal enzymes involved in sterol biosynthesis in *D. discoideum*

5.1 Introduction

Peroxisomal membrane proteins (PMPs) and matrix proteins require different factors for their targeting and insertion into or translocation across the peroxisomal membrane. Matrix protein import relies on the well-characterised peroxisomal targeting signal type 1 or type 2. These PTSs are absent from PMPs, which contain poorly defined sequences that mediate peroxisomal targeting. Two classes of PMPs can be distinguished. Class1 PMPs traffic via the ER to peroxisomes whereas Class2 PMPs are directly inserted into the peroxisomal membrane dependent on Pex3 and Pex19.

The data presented in chapter 4 demonstrate clearly that four of the sterol biosynthesis enzymes in *D.discoideum* are localized to the peroxisomes. Three of these enzymes seem to have a clear PTS1. However, for instance *Dd*squalene synthase also possesses a predicted transmembrane domain located near to its C-terminus, which appears to resemble the transmembrane domain of *A.thaliana* and human squalene synthases (Table 5.1) that are responsible of anchoring these enzymes into the ER membrane (Jennings et al., 1991, Robinson et al., 1993, Busquets et al., 2008). In addition, cycloartenol synthase contains a putative PTS1 and a predicted transmembrane segments (Table 5.2). Squalene epoxidase and cycloartenol-C-24-methyltransferase contain a transmembrane segment or a PTS1, respectively (Table 5.2). It therefore appeared important to investigate whether *Dd*squalene synthase and other sterol biosynthesis enzymes are associated with the peroxisomal membrane.

Organism	The predicted C-terminal TM	Position	Uniprot number	Length
D. discoidium	FISYDWMAVTSLAVSSAFLIA	386-406	Q54DR1	21
A.thaliana	QPNSVFIIMVVILLAIVFAYL	387-407	P53799	21
S.cerevisiae	FNMVLSIILSVLLGFYYIYTL	421-441	P29704	21
H.sapiens	PIYLSFVMLLAALSWQYLTTL	384-404	P37268	21

Table 5.1: Predicted transmembrane domains of squalene synthase from different organisms as predicted by Uniprot.

Protein	Predicted TM position	Length	PTS1
Squalene synthase	386 - 406	21	SKL
Squalene epoxidase	439 - 456	17	___
Cycloartenol synthase	290 – 306	16	SKI
Cycloartenol –C-24 methyltransferase	___	___	AKL

Table 5.2: Predicted transmembrane domains and the putative PTS1 of the four sterol biosynthesis enzymes in *D.discoideum*.

To investigate the possible membrane association of the four *D. discoideum* sterol biosynthesis enzymes, two biochemical methods were used. First, disrupted amoebae were divided into soluble and insoluble fractions by centrifugation. The insoluble fraction was extracted with 1M NaCl at 0ºC for 30 min in order to remove any protein that associated with the membrane by non-specific ionic interactions. Furthermore, Na_2CO_3 pH 11.4 at 0ºC treatment was used on a second sample of the insoluble fraction to distinguish between the peripheral and integral

membrane proteins (Fujiki et al., 1982, Elgersma et al., 1997). Only peripheral membrane proteins are released by this treatment whereas integral membrane proteins remain embedded wihin the membrane.

The aim of this chapter is therefore to describe investigations of the membrane association of squalene synthase and the other sterol biosynthesis enzymes because it would be unusual for a peroxisomal matrix protein to be associated with the membrane.

5.2 Results

5.2.1 Control conditions

Amoebae transformed with either pGFP-PTS1 or pMA23 encoding *Dd*methylsterol monooxygenase-GFP were disrupted and the insoluble fractions were treated with 1M NaCl or 100mM carbonate pH 11.4 respectively (section 2.9.3 Materials and Methods). GFP-PTS1 was used as a control for a peroxisomal matrix protein and it was found that most of the GFP was released immediately into the soluble fraction from amoebae disrupted by sonication (Figure 5.1 A) whereas *Dd*methylsterol monooxygenase, used as control for an integral membrane protein, was, as expected, not extracted by Na_2CO_3 pH 11.4 (Figure 5.1 B).

Figure 5.1: Control conditions. (A) Amoebae transformed with pGFP-PTS1 were disrupted by sonication and the insoluble fraction was treated with 1M NaCl followed by high speed centrifugation ~ 233,000 g_{max}. (B) Amoebae transformed with *Dd*methylsterol monooxygenase 1-GFP were disrupted and the insoluble fraction was treated with 100mM sodium carbonate pH 11.4 followed by high speed centrifugation ~ 233,000 g_{max}. Each sample on the immunoblot was derived from approximately the same number of cells. Total (the whole lysate), First s (the supernatant after the first centrifugation), Pellet (the insoluble fraction after 1M NaCl or 100mM Na_2CO_3 pH 11.4 treatment), Final s (the supernatant after 1M NaCl or 100mM Na_2CO_3 pH 11.4 treatment).

5.2.2 Squalene synthase is tightly bound to the peroxisomal membrane

Although the *Dd*squalene synthase possesses the most efficient PTS1 (-SKL) there is a predicted trans-membrane domain (TM) located near to the C-terminus (Table 5.1) of this enzyme which implies that *Dd*squalene synthase might be associated with the peroxisomal membrane. We therefore, decided to investigate the membrane association of *Dd*squalene synthase by using biochemical methods. Membrane fractions from amoebae expressing *Dd*GFP-SQS were treated with 1M NaCl followed by high speed centrifugation ~233,000 g_{max} (section 2.9.4 Materials and Methods) in order to release any peripheral membrane proteins. It was found that *Dd*squalene synthase remained in the pellet fraction suggesting that this enzyme is strongly associated with the peroxisomal membrane (Figure 5.2 A). Furthermore, we found that *Dd*squalene synthase was not extracted with 100mM Na_2CO_3 pH 11.4 (section 2.9.3 Materials and Methods) (Figure 5.2 B). Together, these results suggested that *Dd*squalene synthase is tightly bound to the peroxisomal membrane and that it behaves like an integral membrane protein.

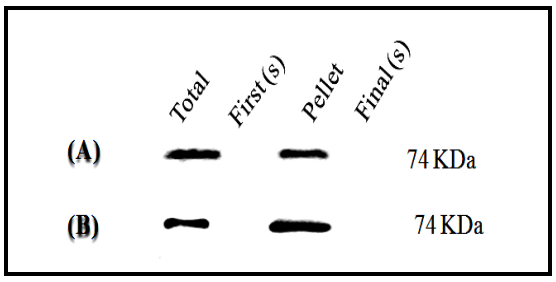

Figure 5.2: Association of *D. discoideum* squalene synthase with the peroxisomal membrane. (A) 1M NaCl treatment. (B) 100mM sodium carbonate pH 11.4 treatment. Amoebal homogenate was centrifuged at 4 ˚C for 1 hour at 50,000 rpm using a Beckman 50 Ti rotor. The supernatant (First s) was separated from the pellet and subjected to SDS- PAGE and western blot analysis using an anti-GFP antibody. The pellet fraction was extracted with either 1M NaCl or 100mM Na_2CO_3 pH 11.4. Extracted proteins were separated from the membranes by high speed centrifugation. Samples of the pellet and supernatant fractions were

analyzed by immunoblot analyses using the anti-GFP antibody. Each sample on the immunoblot was derived approximately from the same number of cells. Total (the whole lysate), First s (the supernatant after the first centrifugation), Pellet (the insoluble fraction after 1M NaCl or 100mM Na_2CO_3 pH 11.4 treatment), Final s (the supernatant after 1M NaCl or 100mM Na_2CO_3 pH 11.4 treatment).

5.2.3 Squalene epoxidase is associated with the peroxisomal membrane

Analysis of the hydrophobicity plot (Krogh et al., 2001) *Dd*squalene epoxidase indicated that the enzyme possessess a highly hydrophobic C-terminal sequence (amino acid residues 439 to 456) (Figure 5.3). In addition, the N-terminus contains a less hydrophobic sequence extending from residues 15 to 33. This led to the hypothesis that squalene epoxidase might be associated with the peroxisomal membrane.

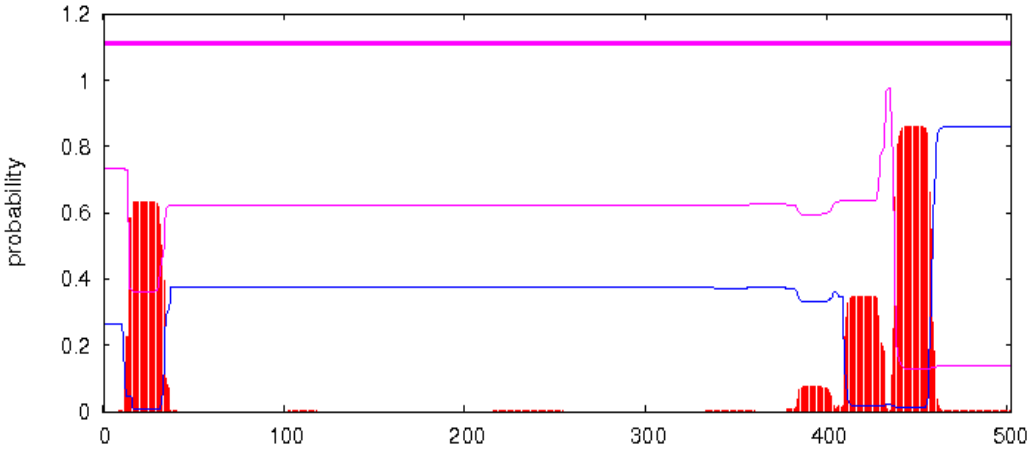

Figure 5.3: Hydropathy plot of *Dd*squalene epoxidase using TMHMM (www.cbs.dtu.dk/services/TMHMM). The red columns indicate the predicted transmembrane domains.

In order to investigate the membrane association of *Dd*squalene epoxidase we applied both treatments, 1M NaCl and 100mM Na_2CO_3 pH11.4 (section 2.9.3 and 2.9.4 Materials and Methods), to the insoluble fractions from amoebae overexpressing *Dd*squalene epoxidase-GFP. *Dd*squalene epoxidase was not removed by 1M NaCl suggesting that this enzyme is strongly associated with the

peroxisomal membrane and therefore is not a peripheral membrane protein (Figure 5.4 A). By contrast, *Dd*squalene epoxidase was removed after extraction with 100mM Na_2CO_3 pH11.4 (Figure 5.4 B). Thus, *Dd*squalene epoxidase is strongly associated with the peroxisomal membrane but it is not an integral membrane protein.

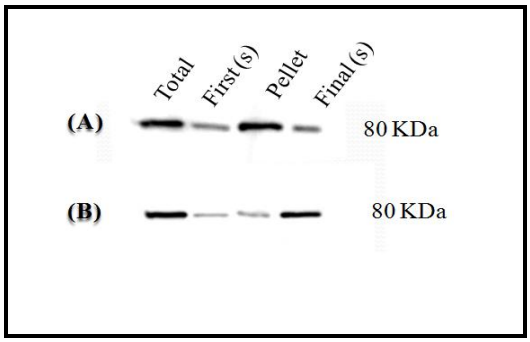

Figure 5.4: Association of *D. discoideum* squalene epoxidase with the peroxisomal membrane. (A) 1M NaCl treatment. (B) 100mM sodium carbonate pH 11.4 treatment. Further details are given in the legend to Figure 5.2. Total (the whole lysate), First s (the supernatant after the first centrifugation), Pellet (the insoluble fraction after 1M NaCl or 100mM Na_2CO_3 pH 11.4 treatment), Final s (the supernatant after 1M NaCl or 100mM Na_2CO_3 pH 11.4 treatment).

5.2.4 Oxidosqualene cyclase (Cycloartenol synthase) is associated with the peroxisomal membrane

Previously, we determined the intracellular location of *D. discoideum* oxidosqualene cyclase which was found to be peroxisomal. In addition, in this chapter we showed that two of the sterol biosynthesis enzymes are associated with the peroxisomal membrane (i.e. squalene synthase and squalene epoxidase). On the basis of these results, it seemed probable that *Dd*OSC would also be associated with the peroxisomal membrane because the product of the enzyme-catalysed reaction is highly hydrophobic and therefore must be released temporarily into a membrane prior to the subsequent methylation reaction.

To investigate the membrane association of *D. discoideum* oxidosqualene cyclase the insoluble fraction obtained from disrupted amoebae was treated with either 1M NaCl or 100mM Na_2CO_3 pH11.4. We found that GFP-*Dd*OSC was not removed by 1M NaCl suggesting that the enzyme is strongly bound to the peroxisomal membrane (Figure 5.5 A). By contrast, when the pellet fraction was treated with carbonate approximately half of the protein remained in the pellet fraction while 50% of the protein was released in the supernatant (Figure 5.5 B). Thus, these results indicated that *Dd*oxidosqualene cyclase is strongly associated with the peroxisomal membrane.

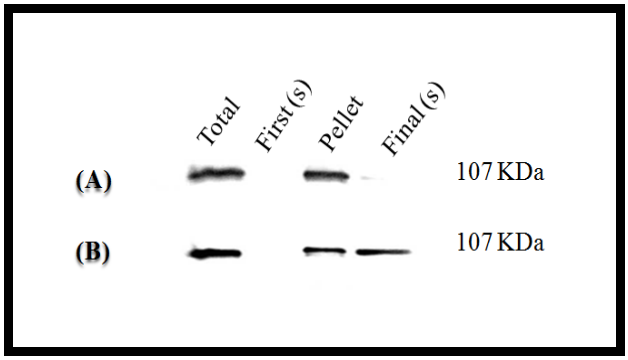

Figure 5.5: Biochemical analysis of *D. discoideum* oxidosqualene cyclase. (A) 1M NaCl treatment. (B) 100mM sodium carbonate pH 11.4 treatment. Further details are given in the legend to Figure 5.2. Total (the whole lysate), First s (the supernatant after the first centrifugation), Pellet (the insoluble fraction after 1M NaCl or 100mM Na_2CO_3 pH 11.4 treatment), Final s (the supernatant after 1M NaCl or 100mM Na_2CO_3 pH 11.4 treatment).

5.2.5 Cycloartenol-C-24-methyltransferase is tightly bound to the peroxisomal membrane

It appeared that, because the first three enzymes of sterol biosynthesis from farnesyl diphosphate are associated with the peroxisomal membrane, it was necessary to determine whether the next enzyme was also peroxisomal membrane protein. Therefore, in experiments intended to investigate whether *Dd*cycloartenol-C-24-methyltransferase is also associated with the peroxisomal membrane, we treated the pellet fraction from amoebae that overexpressd *Dd*SMT with Na_2CO_3 pH 11.4. It was found that *Dd*SMT cannot be extracted by carbonate at pH 11.4 (Figure 5.6), suggesting that *Dd*cycloartenol-C-24-methyltransferase is tightly bound to the peroxisomal membrane and behaves like an integral membrane protein.

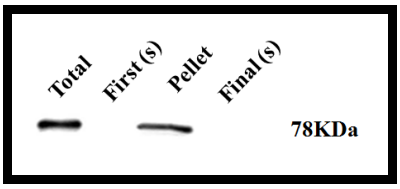

Figure 5.6: Association of *D. discoideum* cycloartenol-C-24-methyltransferase with the peroxisomal membrane. Amoebae were treated with 100mM sodium carbonate pH 11.4. Total (the whole lysate), First s (the supernatant after the first centrifugation), Pellet (the insoluble fraction after the carbonate treatment), Final s (the supernatant after the carbonate treatment).

5.2.6 Is the PTS1 on squalene synthase, oxidosqualene cyclase and cycloartenol -C-24-methyltransferase functional?

By definition, peroxisomal matrix proteins do not associate with the peroxisomal membrane. Furthermore, proteins with a PTS1 are believed to be matrix proteins and thus not to be membrane proteins. Peroxisomal membrane proteins (PMPs) require an entirely different pathway for their sorting into the peroxisomes (Pex19p and Pex3p pathways). Therefore, it seemed necessary to test whether the putative PTS1 of *Dd*squalene synthase, *Dd*oxidosqualene cyclase and *Dd*C-24-methyltransferase is involved in peroxisomal import because these appear to be membrane-associated proteins rather than matrix proteins.

5.2.7 Squalene synthase

A PCR product encoding *Dd*squalene synthase, lacking the last three amino acids comprising the PTS1 (-Ser-Lys-Lue$_{COOH}$), was generated using pMA16 as a DNA template and VIP1892 plus VIP2184 as primers. This cDNA fragment was digested with BamHI and XbaI and ligated into BamHI – XbaI digested pDXA3C-MA to obtain pMA27. When amoebae expressed pMA27 encoding GFP-*Dd*SQSΔPTS1 a punctate distribution of fluorescence was mainly observed in addition to some cytosolic background (Figure 5.7).

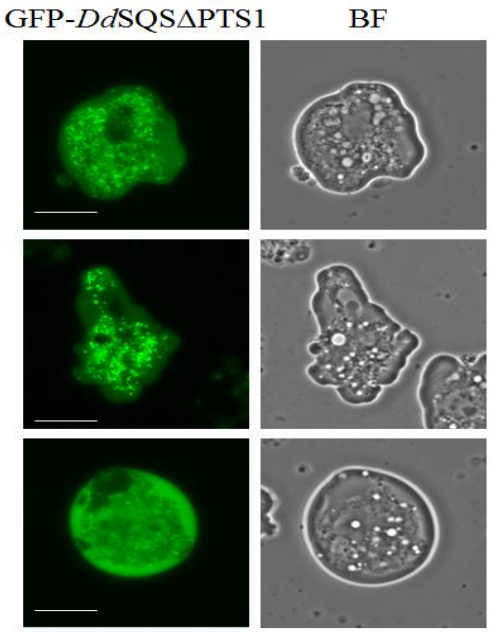

Figure 5.7: Analysis of GFP-*Dd*SQSΔPTS1 expression in *D. discoideum*. Amoebae expressing GFP-*Dd*SQSΔPTS1exhibited an apparently typical peroxisomal pattern of green fluorescence in addition to some cytosolic fluorescence distribution. Scale bars 5µm.

Amoebae expressing pMA27 were re-transformed to express the peroxisomal marker mRFP-PTS1 in order to investigate whether the punctate fluorescence was peroxisomal. It was found that GFP-*Dd*SQSΔPTS1, despite the absence of the PTS1, co-localized with the peroxisomal marker was partially observed (Figure 5.8).

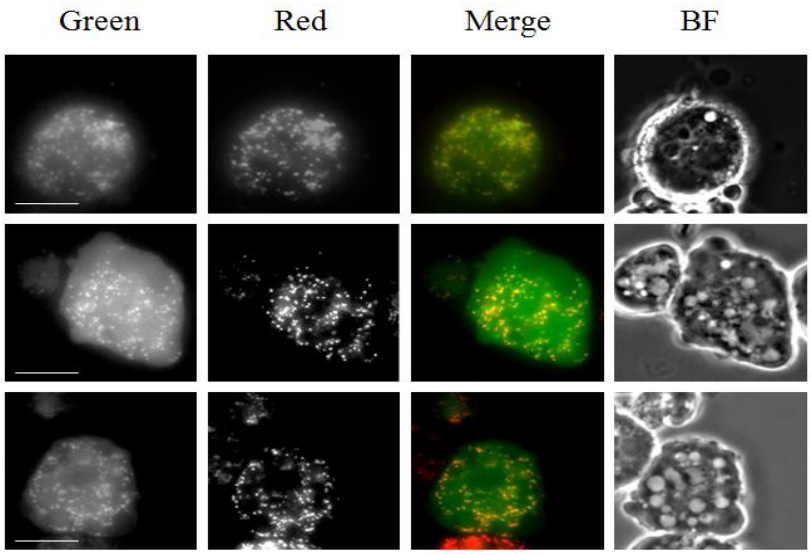

Figure 5.8: The intracellular localization of GFP-*Dd*SQSΔPTS1 in *D. discoideum*. Amoebae co-expressing GFP-*Dd*SQSΔPTS1 and the peroxisomal marker mRFP-PTS1. The co-localization of the GFP and mRFP fluorescence was partially observed in the peroxisomes. Scale bars 5μm.

5.2.8 Oxidosqualene cyclase

To determine whether the putative PTS1 (-SKI$_{COOH}$) of *Dd*oxidosqualene cyclase is responsible for the peroxisomal localization, a truncated version of *Dd*OSC, encoded by pMA28, lacking the putative PTS1 was expressed in amoebae. When *D. discoideum* amoebae expressed pMA28, encoding GFP-*Dd*OSCΔPTS1, the fusion protein was mislocalized to the cytosol where it was associated with unusual structures (Figure 5.9). This suggested that *Dd*OSC PTS1 is responsible of targeting the enzyme into the peroxisomes.

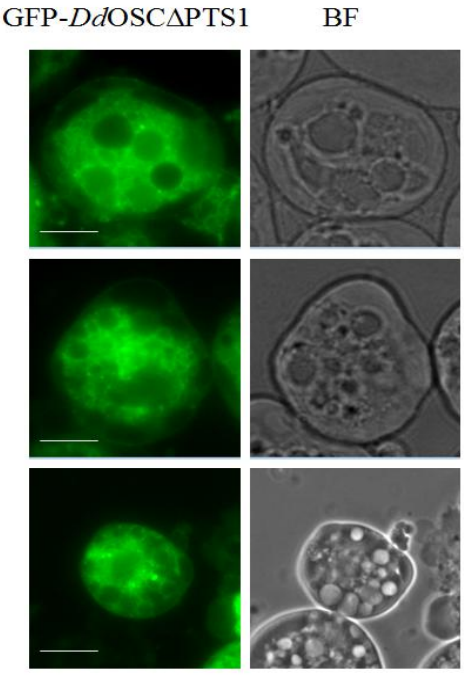

Figure 5.9: Analysis of GFP-*Dd*OSCΔPTS1 expression in *D. discoideum*. The GFP fluorescence appeared to be associated with components of the cytosol. Scale bars 5μm.

Further experiments were carried out in order to investigate the possible intracellular location of *Dd*OSC-ΔPTS1. *D. discoideum* amoebae were therefore re-transformed either with pMA26 encoding *Dd*Calnexin-mRFP (ER membrane marker) or pMA30 encoding *Dd*Top2-isomerase-mRFP (mitochondrial marker). When amoebae were co-expressing GFP-*Dd*OSC-ΔPTS1and *Dd*Calnexin-mRFP, the fluorescence of the GFP partially co-localized with the mRFP fluorescence (Figure 5.10). In addition, in some cells, there was a ring of GFP fluorescence coinciding with the plasma membrane (Figure 5.10).

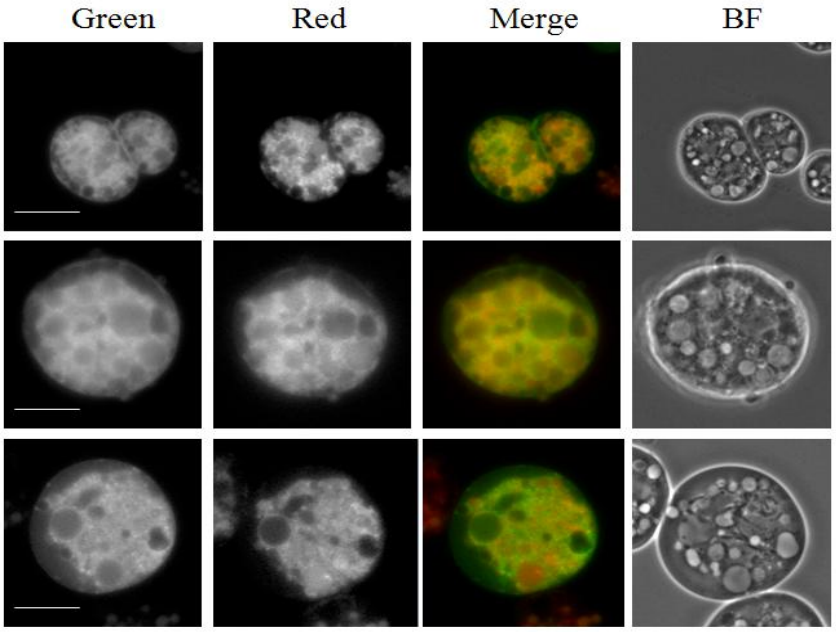

Figure 5.10: Association of GFP-*Dd*OSC-ΔPTS1 with the ER membrane. Amoebae expressing both GFP-*Dd*OSC-ΔPTS1 and an ER marker (*Dd*Calnexin-mRFP). Co-localization of the GFP and mRFP fluorescence was observed in the ER. Scale bars 5μm.

Furthermore, when amoebae were co-expressing GFP-*Dd*OSC-ΔPTS1 and *Dd*Top2-isomerase-mRFP, the fluorescence patterns of GFP and mRFP partially superimposed (Figure 5.11).

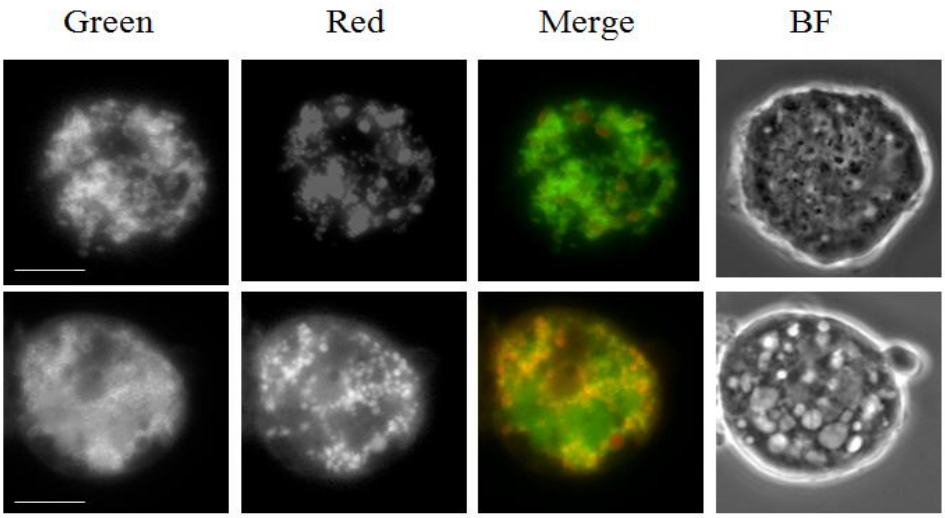

Figure 5.11: Association of GFP-*Dd*OSC-ΔPTS1 with the mitochondria. Amoebae co-expressing GFP-*Dd*OSC-ΔPTS1 and *Dd*Top2-isomerase-mRFP (mitochondrial marker). Co-localization of GFP and mRFP fluorescence was observed around the mitochondria. Scale bars 5μm.

5.2.9 Cycloartenol -C-24-methyltransferase

In order to investigate whether the putative PTS1 (-AKL) of *Dd*cycloartenol-C-24-methyltransferase targets the enzyme to the peroxiomes, a GFP-*Dd*SMT minus PTS1 construct (pMA29) was generated. In amoebae expressing pMA29, encoding GFP-*Dd*SMTΔPTS1, the fusion protein accumulated entirely in the cytosol (Figure 5.12). Thus, this result indicated that the putative PTS1 is essential for the peroxisomal localization of *Dd*cycloartenol-C-24-methyltransferase.

`

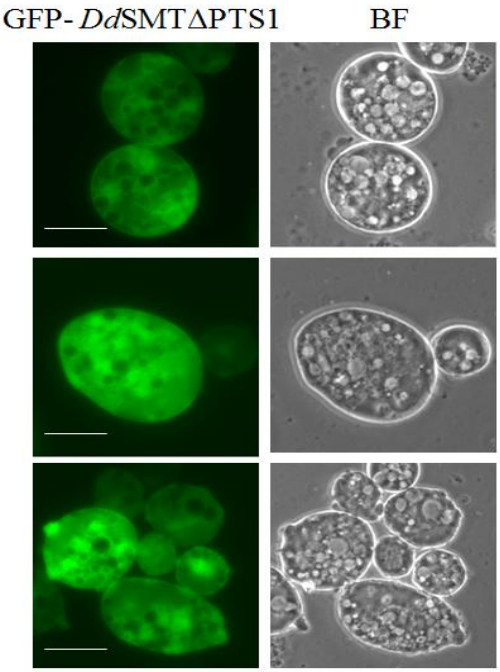

Figure 5.12: Analysis of GFP-*Dd*SMTΔPTS1 expression in *D. discoideum*. Amoebae expressing GFP- *Dd*SMTΔPTS1 showed green fluorescence only in the cytosol. Scale bars 5μm.

5.3 Discussion

The biochemical approaches making use of 1M NaCl and 100mM carbonate extraction of the membrane-containing fraction from amoebae, demonstrated that the first four enzymes involved in converting farnesyl diphosphate into sterols in *D. discoideum* are associated with the peroxisoml membrane. Squalene synthase and cycloartenol-C-24-methyltransferase are tightly bound to the peroxisomal membrane and seem to behave as integral membrane proteins. Oxidosqualene cyclase was partially extracted by 100mM carbonate whereas squalene epoxidase was not extracted by high salt treatment but it was released completely into the supernatant by the carbonate. It appeared that these two enzymes cannot be transmembrane membrane proteins although they must, nevertheless, be tightly bound to the peroxisomal membrane.

Treatment with 100mM carbonate revealed that *Dd*squalene synthase behaves as an integral membrane protein. The C-terminal hydrophobic sequence of human, yeast and *A. thaliana* squalene synthase contains a predicted trans-membrane domain (Jennings et al., 1991, Robinson et al., 1993, Kribii et al., 1997, Busquets et al., 2008). This sequence plays an important role in anchoring squalene synthase into the ER membrane. Furthermore, the bioinformatic predication for trans-membrane domains (TM) suggests the existence of a similar TM domain in the *Dd*squalene synthase which is again located very close to the carboxy terminus. This evidence suggests that *Dd*squalene synthase may be tail-anchored into the peroxisomal mermbrane.

Although the bioinformatic data support the presence of the trans-membrane domain at the C-terminus of *Dd*squalene epoxidase, our results suggested that this protein does not act as an integral membrane protein. The mechanism by which the *Dd*squalene epoxidase becomes asssociated with the peroxisomal membrane remains unclear. It is also unclear how the epoxidase enters the peroxisomes because it lacks a PTS.

*Dd*oxidosqualene cyclase (cycloartenol synthase) is associated with the peroxisomal membrane but it is not tightly bound. In addition, it has been postulated that the human lanosterol synthase (oxidosqualene cyclase) is a monotopic integral

membrane protein (Figure 5.13) (Thoma et al., 2004, Ruf et al., 2004). Furthermore, it was found that there is a predicted amphipathic membrane anchor helix in *Dd*oxidosqualene cyclase that corresponds to the membrane anchor helix of human lanosterol synthase (Figure 5.14). X-ray crystal structure analysis demonstrated that squalene-hopene cyclase, homologous to the eukaryotic OSC, from the bacterium *Alicyclobacillus acidocaldarius* is integrated partially into the membrane (Wendt et al., 1997, Bracey et al., 2004, Siedenburg and Jendrossek, 2011). Therefore, the membrane association of *Dd*oxidosqualene cyclase might be classified as a monotopic membrane protein (a protein that inserts within one leaflet of the membrane bilayer but does not span the membrane).

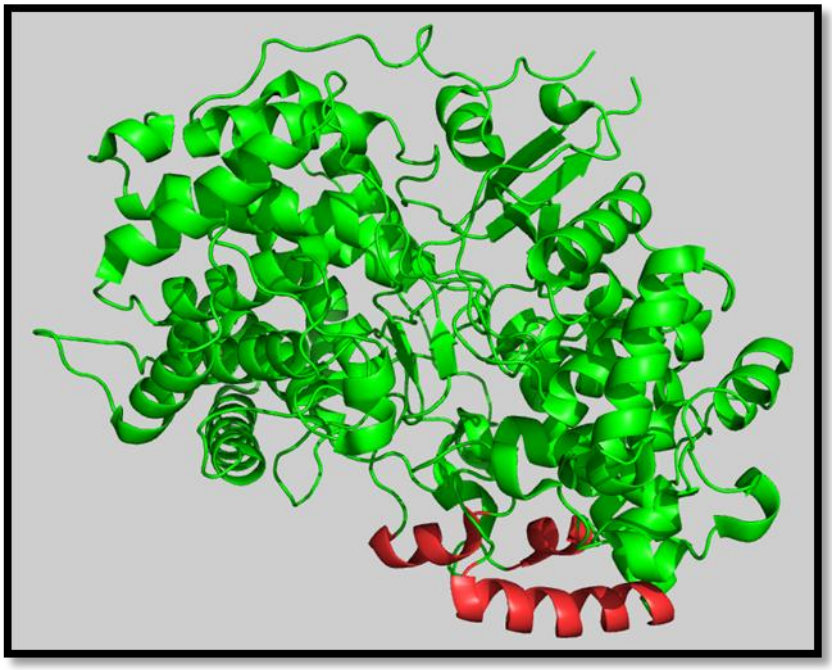

Figure 5.13: Three dimensional structure of human lanosterol synthase. The predicted membrane anchor helix is shown in red. This image was kindly provided by Dr Patrick Baker and is derived from the structure elucidated by Thoma et al, (2004).

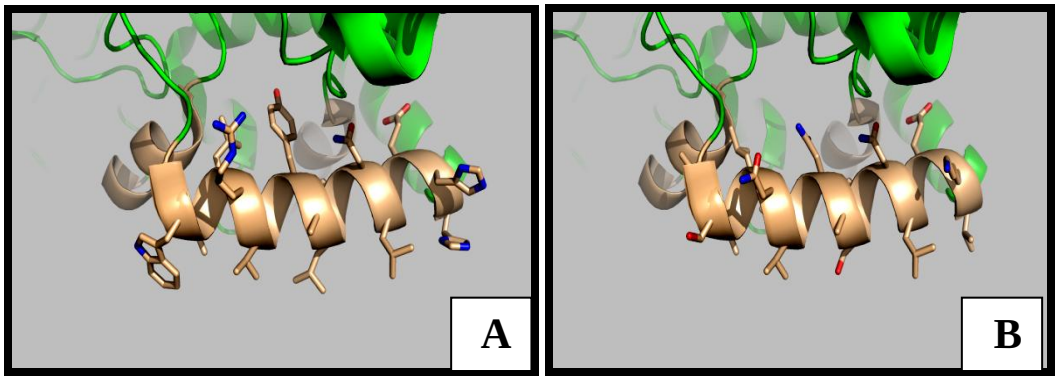

Figure 5.14: Predicted membrane anchor helix of human lanosterol synthase (A) and *D. discoideum* cycloartenol synthase(B). It seems that a similar helix is present in *Dd*cycloartenol synthase. These structures were kindly provided by Dr Patrick Baker.

Previous studies have suggested that the import of peroxisomal matrix proteins and the insertion of peroxisomal membrane proteins occur by two independent pathways (Erdmann and Blobel, 1996, Gould et al, 1996). In addition, it has been postulated that the PTS1 and PTS2 pathways are responsible for the entry of the peroxisomal matrix protein but not the membrane proteins. It remains unclear how at least oxidosqualene cyclase and cycloartenol-C-24-methyltransferase apparently behave as peroxisomal matrix proteins but also associate with the peroxisomal membrane.

Chapter 6

General discussion and Future directions

The initial aim of this study was to determine the intracellular compartmentalization of the mevalonate pathway enzymes in *Dictyostelium discoideum*. The evidence presented, based upon generating fusion proteins, demonstrates that three enzymes of the pathway are localized to the peroxisomes: the second isozyme of HMG-CoA synthase, phosphomevalonate kinase and farnesyl diphosphate synthase. The latter had been identified previously as a peroxisomal enzyme in *D.discoideum* (Nuttall et al., 2012). HMG-CoA reductase, as in other organisms, is localized to the ER whereas four enzymes of the MVA pathway are cytosolic.

It has been shown in mammals that the peroxisomal membrane is permeable to small molecules whereas it does not allow uptake of large molecules such as the cofactors NAD/H, NADP/H and phosphorylated components by simple diffusion (Antonenkov et al., 2004b). Due to the compartmentalization of the *D.discoideum* MVA pathway into three cellular compartments: perosixsome, cytosol and ER, all of the pathway phosphorylated intermediates need to cross the peroxisomal membrane: phosphomevalonate, isopentenyl diphosphate and dimethylallyl diphosphate must have to immigrate from the cytosol into the peroxisomes. However, some of the phosphorylated components need to travel in the opposite direction such as diphosphomevalonate and farnesyl diphosphate (Figure 1.6). In *S.cerevisiae*, it has been proposed that the passage of the phosphorylated compound ADP from the cytosol into the peroxisomal matrix requires a specific transport system (Palmieri et al., 2001, Lasorsa et al., 2004). This implies that the shuttle of MVA pathway phosphorylated compounds across the peroxisomal membrane will also require a transport system although this has yet to be identified.

Although there is evidence that most of the mammalian MVA pathway enzymes are peroxisomal (reviewed by Kovacs et al, 2007), the localization of the pathway enzymes in *D.discoideum* is only partially consistent with the mammalian

distribution proposed by Kovacs et al, (2007). As in *D.discoideum*, it has been shown previously in mammals that the second isozyme of HMG-CoA synthase, phosphomevalonate kinase and FDP-synthase are localized to the peroxisomes (Olivier et al., 2000, Kovacs et al., 2007). Indeed, the peroxisomal location of the *D.discoideum* enzymes is consistent with the presence of strong PTS sequences. By contrast, *D.discoideum* isopentenyl diphosphate isomerase was found to be localized to the cytosol wherease the two isozymes of human IDP- isomease were identified as peroxisomal enzymes (Clizbe et al., 2007). This peroxisomal targeting is facilitated by unusual tripeptide combinations which each seem to act as a functional PTS1. However, much evidence (discussed previously in Chapter 3) supports the conclusion that the amino acid triplet at the C-terminus of *D.discoideum* IDP-isomerase does not act as a PTS1. Furthermore, our data support a cytosolic location of both mevalonate kinase and diphosphomevalonate decarboxylase as described by (Hogenboom et al., 2004b, Hogenboom et al., 2004a) for mammalian cells. Nevertheless, Krisans' group appears to have demonstrated a peroxisomal location for mevalonate kinase and the decarboxylase in mammals (Kovacs et al., 2007).

Investigations of the intracellular locations of the mevalonate pathway in mammals mainly rely on subcellular fractionation and immunofluorescence microscopy studies. Use of the subcellular fraction method requires great care because the peroxiomal membrane is known to be fragile. Furthermore, it has been reported that some of the peroxisomal matrix protein can seep out easily from the peroxisome during the fractionation (Antonenkov et al., 2004b, Antonenkov et al., 2004a) which may lead to misinterpretation of the enzyme subcellular location. One limitation of using immunofluorescence microscopy is that the antibody may be able to detect its antigen only when the antigen is at a higher concentration than is usually present in cells. Therefore, the antibody cannot recognize its target in the cytosol. The limitations of the subcellular fractions and immunofluorescence microscopy approaches discussed above may explain the conflicting results that have been reported on the role of peroxisomes in the mammalian mevalonate pathway.

In plants, the experimental data regarding the intracellular compartmentalization of the MVA pathway is very limited. However, as in *D.discoideum,* it has been demonstrated that plant mevalonate kinase is a cytosolic enzyme and phosphomevalonate kinase have been identified as a peroxisomal enzyme (Simkin et al., 2011). By contrast, the cytosolic location of both *D.discoideum* diphosphomevalonate decarboxylase and IDP-isomerase does not agree with the data from plants system which apparently support a peroxisomal location for each enzyme (Sapir-Mir et al., 2008, Simkin et al., 2011).

Based upon the data and the arguments presented above a new model describing the compartmentalization of the MVA pathway in the unicellular organism *D.discoideum* can be proposed (Figure 1.6). This model provides a clear picture, at least in one organism, as to where each substrate must be present to allow each enzyme reaction to occur. Nevertheless, the reason for distribution of the MVA pathway enzymes between the three cellular compartments has not been identified.

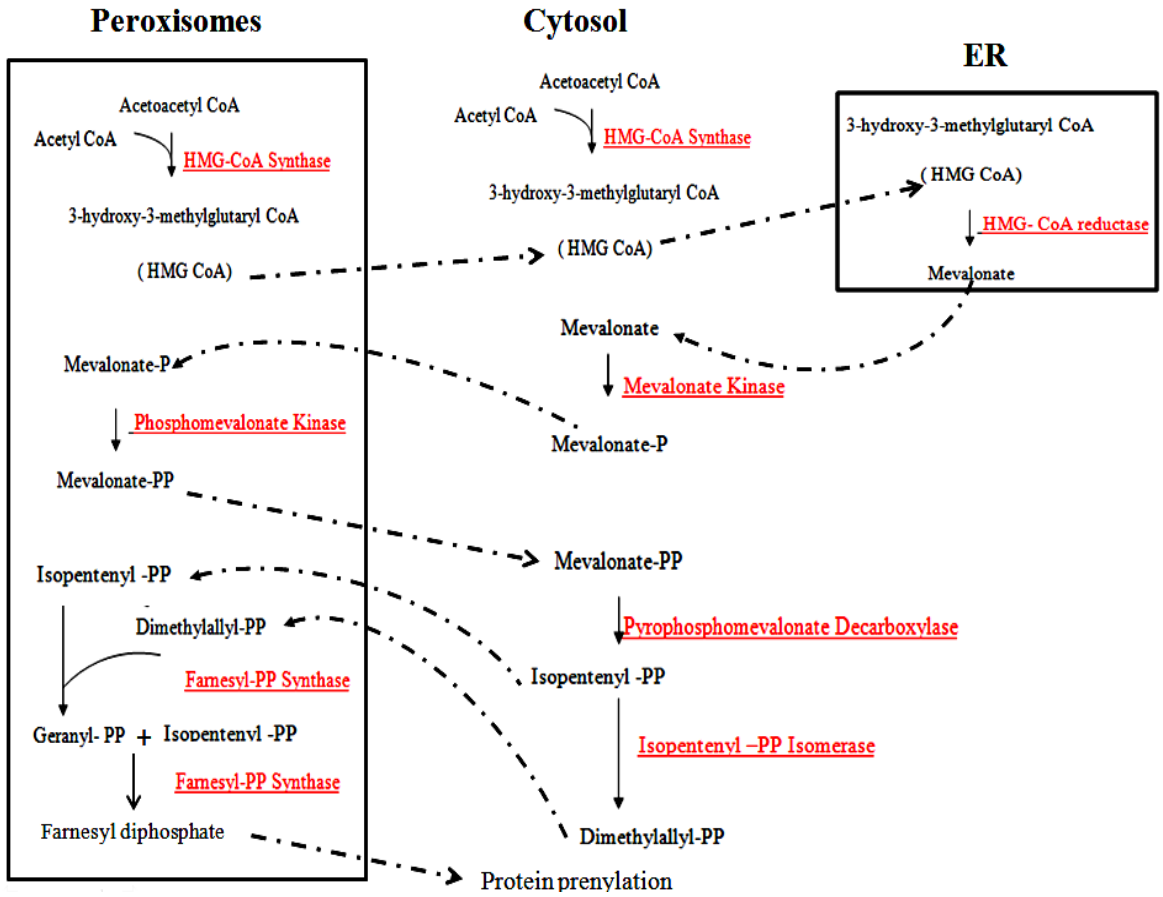

Figure 6.1: A current view of the intracellular locations of the mevalonate pathway enzymes in the unicellular organism *Dictyostelium discoideum*.

The successful used of the fusion protein approach to investigate the intracellular location of the MVA pathway encourages us to characterize the intracellular compartmentalization of the following pathway (sterol biosynthesis) because it appeared that, unusually, the first enzyme on this pathway has a PTS1 in *D. discoideum*. A further aim of this study was therefore, to investigate the intracellular locations of the first five enzymes involved in converting farnesyl diphosphate to sterol in *D. discoideum*. The peroxisomal location of the first four enzymes of sterol biosynthesis is uniquely observed in the slime mold *D. discoideum*. Three of the pathway enzymes in *D. discoideum* possess a putative PTS1 and these have been identified as peroxisomal proteins: squalene synthase, oxidosqualene cyclase and cycloartenol -C-24-methyltransferase. Despite lacking a PTS, *Dd*squalene epoxidase, which catalyzes the second reaction of the sterol biosynthesis, was also found in the peroxisomes. Nevertheless, the two isozymes of the methylsterol monooxygenase are associated with the endoplasmic reticulum. Therefore, one would expect that the enzymes catalyzing the later steps of the sterol biosynthetic pathway in *D. discoideum* will be localized as in other organisms to the ER, because these enzymes seem to possess an ER-directed signal but do not possess a PTS. The reasons for the enzymes' distribution between the two cellular compartments: peroxisomes and ER is not clear. In addition, it is assumed that there is a mechanism by which the intermediate C-24 methylcycloartenol is transferred from the peroxisomes to the ER. Different mechanisms can be envisaged including vesicular transport, lipid transfer protein mediated transport or diffusion via membrane continuations or contact sites. The mechanism has yet to be elucidated.

Furthermore, another unique aspect of the sterol biosynthesis enzymes in *D. discoideum* is that although the first four enzymes appear to enter the peroxisome as peroxisomal matrix proteins, they have been shown to be associated with the peroxisomal membrane. Two of these enzymes are tightly bound to the peroxisomal membrane: squalene synthase and cycloartenol-C-24-methyltransferase. Oxidosqualene cyclase is not as strongly bound as the previous enzyme whereas squalene epoxidase is loosely bound to the peroxisomal membrane. It is possible that these enzymes become associated with the peroxisomal membrane after being imported into the peroxisomal matrix and this

requires a specific mechanism that has not been investigated. However, one would assume that squalene sythase might be anchoring into the peroxisomal membrane via its possible C-terminus TM domain. Therefore, one could investigate the possible role of the TM domain by generating a truncated version of squalene synthase lacking the C-terminus TM domain but retaining the PTS1 and analyzing the location of the truncated enzyme by immunoblot analysis. It is also not clear how cycloartenol-C-24-methyltransferase is associated with the peroxisomal membrane. However, one could assume that the N-terminal extension (114 amino acids) of *Dd*cycloartenol-C-24-methyltransferase may have a role in anchoring the enzyme into the peroxisomal membrane. Therefore, further research should be carried out to clarify the possible function of the N-terminal extension of *Dd*SMT1. Overall, the association of these enzymes with the peroxisomal membrane indicates a significant role for peroxisomes in sterol biosynthesis in *D.discoideum*.

Since squalene synthase, oxidosqualene cyclase and cycloartenol-C-24-methyltransferase are membrane associated proteins in *D. discoideum* it was therefore necessary to investigate whether their putative PTS1 is functional. Although squalene synthase possesses the most efficient targeting signal (-SKL), it was found that this enzyme is still able to accumulate in the peroxisomes after deletion of its targeting signal. It is still unclear how squalene synthase is targeted to the peroxisome.

By contrast, the putative PTS1 sequences of oxidosqualene cyclase and cycloartenol-C-24-methyltransferase have been shown to be responsible for targeting these two enzymes into the peroxisomes. Oxidosqualene cyclase ΔPTS1 seems to associate with most cellular membranes. It is probable that cycloartenol synthase in *D.discoideum*, like the human lanosterol synthase, is a monotopic protein. Therefore, it is possible that, after deletion of the putative targeting signal, its amphipathic helix tends to insert into any membrane. Cycloartenol-C-24-methyltransferase ΔPTS1 accumulated in the cytosol. This suggests that this enzyme does not contain a hydrophobic region and probably does not contain a TM domain. Based on this observation, it is possible that the association of this enzyme with the peroxisomal membrane occurs via the interaction of this enzyme with some peroxisomal membrane protein.

During this study the intracellular locations of the mevalonate pathway enzymes from HMG-CoA synthase have been determined in the unicellular organism *D.discoideum*. Our data clearly show that three of the pathway enzymes are peroxisomal and four enzymes are most likely cytosolic and one enzyme is localized to the ER. Furthermore, we determined the intracellular locations of the first five enzymes involved in converting farnesyl diphosphate to dictysterol in *D. discoidium*. It has been shown that the first four enzymes are peroxisomal and the fifth one was identified as an ER enzyme. This study provides a clear picture of the intracellular compartmentalization of the sterol biosynthesis enzymes in one organism. Further investigations will be needed to determine the reasons for the enzymes' distribution between the different cellular compartments and to discover how the four of the sterol biosynthesis enzymes are bound to the peroxisomal membrane.

REFRENCES

AGNE, B., MEINDL, N. M., NIEDERHOFF, K., EINWACHTER, H., REHLING, P., SICKMANN, A., MEYER, H. E., GIRZALSKY, W. & KUNAU, W. H. 2003. Pex8p: an intraperoxisomal organizer of the peroxisomal import machinery. ***Mol Cell,*** **11, 635-46**

ANTONENKOV, V. D., SORMUNEN, R. T. & HILTUNEN, J. K. 2004a. The behavior of peroxisomes in vitro: mammalian peroxisomes are osmotically sensitive particles. ***Am J Physiol Cell Physiol,*** **287, C1623-35**

ANTONENKOV, V. D., SORMUNEN, R. T. & HILTUNEN, J. K. 2004b. The rat liver peroxisomal membrane forms a permeability barrier for cofactors but not for small metabolites in vitro. ***J Cell Sci,*** **117, 5633-42**

AYTE, J., GIL-GOMEZ, G., HARO, D., MARRERO, P. F. & HEGARDT, F. G. 1990. Rat mitochondrial and cytosolic 3-hydroxy-3-methylglutaryl-CoA synthases are encoded by two different genes. ***Proc Natl Acad Sci U S A,*** **87, 3874-8**

BAKER, A. & SPARKES, I. A. 2005. Peroxisome protein import: some answers, more questions. ***Curr Opin Plant Biol,*** **8, 640-7**

BAUDHUIN, P., BEAUFAY, H. & DE DUVE, C. 1965. Combined biochemical and morphological study of particulate fractions from rat liver Analysis of preparations enriched in lysosomes or in particles containing urate oxidase, D-amino acid oxidase, and catalase. ***J Cell Biol,*** **26, 219-43**

BERGERON, J. J., BRENNER, M. B., THOMAS, D. Y. & WILLIAMS, D. B. 1994. Calnexin: a membrane-bound chaperone of the endoplasmic reticulum. ***Trends Biochem Sci,*** **19, 124-8**

BIARDI, L., SREEDHAR, A., ZOKAEI, A., VARTAK, N. B., BOZEAT, R. L., SHACKELFORD, J. E., KELLER, G. A. & KRISANS, S. K. 1994. Mevalonate kinase is predominantly localized in peroxisomes and is defective in patients with peroxisome deficiency disorders. ***J Biol Chem,*** **269, 1197-205**

BIRSCHMANN, I., STROOBANTS, A. K., VAN DEN BERG, M., KUNAU, W. H. & TABAK, H. F. „.SCHAFER, A., ROSENKRANZ, K 2003. Pex15p of Saccharomyces cerevisiae provides a molecular basis for recruitment of the AAA peroxin Pex6p to peroxisomal membranes. ***Mol Biol Cell,*** **14, 2226-36**

BOUVIER-NAVE, P., HUSSELSTEIN, T. & BENVENISTE, P. 1998. Two families of sterol methyltransferases are involved in the first and the second methylation steps of plant sterol biosynthesis. ***Eur J Biochem,*** **256, 88-96**

BOUVIER, F., RAHIER, A. & CAMARA, B. 2005. Biogenesis, molecular regulation and function of plant isoprenoids. ***Prog Lipid Res,*** **44, 357-429**

BRACEY, M. H., CRAVATT, B. F. & STEVENS, R. C. 2004. Structural commonalities among integral membrane enzymes. ***FEBS Lett,*** **567, 159-65**

BROWN, L. A. & BAKER, A. 2003. Peroxisome biogenesis and the role of protein import. ***J Cell Mol Med,*** **7, 388-400**

BROWN, L. A. & BAKER, A. 2008. Shuttles and cycles: transport of proteins into the peroxisome matrix (review). ***Mol Membr Biol,*** **25, 363-75**

BUSQUETS, A., KEIM, V., CLOSA, M., DEL ARCO, A., BORONAT, A., ARRO, M. & FERRER, A. 2 .008Arabidopsis thaliana contains a single gene encoding squalene synthase. ***Plant Mol Biol,*** **67, 25-36**

CHEN, D. C., YANG, B. C. & KUO, T. T. 1992. One-step transformation of yeast in stationary phase. ***Curr Genet,*** **21, 83-4**

CIOSEK, C. P., JR., MAGNIN, D .R., HARRITY, T. W., LOGAN, J. V., DICKSON, J. K., JR., GORDON, E. M., HAMILTON, K. A., JOLIBOIS, K. G., KUNSELMAN, L. K., LAWRENCE, R. M. & ET AL. 1993. Lipophilic 1,1-bisphosphonates are potent squalene synthase inhibitors and orally active cholesterol lowering agents in vivo. ***J Biol Chem,*** **268, 24832-7**

CLIZBE, D. B., OWENS, M. L., MASUDA, K. R., SHACKELFORD, J. E. & KRISANS, S. K. 2007. IDI2, a second isopentenyl diphosphate isomerase in mammals. ***J Biol Chem,*** **282, 6668-76**

CLOUSE, S. D. 2002. Arabidopsis mutants reveal multiple roles for sterols in plant development. ***Plant Cell,*** **14, 1995-2000**

DAMMAI, V. & SUBRAMANI, S. 2001. The human peroxisomal targeting signal receptor, Pex5p, is translocated into the peroxisomal matrix and recycled to the cytosol .*Cell,* 105, 187-96

DARNET, S. & RAHIER, A. 2004. Plant sterol biosynthesis: identification of two distinct families of sterol 4alpha-methyl oxidases. ***Biochem J,*** **378, 889-98**

DE DUVE, C. & BAUDHUIN, P. 1966. Peroxisomes (microbodies and related particles) .*Physiol Rev,* 46, 323-57

DISTEL, B., ERDMANN, R., GOULD, S. J., BLOBEL, G., CRANE, D. I., CREGG, J. M., DODT, G., FUJIKI, Y., GOODMAN, J. M., JUST, W. W., KIEL, J. A., KUNAU, W. H., LAZAROW, P. B., MANNAERTS, R. A., ,G. P., MOSER, H. W., OSUMI, T., RACHUBINSKI ROSCHER, A., SUBRAMANI, S., TABAK, H. F., TSUKAMOTO, T., VALLE, D., VAN DER KLEI, I., VAN VELDHOVEN, P. P. & VEENHUIS, M. 1996. A unified nomenclature for peroxisome biogenesis factors. *J Cell Biol,* 135, 1-3

EICHINGER, L., PACHEBAT, J. A., GLOCKNER, G., RAJANDREAM, M. A., SUCGANG, R., BERRIMAN, M., SONG, J., OLSEN, R., SZAFRANSKI, K., XU, Q., TUNGGAL, B., KUMMERFELD, S., MADERA, M., KONFORTOV, B. A., RIVERO, F., BANKIER, A. T., LEHMANN, R., HAMLIN, N., DAVIES, R., GAUDET, P., FEY, P., PILCHER, K ,.CHEN, G., SAUNDERS, D., SODERGREN, E., DAVIS, P., KERHORNOU, A., NIE, X., HALL, N., ANJARD, C., HEMPHILL, L., BASON, N., FARBROTHER, P., DESANY, B., JUST, E., MORIO, T., ROST, R., CHURCHER, C., COOPER, J., HAYDOCK, S., VAN DRIESSCHE, N., CRONIN, A., GOODHEAD, I., MUZNY, D., MOURIER, T., PAIN, A., LU, M., HARPER, D., LINDSAY, R., HAUSER, H., JAMES, K., QUILES, M., MADAN BABU, M., SAITO, T., BUCHRIESER, C., WARDROPER, A., FELDER, M., THANGAVELU, M., JOHNSON, D., KNIGHTS, A., LOULSEGED, H., MUNGALL, K., OLIVER, K., PRICE, C., QUAIL, M. A., URUSHIHARA, H., HERNANDEZ, J., RABBINOWITSCH, E., STEFFEN, D., SANDERS, M., MA, J., KOHARA, Y., SHARP, S., SIMMONDS, M., SPIEGLER, S., TIVEY, A., SUGANO, S., WHITE, B., WALKER, D., WOODWARD, J., WINCKLER, T., TANAKA, Y ,.SHAULSKY, G., SCHLEICHER, M., WEINSTOCK, G., ROSENTHAL, A., COX, E. C., CHISHOLM, R. L., GIBBS, R., LOOMIS, W. F., PLATZER, M., KAY, R. R., WILLIAMS, J.,

DEAR, P. H., NOEGEL, A. A., BARRELL, B. & KUSPA, A. 2005. The genome of the social amoeba Dictyostelium discoideum. ***Nature,*** **435, 43-57**

EITZEN, G. A., SZILARD, R. K. & RACHUBINSKI, R. A. 1997. Enlarged peroxisomes are present in oleic acid-grown Yarrowia lipolytica overexpressing the PEX16 gene encoding an intraperoxisomal peripheral membrane peroxin. ***J Cell Biol,*** **137, 1265-78**

ELGERSMA, Y., KWAST, L., VAN DEN BERG, M., SNYDER, W. B., DISTEL, B., SUBRAMANI, S. & TABAK, H. F. 1997. Overexpression of Pex15p, a phosphorylated peroxisomal integral membrane protein required for peroxisome assembly in S.cerevisiae, causes proliferation of the endoplasmic reticulum membrane. ***EMBO J,*** **16, 7326-41**

ERDMANN, R. & BLOBEL, G. 1996. Identification of Pex13p a peroxisomal membrane receptor for the PTS1 recognition factor. ***J Cell Biol,*** **135, 111-21**

ERDMANN, R. & SCHLIEBS, W. 2005. Peroxisomal matrix protein import: the transient pore model. ***Nat Rev Mol Cell Biol,*** **6, 738-42**

ERDMANN, R., VEENHUIS, M., MERTENS, D. & KUNAU, W. H. 1989. Isolation of peroxisome-deficient mutants of Saccharomyces cerevisiae. ***Proc Natl Acad Sci U S A,*** **86, 5419-23**

FISCHER, M., HAASE, I., SIMMETH, E., GERISCH, G. & MULLER-TAUBENBERGER, A. 2004. A brilliant monomeric red fluorescent protein to visualize cytoskeleton dynamics in Dictyostelium. ***FEBS Lett,*** **577, 227-32**

FU, Z., WANG, M., POTTER, D ,.MIZIORKO, H. M. & KIM, J. J. 2002. The structure of a binary complex between a mammalian mevalonate kinase

and ATP: insights into the reaction mechanism and human inherited disease. ***J Biol Chem,*** **277, 18134-42**

FLEISCH, H. 1995. Bisphosphonates in Bone Disease. From the Laboratory to the Patient. The Parthenon Publishing Group, New York and London

FUJIKI, Y. 2000. Peroxisome biogenesis and peroxisome biogenesis disorders. ***FEBS Lett,*** **476, 42-6**

FUJIKI, Y., HUBBARD, A. L., FOWLER, S. & LAZAROW, P. B. 1982. Isolation of intracellular membranes by means of sodium carbonate treatment: application to endoplasmic reticulum. ***J Cell Biol,*** **93, 97-102**

GABER, R. F., COPPLE, D. M., KENNEDY, B. K., VIDAL, M. & BARD, M. 1989. The yeast gene ERG6 is required for normal membrane function but is not essential for biosynthesis of the cell-cycle-sparking sterol. ***Mol Cell Biol,*** **9, 3447-56**

GEISBRECHT, B. V., ZHANG, D., SCHULZ, H. & GOULD, S. J. 1999. Characterization of PECI, a novel monofunctional Delta(3), Delta(2)-enoyl-CoA isomerase of mammalian peroxisomes. ***J Biol Chem,*** **274, 21797-803.**

GIETZ, D., ST JEAN, A., WOODS, R. A. & SCHIESTL, R. H. 1992. Improved method for high efficiency transformation of intact yeast cells. ***Nucleic Acids Res,*** **20, 1425**

GIRZALSKY, W., HOFFMANN, L. S., SCHEMENEWITZ, A., NOLTE, A., KUNAU, W. H. & ERDMANN, R. 2006. Pex19p-dependent targeting of Pex17p, a peripheral component of the peroxisomal protein import machinery. ***J Biol Chem,*** **281, 19417-25**

GOEPFERT, S., VIDOUDEZ, C., TELLGREN-ROTH, C., DELESSERT, S., HILTUNEN, J. K. & POIRIER, Y. 2008. Peroxisomal Delta(3),Delta(2)-enoyl CoA isomerases and evolution of cytosolic paralogues in embryophytes. ***Plant J,*** **56, 728-42**

GOLDFARB, S. 1972. Submicrosomal localization of hepatic 3-hydroxy-3-methylglutaryl coenzyme a (HMG-CoA) reductase. ***FEBS Lett,*** **24, 153-155.**

GOLDSTEIN, J. L. & BROWN, M. S. 1990. Regulation of the mevalonate pathway. ***Nature,*** **343, 425-30**

GOTTE, K., GIRZALSKY, W., LINKERT, M., BAUMGART, E., KAMMERER, S., KUNAU, W. H. & ERDMANN, R. 1998. Pex19p, a farnesylated protein essential for peroxisome biogenesis. ***Mol Cell Biol,*** **18, 616-28**

GOULD, S. J., KELLER, G. A., HOSKEN, N., WILKINSON, J. & SUBRAMANI, S. 1989. A conserved tripeptide sorts proteins to peroxisomes. ***J Cell Biol,*** **108, 1657-64**

GOULD, S. J., MCCOLLUM, D., SPONG, A. P., HEYMAN, J. A. & SUBRAMANI, S. 1992. Development of the yeast Pichia pastoris as a model organism for a genetic and molecular analysis of peroxisome assembly. ***Yeast,*** **8, 613-28**

GOUVEIA, A. M., REGUENGA, C., OLIVEIRA, M. E., SA-MIRANDA, C. & AZEVEDO, J. E. 2000. Characterization of peroxisomal Pex5p from rat liver. Pex5p in the Pex5p-Pex14p membrane complex is a transmembrane protein. ***J Biol Chem,*** **275, 32444-51**

GROVE, J. E., BROWN, R. J. & WATTS, D. J. 2000. The intracellular target for the antiresorptive aminobisphosphonate drugs in Dictyostelium

discoideum is the enzyme farnesyl diphosphate synthase. *J Bone Miner Res,* 15, 971-81

GUPTA, S. D., MEHAN, R. S., TANSEY, T. R., CHEN, H. T., GOPING, G., GOLDBERG, I. & SHECHTER, I. 1999. Differential binding of proteins to peroxisomes in rat hepatoma cells: unique association of enzymes involved in isoprenoid metabolism. *J Lipid Res,* 40, 1572-84

GUNNING, B.E.S. 1998. The identity of mystery organelles in *Arabidopsis* plants expressing GFP. *in Plant Science* 3, 417

HARTMANN MA. 1998. Plant sterols and the membrane environment. Trends Plant Sci 3 170–175

HANAHAN, D. 1983. Studies on transformation of Escherichia coli with plasmids. *J Mol Biol,* 166, 557-80.

HAWES, C., SAINT-JORE, C., MARTIN, B. & ZHENG, H. Q. 2001. ER confirmed as the location of mystery organelles in Arabidopsis plants expressing GFP! *Trends Plant Sci,* 6, 245-6

HEGARDT, F. G. 1999. Mitochondrial 3-hydroxy-3-methylglutaryl-CoA synthase: a control enzyme in ketogenesis. *Biochem J,* 338 (Pt 3), 569-82

HERVET, E., CHARPENTIER, X., VIANNEY, A., LAZZARONI, J. C., GILBERT, C., ATLAN, D. & DOUBLET, P. 2011. Protein kinase LegK2 is a type IV secretion system effector involved in endoplasmic reticulum recruitment and intracellular replication of Legionella pneumophila. *Infect Immun,* 79, 1936-50

HETTEMA, E. H., GIRZALSKY, W., VAN DEN BERG, M., ERDMANN, R. & DISTEL, B. 2000. Saccharomyces cerevisiae pex3p and pex19p are

required for proper localization and stability of peroxisomal membrane proteins. *EMBO J,* 19, 223-33

HOGENBOOM, S., TUYP, J. J., ESPEEL, M., KOSTER, J., WANDERS, R. J. & WATERHAM, H. R. 2004a. Human mevalonate pyrophosphate decarboxylase is localized in the cytosol. *Mol Genet Metab*.24-216 ,81

HOGENBOOM, S., TUYP, J. J., ESPEEL, M., KOSTER, J., WANDERS, R. J. & WATERHAM, H. R. 2004b. Mevalonate kinase is a cytosolic enzyme in humans. *J Cell Sci,* 117, 631-9

HOGENBOOM, S., TUYP, J. J., ESPEEL, M., KOSTER, J., WANDERS, R. J. & WATERHAM, H. R. 2004c. Phosphomevalonate kinase is a cytosolic protein in humans. *J Lipid Res,* 45, 697-705

HONSHO, M., TAMURA, S., SHIMOZAWA, N., SUZUKI, Y., KONDO, N. & FUJIKI, Y. 1998. Mutation in PEX16 is causal in the peroxisome-deficient Zellweger syndrome of complementation group D. *Am J Hum Genet,* 63, 1622-30.

HOUTEN, S. M., WANDERS, R. J. & WATERHAM, H. R. 2000. Biochemical and genetic aspects of mevalonate kinase and its deficiency. *Biochim Biophys Acta,* 1529, 19-32

HSIEH, M. H., CHANG, C. Y., HSU, S .J. & CHEN, J. J. 2008. Chloroplast localization of methylerythritol 4-phosphate pathway enzymes and regulation of mitochondrial genes in ispD and ispE albino mutants in Arabidopsis. *Plant Mol Biol,* 66, 663-73

ISLINGER, M., LI, K. W., SEITZ, J., VOLKL, A & .LUERS, G. H. 2009. Hitchhiking of Cu/Zn superoxide dismutase to peroxisomes--evidence for a natural piggyback import mechanism in mammals. *Traffic,* 10, 1711-21

JENNINGS, S. M., TSAY, Y. H., FISCH, T. M. & ROBINSON, G. W. 1991. Molecular cloning and characterization of the yeast gene for squalene synthetase. ***Proc Natl Acad Sci U S A,*** **88, 6038-42**

JONES, J. M., MORRELL, J. C. & GOULD, S. J. 2004. PEX19 is a predominantly cytosolic chaperone and import receptor for class 1 peroxisomal membrane proteins .*J Cell Biol,* 164, 57-67

KELLER, G. A., PAZIRANDEH, M. & KRISANS, S. 1986. 3-Hydroxy-3-methylglutaryl coenzyme A reductase localization in rat liver peroxisomes and microsomes of control and cholestyramine-treated animals: quantitative biochemical and immunoelectron microscopical analyses. ***J Cell Biol,*** **103, 875-86**

KIEL, J. A., VEENHUIS, M. & VAN DER KLEI, I. J. 2006. PEX genes in fungal genomes: common, rare or redundant. ***Traffic,*** **7, 1291-303**

KLEIN, A. T., VAN DEN BERG, M., BOTTGER, G., TABAK, H. F *&* . DISTEL, B. 2002. Saccharomyces cerevisiae acyl-CoA oxidase follows a novel, non-PTS1, import pathway into peroxisomes that is dependent on Pex5p. ***J Biol Chem,*** **277, 25011-9**

KOVACS, W. J., TAPE, K. N., SHACKELFORD, J. E., DUAN, X., KASUMOV, T., KELLEHER, J .K., BRUNENGRABER, H. & KRISANS, S. K. 2007. Localization of the pre-squalene segment of the isoprenoid biosynthetic pathway in mammalian peroxisomes. ***Histochem Cell Biol,*** **127, 273-90**

KRIBII, R., ARRO, M., DEL ARCO, A., GONZALEZ, V., BALCELLS, L., DELOURME, D., FERRER, A., KARST, F. & BORONAT, A. 1997. Cloning and characterization of the Arabidopsis thaliana SQS1 gene encoding squalene synthase--involvement of the C-terminal region of the enzyme in the channeling of squalene through the sterol pathway .*Eur J Biochem,* 249, 61-9

KRISANS, S. K. 1996. Cell compartmentalization of cholesterol biosynthesis. ***Ann N Y Acad Sci,*** **804, 142-64**

KRISANS, S. K., ERICSSON, J., EDWARDS, P. A. & KELLER, G. A. 1994. Farnesyl-diphosphate synthase is localized in peroxisomes. ***J Biol Chem,*** **269, 14165-9**

KROGH, A., LARSSON, B., VON HEIJNE, G. & SONNHAMMER, E. L. 2001. Predicting transmembrane protein topology with a hidden Markov model: application to complete genomes. ***J Mol Biol,*** **305, 567-80**

KUNAU, W. H. 2001. Peroxisomes :the extended shuttle to the peroxisome matrix. ***Curr Biol,*** **11, R659-62**

LAEMMLI, U.K. 1970. Cleavage of structural proteins during the assembly of the head of bacterophage T4. ***Nature*****. 227, 680-685**

LASORSA, F. M., SCARCIA, P., ERDMANN, R., PALMIERI, F., ROTTENSTEINER, H. & PALMIERI, L. 2004. The yeast peroxisomal adenine nucleotide transporter: characterization of two transport modes and involvement in DeltapH formation across peroxisomal membranes. ***Biochem J,*** **381, 581-5**

LAZAROW, P. B. & FUJIKI, Y. 1985. Biogenesis of peroxisomes. ***Annu Rev Cell Biol,*** **1, 489-530**

LEBER, R., LANDL, K., ZINSER, E., AHORN, H., SPOK, A., KOHLWEIN, S .D., TURNOWSKY, F. & DAUM, G. 1998. Dual localization of squalene epoxidase, Erg1p, in yeast reflects a relationship between the endoplasmic reticulum and lipid particles. ***Mol Biol Cell,*** **9, 375-86**

LEIVAR, P., GONZALEZ, V. M., CASTEL, S., TRELEASE, R. N ,.LOPEZ-IGLESIAS, C., ARRO, M., BORONAT, A., CAMPOS, N., FERRER, A. & FERNANDEZ-BUSQUETS, X. 2005. Subcellular localization of Arabidopsis 3-hydroxy-3-methylglutaryl-coenzyme A reductase. ***Plant Physiol,*** **137, 57-69**

LICHTENTHALER, H. K. 1999. The 1-Deoxy-D-Xylulose-5-Phosphate Pathway of Isoprenoid Biosynthesis in Plants. ***Annu Rev Plant Physiol Plant Mol Biol,*** **50, 47-65**

LISCUM, L., FINER-MOORE, J., STROUD, R. M., LUSKEY, K. L., BROWN, M. S. & GOLDSTEIN, J. L. 1985. Domain structure of 3-hydroxy-3-methylglutaryl coenzyme A reductase, a glycoprotein of the endoplasmic reticulum. ***J Biol Chem,*** **260, 522-30**

LISENBEE, C. S., KARNIK, S. K. & TRELEASE, R. N. 2003. Overexpression and mislocalization of a tail-anchored GFP redefines the identity of peroxisomal ER .*Traffic,* 4, 491-501

LIU, H., TAN, X., VEENHUIS, M., MCCOLLUM, D. & CREGG, J. M. 1992. An efficient screen for peroxisome-deficient mutants of Pichia pastoris. ***J Bacteriol,*** **174, 4943-51**

MANSTEIN, D. J., SCHUSTER, H. P., MORANDINI, P. & HUNT, D. M. 1995 .Cloning vectors for the production of proteins in Dictyostelium discoideum. ***Gene,*** **162, 129-34**

MATSUMOTO, N., TAMURA, S. & FUJIKI, Y. 2003. The pathogenic peroxin Pex26p recruits the Pex1p-Pex6p AAA ATPase complexes to peroxisomes. ***Nat Cell Biol,*** **5, 454-60**

MATSUZAKI, T. & FUJIKI, Y. 2008. The peroxisomal membrane protein import receptor Pex3p is directly transported to peroxisomes by a novel Pex19p- and Pex16p-dependent pathway. ***J Cell Biol,*** **183, 1275-86**

MATSUZONO, Y., MATSUZAKI, T. & FUJIKI, Y. 2006. Functional domain mapping of peroxin Pex19p: interaction with Pex3p is essential for function and translocation. ***J Cell Sci,*** **119, 3539-50**

MCGARVEY, D. J. & CROTEAU, R. 1995. Terpenoid metabolism. ***Plant Cell,*** **7, 1015-26**

MICHIHARA, A., SAWAMURA, M., YAMORI ,Y., AKASAKI, K. & TSUJI, H. 2001. Mevalonate pyrophosphate decarboxylase is predominantly located in the cytosol of rat hepatocytes. ***Biol Pharm Bull,*** **24, 1235-40**

MIYATA, N. & FUJIKI, Y. 2005. Shuttling mechanism of peroxisome targeting signal type 1 receptor Pex5: ATP-independent import and ATP-dependent export. ***Mol Cell Biol,*** **25, 10822-32**

MIZUNO, Y., KUROCHKIN, I. V., HERBERTH, M., OKAZAKI, Y. & SCHONBACH, C. 2008. Predicted mouse peroxisome-targeted proteins and their actual subcellular locations. ***BMC Bioinformatics,*** **9 Suppl 12, S16**

MONNAT, J., HACKER, U., GEISSLER, H., RAUCHENBERGER, R., NEUHAUS, E. M., MANIAK, M. & SOLDATI, T. 1997. Dictyostelium discoideum protein disulfide isomerase, an endoplasmic reticulum resident enzyme lacking a KDEL-type retrieval signal. ***FEBS Lett,*** **418, 357-62**

MOTLEY, A. M., HETTEMA, E. H., KETTING, R., PLASTERK, R. & TABAK, H. F. 2000. Caenorhabditis elegans has a single pathway to target matrix proteins to peroxisomes. ***EMBO Rep,*** **1, 40-6**

NAIR, D. M., PURDUE, P. E. & LAZAROW, P. B. 2004. Pex7p translocates in and out of peroxisomes in Saccharomyces cerevisiae. ***J Cell Biol,*** **167, 599-604**

NAKAMURA, A., SHIMADA, H., MASUDA, T., OHTA, H. & TAKAMIYA, K. 2001. Two distinct isopentenyl diphosphate isomerases in cytosol and plastid are differentially induced by environmental stresses in tobacco. ***FEBS Lett,*** **506, 61-4**

NES, W. D. 2011. Biosynthesis of cholesterol and other sterols. ***Chem Rev,*** **111, 6423-51**

NES, W. D., NORTON, R. A., CRUMLEY, F. G., MADIGAN, S. J. & KATZ, E. R. 1990. Sterol phylogenesis and algal evolution. ***Proc Natl Acad Sci U S A,*** **87, 7565-9**

NUTTALL, J. M., HETTEMA, E. H. & WATTS, D. J. 2012. Farnesyl diphosphate synthase, the target for nitrogen-containing bisphosphonate drugs, is a peroxisomal enzyme in the model system Dictyostelium discoideum. ***Biochem J,*** **447, 353-61**

NUTTALL, J. M., MOTLEY, A. & HETTEMA, E. H. 2011. Peroxisome biogenesis: recent advances. ***Curr Opin Cell Biol,*** **23, 421-6**

OKADA, K., KASAHARA, H., YAMAGUCHI, S., KAWAIDE, H., KAMIYA, Y., NOJIRI ,H. & YAMANE, H. 2008. Genetic evidence for the role of isopentenyl diphosphate isomerases in the mevalonate pathway and plant development in Arabidopsis. ***Plant Cell Physiol,*** **49, 604-16**

OLIVIER, L. M., KOVACS, W., MASUDA, K., KELLER, G. A. & KRISANS, S .K. 2000. Identification of peroxisomal targeting signals in

cholesterol biosynthetic enzymes. AA-CoA thiolase, hmg-coa synthase, MPPD, and FPP synthase. ***J Lipid Res,*** **41, 1921-35**

OTERA, H., HARANO, T., HONSHO, M., GHAEDI, K., MUKAI, S., TANAKA, A., KAWAI ,A., SHIMIZU, N. & FUJIKI, Y. 2000. The mammalian peroxin Pex5pL, the longer isoform of the mobile peroxisome targeting signal (PTS) type 1 transporter, translocates the Pex7p.PTS2 protein complex into peroxisomes via its initial docking site, Pex14p. ***J Biol Chem,*** **275, 21703-14**

PALMIERI, L., ROTTENSTEINER, H., GIRZALSKY, W., SCARCIA, P., PALMIERI, F. & ERDMANN, R. 2001. Identification and functional reconstitution of the yeast peroxisomal adenine nucleotide transporter. ***EMBO J,*** **20, 5049-59**

POULTER, D. C., AND H. C. RILLING. 1981. Conversion of farnesyl pyrophosphate to squalene, p. 414-441. In J. W. Porter and S. L. Spurgeon (ed.), Biosynthesis of isoprenoid compounds, vol. 1. Wiley & Sons, New York

PANG, K. M ,.LYNES, M. A. & KNECHT, D. A. 1999. Variables controlling the expression level of exogenous genes in Dictyostelium. ***Plasmid,*** **41, 187-97**

PATON, V. G., SHACKELFORD, J. E. & KRISANS, S. K. 1997. Cloning and subcellular localization of hamster and rat isopentenyl diphosphate dimethylallyl diphosphate isomerase. A PTS1 motif targets the enzyme to peroxisomes. ***J Biol Chem,*** **272, 18945-50**

PETRIV, O. I., PILGRIM, D. B., RACHUBINSKI, R. A. & TITORENKO, V. I. 2002. RNA interference of peroxisome-related genes in C .elegans: a new model for human peroxisomal disorders. ***Physiol Genomics,*** **10, 79-91**

PETRIV, O. I., TANG, L., TITORENKO, V. I. & RACHUBINSKI, R. A. 2004. A new definition for the consensus sequence of the peroxisome targeting signal type 2. *J Mol Biol,* 34.34-119 ,1

PHILLIPS, M. A., D'AURIA, J. C., GERSHENZON, J. & PICHERSKY, E. 2008. The Arabidopsis thaliana type I Isopentenyl Diphosphate Isomerases are targeted to multiple subcellular compartments and have overlapping functions in isoprenoid biosynthesis .*Plant Cell,* 20, 677-96

PLATTA, H. W., EL MAGRAOUI, F., BAUMER, B. E., SCHLEE, D., GIRZALSKY, W. & ERDMANN, R. 2009. Pex2 and pex12 function as protein-ubiquitin ligases in peroxisomal protein import. *Mol Cell Biol,* 29, 5505-16

PLATTA, H. W., EL MAGRAOUI, F., SCHLEE, D., GRUNAU, S., GIRZALSKY, W. & ERDMANN, R. 2007. Ubiquitination of the peroxisomal import receptor Pex5p is required for its recycling. *J Cell Biol,* 177, 197-204

PLATTA, H. W. & ERDMANN, R. 2007a. Peroxisomal dynamics. *Trends Cell Biol.*84-474 ,17

PLATTA, H. W. & ERDMANN, R. 2007b. The peroxisomal protein import machinery. *FEBS Lett,* 581, 2811-9

PLATTA, H. W., GRUNAU, S., ROSENKRANZ, K., GIRZALSKY, W. & ERDMANN, R. 2005. Functional role of the AAA peroxins in dislocation of the cycling PTS1 receptor back to the cytosol. *Nat Cell Biol,* 7, 817-22

POIRIER, Y., ANTONENKOV, V. D., GLUMOFF, T. & HILTUNEN, J. K. 2006. Peroxisomal beta-oxidation--a metabolic pathway with multiple functions. *Biochim Biophys Acta,* 1763, 1413-26

PURDUE, P. E & .LAZAROW, P. B. 1994. Peroxisomal biogenesis: multiple pathways of protein import. ***J Biol Chem,*** **269, 30065-8**

PURDUE, P. E., YANG, X. & LAZAROW, P. B. 1998. Pex18p and Pex21p, a novel pair of related peroxins essential for peroxisomal targeting by the PTS 2 pathway. ***J Cell Biol,*** **143, 1859-69**

RACHUBINSKI, R. A. & SUBRAMANI, S. 1995. How proteins penetrate peroxisomes. ***Cell,*** **83, 525-8**

RAYAPURAM, N. & SUBRAMANI, S. 2006. The importomer--a peroxisomal membrane complex involved in protein translocation into the peroxisome matrix. ***Biochim Biophys Acta,*** **1763, 1613-9**

RECALCATI, S., MENOTTI, E. & KUHN, L. C. 2001. Peroxisomal targeting of mammalian hydroxyacid oxidase 1 requires the C-terminal tripeptide SKI. ***J Cell Sci,*** **114, 1625-9**

REHLING, P., SKALETZ-ROROWSKI, A., GIRZALSKY, W., VOORN-BROUWER, T., FRANSE, M. M., DISTEL, B., VEENHUIS, M., KUNAU, W. H. & ERDMANN, R. 2000. Pex8p, an intraperoxisomal peroxin of Saccharomyces cerevisiae required for protein transport into peroxisomes binds the PTS1 receptor pex5p .*J Biol Chem,* **275, 3593-602**

REUMANN, S. 2004. Specification of the peroxisome targeting signals type 1 and type 2 of plant peroxisomes by bioinformatics analyses. ***Plant Physiol,*** **135, 783-800**

REUMANN, S., BABUJEE, L., MA, C., WIENKOOP, S., SIEMSEN, T ,. ANTONICELLI, G. E., RASCHE, N., LUDER, F., WECKWERTH, W. & JAHN, O. 2007. Proteome analysis of Arabidopsis leaf peroxisomes reveals

novel targeting peptides, metabolic pathways, and defense mechanisms. ***Plant Cell,*** **19, 3170-93**

REUMANN, S., QUAN, S., AUNG ,K., YANG, P., MANANDHAR-SHRESTHA, K., HOLBROOK, D., LINKA, N., SWITZENBERG, R., WILKERSON, C. G., WEBER, A. P., OLSEN, L. J. & HU, J. 2009. In-depth proteome analysis of Arabidopsis leaf peroxisomes combined with in vivo subcellular targeting verification indicates novel metabolic and regulatory functions of peroxisomes. ***Plant Physiol,*** **150, 125-43**

ROBINSON, G. W., TSAY, Y. H., KIENZLE, B. K., SMITH-MONROY, C. A. & BISHOP, R. W. 1993. Conservation between human and fungal squalene synthetases: similarities in structure, function, and regulation. ***Mol Cell Biol,*** **13, 2706-17**

ROGERS, M. J., WATTS, D. J., RUSSELL, R. G., JI, X., XIONG, X., BLACKBURN, G. M., BAYLESS, A. V. & EBETINO, F. H. 1994. Inhibitory effects of bisphosphonates on growth of amoebae of the cellular slime mold Dictyostelium discoideum. ***J Bone Miner Res,*** **9, 1029-39**

ROGERS, M. J., XIONG, X., BROWN, R. J., WATTS, D. J., RUSSELL, R. G., BAYLESS, A. V. & EBETINO, F. H. 1995. Structure-activity relationships of new heterocycle-containing bisphosphonates as inhibitors of bone resorption and as inhibitors of growth of Dictyostelium discoideum amoebae. ***Mol Pharmacol,*** **47, 398-402**

ROTTENSTEINER, H., KRAMER, A., LORENZEN, S., STEIN, K., LANDGRAF, C., VOLKMER-ENGERT, R. & ERDMANN, R. 2004. Peroxisomal membrane proteins contain common Pex19p-binding sites that are an integral part of their targeting signals. ***Mol Biol Cell,*** **15, 3406-17**

RUCKTASCHEL, R., GIRZALSKY, W. & ERDMANN, R. 2011. Protein import machineries of peroxisomes. ***Biochim Biophys Acta,*** **1.900-892 ,808**

RUF, A., MULLER, F., D'ARCY, B., STIHLE, M., KUSZNIR, E., HANDSCHIN, C., MORAND, O. H. & THOMA, R. 2004. The monotopic membrane protein human oxidosqualene cyclase is active as monomer. ***Biochem Biophys Res Commun,*** **315, 247-54**

SACKSTEDER, K .A., JONES, J. M., SOUTH, S. T., LI, X., LIU, Y. & GOULD, S. J. 2000. PEX19 binds multiple peroxisomal membrane proteins, is predominantly cytoplasmic, and is required for peroxisome membrane synthesis. ***J Cell Biol,*** **148, 931-44**

SANTOS, M. J., IMANAKA, T ,.SHIO, H., SMALL, G. M. & LAZAROW, P. B. 1988. Peroxisomal membrane ghosts in Zellweger syndrome--aberrant organelle assembly. ***Science,*** **239, 1536-8**

SAPIR-MIR, M., METT, A., BELAUSOV, E., TAL-MESHULAM, S., FRYDMAN, A., GIDONI, D. & EYAL, Y. 2008. Peroxisomal localization of Arabidopsis isopentenyl diphosphate isomerases suggests that part of the plant isoprenoid mevalonic acid pathway is compartmentalized to peroxisomes. ***Plant Physiol,*** **148, 1219-28**

SCHLIEBS, W. & KUNAU, W. H. 2004. Peroxisome membrane biogenesis: the stage is set. ***Curr Biol,*** **14, R397-9**

SEGURA, M. J., JACKSON, B. E. & MATSUDA, S. P. 2003. Mutagenesis approaches to deduce structure-function relationships in terpene synthases. ***Nat Prod Rep,*** **20, 304-17**

SIEDENBURG, G. & JENDROSSEK, D. 2011 .Squalene-hopene cyclases. ***Appl Environ Microbiol,*** **77, 3905-15**

SIMKIN, A. J., GUIRIMAND, G., PAPON, N., COURDAVAULT, V., THABET, I., GINIS, O., BOUZID, S., GIGLIOLI-GUIVARC'H, N. &

CLASTRE, M. 2011. Peroxisomal localisation of the final steps of the mevalonic acid pathway in planta. *Planta,* 234, 903-14

SMITH, J. J., MARELLI, M., CHRISTMAS, R. H., VIZEACOUMAR, F. J., DILWORTH, D. J., IDEKER, T., GALITSKI, T., DIMITROV, K., RACHUBINSKI, R. A. & AITCHISON, J. D. 2002. Transcriptome profiling to identify genes involved in peroxisome assembly and function. *J Cell Biol,* 158, 259-71

SMITH, M. D. & SCHNELL, D. J. 2001. Peroxisomal protein import. the paradigm shifts. *Cell,* 105, 293-6

SNYDER, W. B., KOLLER, A., CHOY, A. J. & SUBRAMANI, S. 2000. The peroxin Pex19p interacts with multiple, integral membrane proteins at the peroxisomal membrane. *J Cell Biol,* 149, 1171-8

STAMELLOS, K. D., SHACKELFORD, J. E., SHECHTER, I., JIANG, G., CONRAD, D., KELLER, G. A. & KRISANS, S. K. 1993. Subcellular localization of squalene synthase in rat hepatic cells. Biochemical and immunochemical evidence. *J Biol Chem,* 268, 12825-36

STANLEY, W. A., FILIPP, F. V., KURSULA, P., SCHULLER, N., ERDMANN, R., SCHLIEBS, W., SATTLER, M. & WILMANNS, M. 2006. Recognition of a functional peroxisome type 1 target by the dynamic import receptor pex5p. *Mol Cell,* 24, 653-63

STEIN, K., SCHELL-STEVEN, A., ERDMANN, R. & ROTTENSTEINER, H. 2002. Interactions of Pex7p and Pex18p/Pex21p with the peroxisomal docking machinery: implications for the first steps in PTS2 protein import. *Mol Cell Biol,* 22, 6056-69

STEINBERG, S. J., DODT, G., RAYMOND, G. V., BRAVERMAN, N. E., MOSER, A. B. & MOSER, H. W. 2006. Peroxisome biogenesis disorders. ***Biochim Biophys Acta,*** **1763, 1733-48**

TAM, Y. Y., TORRES-GUZMAN, J .C., VIZEACOUMAR, F. J., SMITH, J. J., MARELLI, M., AITCHISON, J. D. & RACHUBINSKI, R. A. 2003. Pex11-related proteins in peroxisome dynamics: a role for the novel peroxin Pex27p in controlling peroxisome size and number in Saccharomyces cerevisiae. ***Mol Biol Cell,*** **14, 4089-102**

THOMA, R., SCHULZ-GASCH, T., D'ARCY, B., BENZ, J., AEBI, J., DEHMLOW, H., HENNIG, M., STIHLE, M. & RUF, A. 2004. Insight into steroid scaffold formation from the structure of human oxidosqualene cyclase. ***Nature,*** **432, 118-22**

TITORENKO, V. I., SMITH, J. J., SZILARD, R. K. & RACHUBINSKI, R. A. 1998. Pex20p of the yeast Yarrowia lipolytica is required for the oligomerization of thiolase in the cytosol and for its targeting to the peroxisome. ***J Cell Biol,*** **142, 403-20**

TSUKAMOTO, T., YOKOTA, S. & FUJIKI, Y. 1990. Isolation and characterization of Chinese hamster ovary cell mutants defective in assembly of peroxisomes. ***J Cell Biol,*** **110, 651-60**

VAN DER KLEI, I. J. & VEENHUIS, M. 2006. PTS1-independent sorting of peroxisomal matrix proteins by Pex5p. ***Biochim Biophys Acta,*** **1763, 1794-800**

VEENHUIS, M., MATEBLOWSKI, M., KUNAU, W. H. & HARDER, W. 1987. Proliferation of microbodies in Saccharomyces cerevisiae. ***Yeast,*** **3, 77-84**

VIZEACOUMAR, F. J., TORRES-GUZMAN, J. C., BOUARD, D., AITCHISON, J .D. & RACHUBINSKI, R. A. 2004. Pex30p, Pex31p, and Pex32p form a family of peroxisomal integral membrane proteins regulating peroxisome size and number in Saccharomyces cerevisiae. ***Mol Biol Cell,*** **15, 665-77**

VIZEACOUMAR, F. J., TORRES-GUZMAN, J. C., TAM ,Y. Y., AITCHISON, J. D. & RACHUBINSKI, R. A. 2003. YHR150w and YDR479c encode peroxisomal integral membrane proteins involved in the regulation of peroxisome number, size, and distribution in Saccharomyces cerevisiae. ***J Cell Biol,*** **161, 321-32**

WADA, I ,.RINDRESS, D., CAMERON, P. H., OU, W. J., DOHERTY, J. J., 2ND, LOUVARD, D., BELL, A. W., DIGNARD, D., THOMAS, D. Y. & BERGERON, J. J. 1991. SSR alpha and associated calnexin are major calcium binding proteins of the endoplasmic reticulum membrane. ***J Biol Chem,*** **266, 19599-610**

WANDERS, R. J. & WATERHAM, H. R. 2006. Biochemistry of mammalian peroxisomes revisited. ***Annu Rev Biochem,*** **75, 295-332**

WATTS, D. J. & ASHWORTH, J. M. 1970. Growth of myxameobae of the cellular slime mould Dictyostelium discoideum in axenic culture. ***Biochem J,*** **119, 171-4**

WENDT, K. U., PORALLA, K. & SCHULZ, G. E. 1997. Structure and function of a squalene cyclase. ***Science,*** **277, 1811-5**

WILLIAMS, C., VAN DEN BERG, M., GEERS, E. & DISTEL, B. 2008. Pex10p functions as an E3 ligase for the Ubc4p-dependent ubiquitination of Pex5p. ***Biochem Biophys Res Commun,*** **374, 620-4**